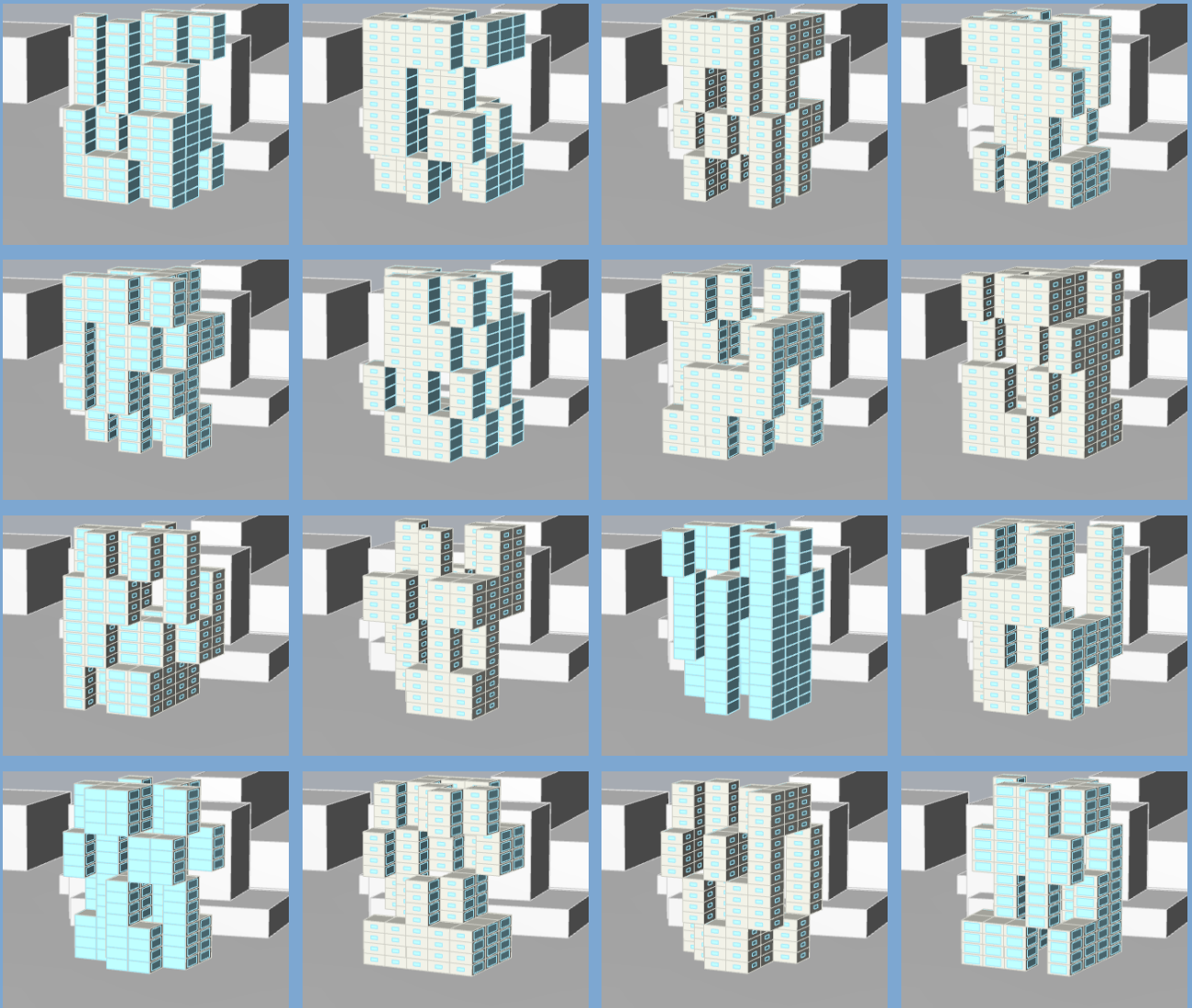


# Shape optimisation of residential mid-rise buildings for reduction of energy demand in temperate climate

MSc thesis Civil Engineering track Building Engineering

B.C. Dorresteyn

Technische Universiteit Delft



# Shape optimisation of residential mid-rise buildings for reduction of energy demand in temperate climate

## MSc thesis Civil Engineering track Building Engineering

by

B.C. Dorresteyn

to obtain the degree of Master of Science  
at the Delft University of Technology,  
to be defended publicly on Thursday August 26, 2020 at 03:30 PM.

Student number:	4218299
Project duration:	November 15, 2019 – August 26, 2020
Thesis committee:	dr. ir. H. R. Schipper, TU Delft Civil Engineering dr. M. Turrin, TU Delft Architecture ir. S. Pasterkamp, TU Delft Civil Engineering ir. N. A. Debets, Arup

An electronic version of this thesis is available at <http://repository.tudelft.nl/>.

# Abstract

Shape has long been an important parameter in improving the internal comfort of buildings and reducing energy demand. In the history of vernacular architecture numerous examples can be found of building typologies that have developed a distinctive shape. These shapes are often result of building physical requirements and principles that follow from local climate. Igloos, having a spherical shape that minimises the thermal loss surface and courtyards which provide shading and improved ventilation are clear examples of this.

Using a shape factor to reduce the building envelope and to minimise thermal loss is incorporated into the Dutch Building codes for a long time, aimed at a comfortable climate and low energy demand. Since living in spherical buildings like igloos, in the Netherlands has a large number of disadvantages, building shape is adapted to fit both demands for low energy use and high thermal comfort, but efficiently using space and allowing for daylight entrance.

Since building design has shifted to becoming more digitised, advantages of increasing computational power can now be used to improve building shape in new ways. Parametric design is a way to generate a large number of building designs in a short amount of time. Optimisation software can assist to analyse and optimise the design.

By making use of Grasshopper a parametric design model is created. Using this model a large variety of building designs was generated which are analysed on their daylight entrance and energy demand using Honeybee and Ladybug. By analysing the outcomes of these performance analyses, the window-to-wall-ratio and shape, quantified by shape factor  $L_c$ , of these designs were optimised using the autonomous optimisation algorithm pilOPT in modeFRONTIER. The optimisation objective is to minimise the total energy demand for heating and cooling. This is assessed by calculating the normalised energy demand for heating and cooling for both a summer and winter period. To execute the optimisation, the Erasmus Campus Student Housing project by Mecanoo in Rotterdam was used as a reference project.

The optimisation which was executed in two parts, for different summer period, shows more compact buildings, with low WWRs have lower energy demands. This can also be seen from the Pearson correlation between the  $L_c$  and the normalised energy demand [ $\text{kWh/m}^2$ ]. Which is found to be -0.624 for the first optimisation and -0.632 for the second optimisation. This confirms current building practice in which the relative building envelope is tried to be reduced.

Low WWRs ( $\leq 0.2$ ) are allowed to obtain a minimum daylight factor of 2.1%, which is lower than current practice. However, the minimum WWR is largely affected by the presence of neighbouring buildings. For facade orientations with adjacent buildings, minimum WWR is significantly higher (up to 0.8). Since buildings outside the own plot are not considered in the daylight calculation according NEN 2057 and the new NEN-EN 17037 situations may occur where buildings will obtain legal requirements but acquire poor daylight entrance.

For future building shape optimisation studies it is recommended to make use of visible part of the sky analysis (VSF) in the assessment of daylight criteria. Using VSF can save minutes of computation time per building analysis thereby speeding up the optimisation process and can be related to the daylight factor with high accuracy.

Recommendations for further research following this thesis are: to enlarge the number of case studies and thereby testing the outcomes of this research on to other cases; Focus on more detailed WWRs in a smaller range, by allowing smaller steps for WWR parameters, more detailed optima may be found; include the effect of installation efficiency, as this will affect the primary energy demand; and assessing the effect of on site energy production such as PV-panels on the building shape and WWR, as increasing the building envelope might not increase the net energy demand of buildings if more energy can be produced.

# Acknowledgements

Finalising my master thesis and thereby concluding my studies in Delft has been an effort I was not able to conduct without the help, assistance and motivation of many people around me.

First of all I would like to thank my committee members who have, from even before the start of my thesis, always been willing to advise me and guide me in the right direction. Starting I would like to thank Roel Schipper, as committee chair, who has helped me both in the process of writing a thesis as well as always keeping me focused on the importance of the practical application of my ideas. This advice and the conversations we had led to a result that, in my opinion, shows a real contribution to the practice of building engineering. Although I often left our meetings having more questions than before, they helped me shaping a clearer view of the direction I had to go. As Roel also was one of the committee members for my bachelor thesis I can truly say he has had a positive impact on my studies, always in a very kind and friendly manner.

Michela Turrin I would like to thank for her understanding and making the problems I encountered during my work clear. Often when I tried to explain my problems she was able to pick out what was the real issue and was able to give a clear example of what I tried to explain. And for always pointing out the importance of a foundation for the choices I made, thereby making me more aware of the subject I was researching and let me get a better grip on the total project.

My third committee member, Noor Debets, I would like to thank for the guidance throughout the entire project. Who has helped me creating an organised view on what I was doing and why. Because you were very quick in uncovering where my strengths and weaknesses lie, you were able to offer the perfect guidance and help in planning my research. Next to that clear examples of your own projects and always pleasant weekly meetings made your help really appreciated.

Sander Pasterkamp I would like to thank for stepping in at the last moment to complete my committee. I appreciate you making time to read my report on joining my presentation while not having been a witness of the rest of my graduation process.

Next to my committee members I would like to thank Jasper Tonk and Martijn Meester from Mecanoo for providing me with information about the Erasmus student housing project, enabling me to use this as a case study for my research. Also would I like to thank the people from Esteco for providing not only a licence to use modeFRONTIER, but also taking the opportunity to come to Delft to give a very helpful crash course into the software.

Apart from the people mentioned before, I would like to thank my other colleagues at Arup, for their help and providing a welcoming and inspiring working environment. Especially Veronika and Alex for their help with Grasshopper problems and the BuP team, for their interest, enthusiasm and kindness even in the last months working from home.

I would also like to thank all my friends and study mates, who have supported me throughout both my bachelor and master. Especially my roommates with whom I have spent a lot of time in the past few months working from home.

Lastly, I would like to thank my family and especially my brother and parents for always supporting me.



# Preface

There are a number of reasons why parametric optimisation for the reduction of energy demand has my personal interest and why I chose to complete my master degree in this field. First of all, the use of technology to solve complex projects is a large personal motivator. Many challenges in building design can be too complex to promptly understand. The use of parametric optimisation provides a perfect solution to these problems because it can create valuable insights.

The second reason that provides personal motivation lies in the combination of aesthetics and performance. I am a great admirer of modernistic architecture and of the form follows function philosophy. Realising an aesthetically attractive building through high performance should always be a goal in architecture in my opinion. Implementing this philosophy for the energy performance of buildings can contribute both to an efficient and aesthetically attractive built environment.

Using the energy performance of buildings as guiding principle to the design reduces the risk of having to "fix" buildings with installations and thereby wasting both materials and energy. Exemplary to this risk are fully glazed buildings that might look impressive, but require an enormous amount of energy and installations for heating and cooling.

The third and last motivator for this research is comes from my interest in solving problems with a solution range rather than a single answer. In the beginning of my bachelor in civil engineering, the goal in many courses was rather exact. When I did a minor in art history, this changed. There was not just one correct answer, but the "why" and "how" were more important. Although this was something to get used to, it also was an eyeopener and showed me that there are multiple solutions to a problem. Something that appeared to be also valid in designing rather than pure maths or mechanics.

This is the reason I will research the impact of design parameters in residential buildings in my thesis.

*B.C. Dorresteyn  
Rotterdam, August 2020*

# Contents

<b>Abstract</b>	<b>i</b>
<b>Acknowledgements</b>	<b>ii</b>
<b>Preface</b>	<b>iii</b>
<b>List of Figures</b>	<b>vi</b>
<b>List of Tables</b>	<b>viii</b>
<b>Glossary</b>	<b>ix</b>
0.1 Abbreviations . . . . .	ix
0.2 Symbols . . . . .	ix
<b>1 Introduction</b>	<b>1</b>
1.1 Statement of the general problem . . . . .	1
1.1.1 A changing environment . . . . .	1
1.1.2 Change of energy use and regulations . . . . .	1
1.1.3 Vernacular architecture . . . . .	3
1.1.4 Adaptive design process . . . . .	4
1.1.5 Optimisation . . . . .	4
1.1.6 Problem . . . . .	5
1.2 State of knowledge . . . . .	5
1.3 Research question . . . . .	6
1.4 Goal . . . . .	6
1.5 Scope . . . . .	7
1.5.1 Building . . . . .	7
1.5.2 Climate . . . . .	7
<b>2 Literature Review</b>	<b>8</b>
2.1 Energy in Buildings . . . . .	8
2.1.1 Energy balance for residential buildings . . . . .	8
2.1.2 BENG . . . . .	11
2.2 Daylight Entrance in Buildings . . . . .	11
2.2.1 Importance of daylight . . . . .	11
2.3 Design Variables . . . . .	12
2.3.1 Window-to-wall-ratio . . . . .	12
2.3.2 Shape . . . . .	13
2.3.3 Orientation . . . . .	14
2.4 Design Objectives . . . . .	15
2.4.1 Energy demand . . . . .	15
2.4.2 Thermal comfort . . . . .	15
2.4.3 Daylight entrance calculations . . . . .	18
<b>3 Methodology</b>	<b>20</b>
3.1 Framework . . . . .	20
3.2 Form Generation . . . . .	23
3.3 Performance analysis . . . . .	23
3.3.1 Energy performance . . . . .	23
3.3.2 Daylight entrance . . . . .	24
3.4 Optimisation . . . . .	24

<b>4</b>	<b>Reference Project</b>	<b>27</b>
4.1	Building information . . . . .	27
4.1.1	Building selection . . . . .	28
4.1.2	Layout. . . . .	28
4.2	Reference building data . . . . .	29
4.2.1	Daylight analysis of the reference building . . . . .	29
4.3	Massing model . . . . .	32
4.4	Grasshopper model . . . . .	35
4.4.1	Building design . . . . .	35
4.4.2	Performance analysis . . . . .	38
4.5	Optimisation model workflow . . . . .	44
<b>5</b>	<b>Results</b>	<b>46</b>
5.1	Daylight analysis . . . . .	46
5.2	Optimisation study . . . . .	47
5.2.1	Effect of window-to-wall ratio . . . . .	50
5.2.2	Effect of shape . . . . .	54
5.2.3	Visualisation . . . . .	59
<b>6</b>	<b>Discussion</b>	<b>61</b>
6.1	Effect of WWR before optimisation . . . . .	61
6.2	Daylight analysis . . . . .	61
6.3	Optimisation study . . . . .	62
6.3.1	Effect of shape . . . . .	62
6.3.2	Effect of window-to-wall-ratio . . . . .	64
6.3.3	Effect of facade orientation . . . . .	64
<b>7</b>	<b>Conclusion</b>	<b>65</b>
7.1	Sub-research questions . . . . .	65
7.2	Main research question . . . . .	66
<b>8</b>	<b>Recommendations</b>	<b>67</b>
8.1	Recommendations for further research . . . . .	67
8.1.1	Other optimisation studies. . . . .	67
8.1.2	Follow up research . . . . .	67
8.2	Recommendations for building designers . . . . .	68
	<b>Bibliography</b>	<b>69</b>
<b>A</b>	<b>Appendix A - ISSO 74</b>	<b>71</b>
<b>A</b>	<b>Appendix B - Daylight Factor to visible part of the sky</b>	<b>73</b>
<b>A</b>	<b>Appendix C - NEN 2057</b>	<b>75</b>
<b>A</b>	<b>Appendix D - Grasshopper model and input</b>	<b>80</b>
<b>A</b>	<b>Appendix E - Input variables DesignBuilder validation</b>	<b>90</b>
<b>A</b>	<b>Appendix F - Drawings Reference Building Mecanoo</b>	<b>91</b>

# List of Figures

1.1	Household energy use in the EU in 2000 and 2015 (ODYSSEE-MURE, 2015)	2
1.2	Energy efficiency in the EU from 2000 to 2015 (ODYSSEE-MURE, 2015)	3
1.3	Section of an Iranian Baudgeer house (Bahadori, 1978)	4
1.4	Thermal performance of a courtyard or patio (Al-Sallal and Rahmani, 2019)	4
1.5	MacLeamy curve, showing the relation between effort, costs and effect through the design process (MacLeamy, 2004)	5
1.6	Final energy consumption in the commercial and public services (left) and residential sector (right) (IEA19)	6
1.7	Köppen-Geiger climate type map of Europe (adapted from: Beck et al., 2018)	7
2.1	Human sensitivity to daylight (Cawthorne, 1995)	12
2.2	Buildings with WWR 0.2, 0.3 and 0.45	13
2.3	Building shapes with equal volume (27000 m <sup>2</sup> ), but different shape factors ( $L_c$ and (relative) compactness (RC)	14
2.4	Different building orientations	14
2.5	BENG1 requirement, maximum energy use depending on compactness (Als/Ag)	15
2.6	PMV vs PPD (Fanger, 1970)	17
2.7	Class B thermal comfort operative temperature requirements (adapted from (ISSO, 2014))	18
2.8	CIE overcast sky at 20 June 12:00 (Marsh, 2018)	19
3.1	Framework performance driven design applied for this research (adapted from Sariyildiz, 2012)	21
3.2	Buildings used in validation process	23
3.3	Exemplary modeFRONTIER optimisation set-up	26
3.4	Classification of different optimisation algorithms within modeFRONTIER (Esteco, 2018)	26
4.1	Erasmus Student housing by Mecanoo (Mecanoo)	27
4.2	Axonometry of Erasmus Student housing (Mecanoo)	28
4.3	Floor plan Erasmus Student Housing 1 <sup>st</sup> floor (Mecanoo)	29
4.4	View on the patio of the Erasmus Student Housing (Xior)	30
4.5	Daylight factor calculation for critical rooms	30
4.6	Daylight analysis of a representative room by daylight factor analysis (a) and Visible part of the sky analysis (b)	31
4.7	Daylight analysis (VSF) for reference building view on south and east facade	31
4.8	Daylight factor ( $DF_{50\%}$ ) [%] versus the window-to-wall ratio times the visible part of the sky ( $WWR \cdot VSF$ ) [%]	32
4.9	Analysis of reference building floor plans	33
4.10	Even distribution of reference building floor plans	33
4.11	Final distribution of spaces for massing	34
4.12	Massing based on the reference building, when all masses are selected (a) and when a design is created (b)	34
4.13	Grasshopper model check and dispatch for windowless zones	35
4.14	Grasshopper model building block selection	36
4.15	Grasshopper model creation of floors and zones	37
4.16	Grasshopper model addition of glazing based on WWR per facade orientation	37
4.17	Grasshopper model VSF analysis for the north and east facade	39
4.18	Grasshopper model HVAC details	40
4.19	Grasshopper model zone details	41
4.20	Grasshopper model zone thresholds and analysis period selection	42

4.21	Grasshopper model energy calculation properties and summer/winter energy performance calculation . . . . .	43
4.22	modeFRONTIER optimisation workflow, showing all input variables, output variables, objective and constraint . . . . .	45
5.1	Daylight factor ( $DF_{50\%}$ ) [%] versus the window-to-wall ratio times the visible part of the sky ( $WWR \cdot VSF$ ) [%] . . . . .	46
5.2	Overview of randomly selected building designs generated by the pilOPT algorithm (part I) . . . . .	48
5.3	Overview of randomly selected building designs generated by the pilOPT algorithm (part II) . . . . .	49
5.4	WWR [-] for each facade orientation in relation to the shape factor ( $L_c$ ) [m] and the total normalised energy demand [kWh/m <sup>2</sup> ] for the first optimisation, coloured based on the energy demand . . . . .	52
5.5	WWR [-] for each facade orientation in relation to the shape factor ( $L_c$ ) [m] and the total normalised energy demand [kWh/m <sup>2</sup> ] for the second optimisation, coloured based on the energy demand . . . . .	53
5.6	Overview of all building designs of the first optimisation, showing the relation between the shape factor ( $L_c$ ) and the normalised energy demand for heating and cooling . . . . .	55
5.7	Overview of all building designs of the second optimisation, showing the relation between the shape factor ( $L_c$ ) and the normalised energy demand for heating and cooling . . . . .	56
5.8	Showing the relative part of the total facade for each orientation [-] in relation to the shape factor ( $L_c$ ) [m] and total normalised energy demand [kWh/m <sup>2</sup> ] for the first optimisation, coloured based on energy demand . . . . .	57
5.9	Showing the relative part of the total facade for each orientation [-] in relation to the shape factor ( $L_c$ ) [m] and total normalised energy demand [kWh/m <sup>2</sup> ] for the second optimisation, coloured based on energy demand . . . . .	58
5.10	Visualisation of building designs 693 (a), 1382 (b), 1883 (c) and 1900 (d) . . . . .	59
5.11	Overview of all building designs of the first optimisation, showing the relation between the shape factor ( $L_c$ ) and the normalised energy demand for heating and cooling including marked designs . . . . .	60
6.1	Overview of all building designs of the first optimisation, showing the relation between the shape factor ( $L_c$ ) and the normalised energy demand for heating and cooling, highlighting interesting areas . . . . .	63
A.1	Flowchart to determine upper temperature boundaries for comfort (ISSO, 2014) . . . . .	72
A.1	Data and relation between $DF_{50\%}$ and window-to-wall ratio times the visible part of the sky (Sky%) . . . . .	74
A.1	Input data NEN 2057 check reference building room 1 . . . . .	76
A.2	Input data NEN 2057 check reference building room 2 . . . . .	77
A.3	Input data NEN 2057 check reference building room 3 . . . . .	78
A.4	Results equivalent daylight surface area calculation critical rooms reference building . . . . .	79
A.1	Grasshopper model assigning RAD material properties . . . . .	81
A.2	Grasshopper model assign material properties external wall . . . . .	82
A.3	Grasshopper model assign material properties glazing and roof . . . . .	83
A.4	Grasshopper model assign material properties internal floor and wall . . . . .	84
A.5	Grasshopper model assign material properties ground floor . . . . .	85
A.6	Grasshopper model assign materials to building . . . . .	86
A.7	Grasshopper model calculate building properties . . . . .	87
A.8	Grasshopper model VSF calculation for the south and west facade . . . . .	88
A.9	Grasshopper model check if VSF calculation results comply the requirements . . . . .	89
A.10	Grasshopper model normalise energy demand for winter and summer analysis and collect output values for modeFRONTIER . . . . .	89

# List of Tables

2.1	BENG requirements for residential buildings (Ministry of the Interior and Kingdom Relations, 2019a) . . . . .	15
2.2	Seven point thermal sensation scale (Fanger, 1970) . . . . .	16
2.3	Selected months for reference climate year for energy calculations . . . . .	19
3.1	Building requirements . . . . .	21
3.2	Building requirements . . . . .	22
3.3	Validation of Energy demand [kWh] for months January, April and July . . . . .	24
5.1	Required WWR for a certain VSF (left) and required VSF for en certain WWR (right) to reach a $DF_{50\%}$ of 2.1% . . . . .	47
5.2	Correlation matrix between the WWR [-] per orientation and the normalised energy demand for heating and cooling [kWh] . . . . .	50
5.3	Correlation matrix between the WWR [-] per orientation and the normalised energy demand for heating and cooling [kWh] . . . . .	51

# Glossary

## 0.1. Abbreviations

Abbreviation	Meaning
API	application programming interface
BENG	bijna energieneutrale gebouwen
DBD	dutch building decree
DF	daylight factor
EPC	energy performance coefficient
GFA	gross floor area
GH	grasshopper
GHG	green house gas
MOO	multi objective optimisation
NFA	nett floor area
nZEB	near energy neutral buildings
PBD	performance-based design
PMV	predicted mean vote
PPD	predicted percentage of people dissatisfied
PV	photo voltaic
SHGC	solar heat gain coefficient
SVF	sky view factor
WWR	window to wall ratio

## 0.2. Symbols

Symbol	Quantity	Unit
$A_{ls}$	thermal loss surface area	$m^2$
$A_g$	usable floor area	$m^2$
$A_{gl}$	glazed surface area	$m^2$
$DF$	daylight factor	%
$DF_{50\%}$	daylight factor for 50% of the analysed room	%
$L_c$	characteristic length or shape factor	m
$SVF$	sky view factor	%

# Introduction

## 1.1. Statement of the general problem

Computational design is an increasingly important aid in the battle against climate change. This chapter explains how this can be achieved, why computational design is so important and what problem is assessed in this research.

First, the problem of climate change is shortly touched upon, as battling against this is one of the main drivers for this research. After that, measures that have been used before in reducing the energy demand for buildings are discussed, as is regulation regarding energy demand for buildings. Then a number of vernacular architectural typologies are discussed and it is explained what the effect building physical requirements has been on their shape. These typologies are discussed to show the importance of shape and the effect it may have on energy use and comfort. Then, the effect of early design decisions on the design and the design process and the role of computational design are discussed. Finally, the connection between these different subjects is illustrated which forms the problem statement.

### 1.1.1. A changing environment

Since the pre-industrial age, human activity has had an impact on the global environment, increasing the average temperature with 1.0 °C. Another effect of climate change, apart from rising temperatures, is the increase, in both intensity and occurrence, of extreme weather conditions like heavy rainfall or extreme droughts. Without interventions, and active reduction of the emission of green house gasses, these developments will have an increasing impact on global climate (Masson-Delmotte et al., 2018).

As a response to climate change the United Nations agreed to limit the allowable global warming in 2050 to below 2.0 °C above the pre-industrial age. The United Nations furthermore agreed to put an effort into keeping the temperature increase below 1.5 °C (United Nations, 2015). To be able to meet these requirements a reduction in the use of fossil fuels is required. The Dutch Climate Agreement, based on the Paris Agreement, states annual CO<sub>2</sub> emissions should be reduced by 49 % in 2030 and by 95 % in 2050, relative to 1990 (Rijksoverheid, 2019).

Since the built environment is responsible for 40 % of the total energy use and 36 % of the total CO<sub>2</sub> emissions in Europe (European Commission, 2019), reducing both the energy consumption and CO<sub>2</sub> emissions for buildings can contribute to the solution of the global warming problem. As residential buildings are responsible for about 25 % of the total energy use in Europe (ODYSSEE-MURE, 2015), reduction of energy demand and increasing the share of renewable energy for this specific type of buildings are essential in reaching both the Dutch Climate Agreement as the Paris Agreement.

### 1.1.2. Change of energy use and regulations

A number of developments in the built environment have contributed to an alteration and reduction of energy demand. Most important of these changes is wide implementation of thermal insulation. Since the start of regulation in thermal resistance of the building envelope, from the 1970s, buildings have become more air tight and insulation improved which reduced energy demand (van Straalen et al., 2007).



For European buildings, these changes have resulted in a reduction of heat losses which has primarily affected the heating demand as can be seen in Figure 1.1. In addition, heating, cooling and ventilation installations have become more efficient over time. With introduction of LED lamps, energy demand for lighting has also decreased which is shown in Figure 1.2. These changes in the way our buildings are climatized affect the ratio in the energy balance of these buildings, where appliances and thermal heat losses and gains claim a larger share of the total energy consumption. Apart from these adaptations, from 2010 on, there is an increasing amount of PV-cells installed on buildings which provides renewable energy (CBS, 2019).

Reduction of thermal losses, improvement of efficiency of installations and increased use of PV-cells are essential steps towards a more energy efficient built environment that can be classified in three steps which are known as the trias energetica. This strategy developed by Duijvestein (1998) consists of the following steps:

1. Reduce the energy demand
2. Use renewable energy
3. Use efficiently energy from fossil fuels

The improvement of insulation and air tightness contribute to the reduction in energy demand. The increased use of PV-cells and wind energy enlarges the share of renewable energy. And lastly the increasing efficiency of installations helps to make more efficient use of the fossil fuels that are still used.

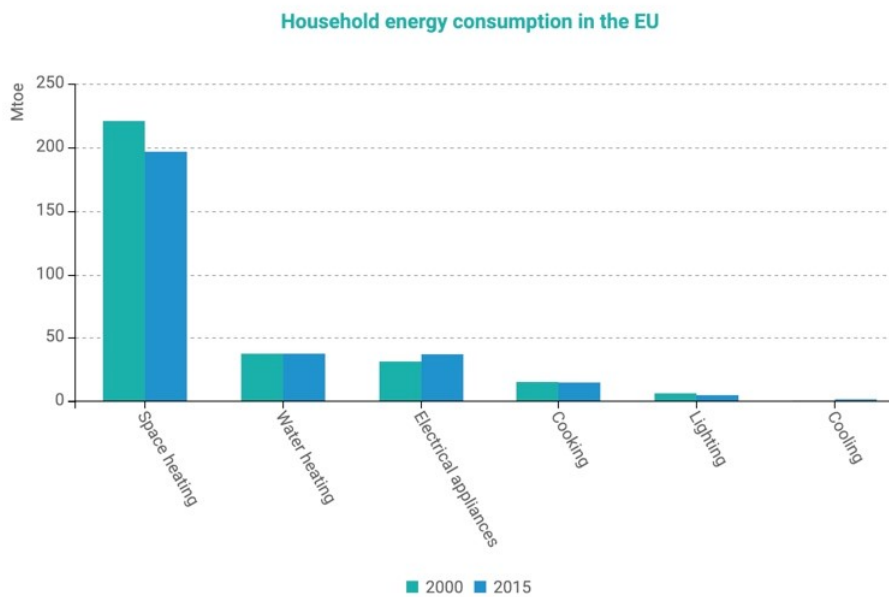


Figure 1.1: Household energy use in the EU in 2000 and 2015 (ODYSSEE-MURE, 2015)

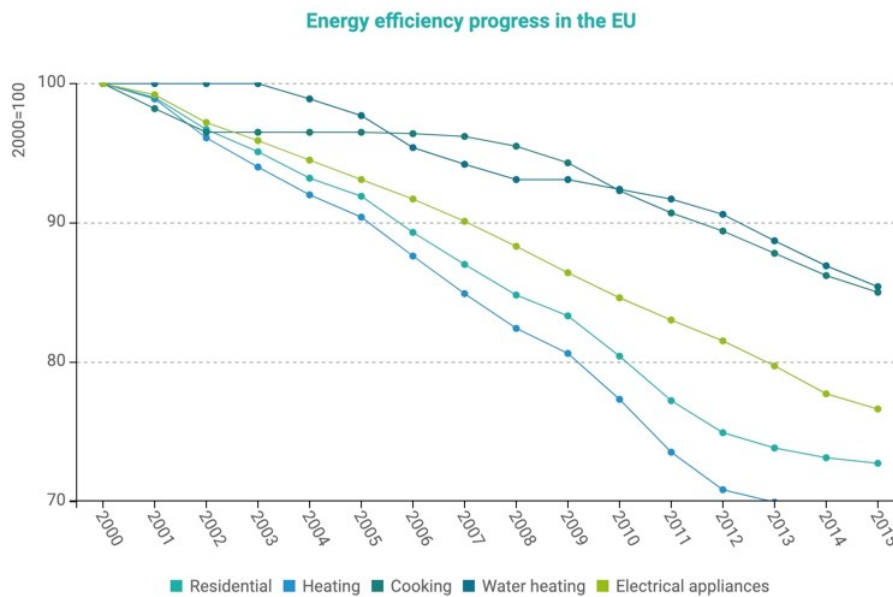


Figure 1.2: Energy efficiency in the EU from 2000 to 2015 (ODYSSEE-MURE, 2015)

### 1.1.3. Vernacular architecture

In the history of vernacular architecture numerous examples can be found of building typologies that have developed a distinctive shape. These shapes are often the result of building physical requirements and principles that follow from local climate. A number of examples is treated here to show the importance of designing with the environment and the effect this has on building shape.

#### Igloo

The Igloo is one of these building typologies that has adapted to an efficient shape for its environment. Extreme weather conditions within the polar circle, where temperatures can drop to  $-45^{\circ}\text{C}$  (Whitsett et al., 2013), raise high demands on thermal insulation. These demands are achieved by applying a range of measures of which the spherical shape is the most important one. By reducing the outdoor surface area, thermal losses are diminished. Additionally, the spherical shape of igloos is an efficient construction, as it can be built without the need for columns. Further measures that increase the internal climate of igloos are a raised floor for the sleeping area and a lowered entrance to exhaust cold air when the igloo warms up. Covered with animal skin and heated by human energy and stone lamps, the temperature inside these igloos can rise up to  $15^{\circ}\text{C}$  (Whitsett et al., 2013).

#### Baudgeers

In Iran, Baudgeers are used to cool a building by capturing and guiding wind through the building as shown in Figure 1.3. Often these towers guide the wind through a long underground shaft or along an underground river. This way the air temperature is decreased before it reaches the houses. Guiding the air along an underground river or fountain helps to reduce the air temperature even further by including the effect of evaporative cooling (Bahadori and Dehghani-sanij, 2014). At night the stack effect is used to exhaust warm internal air through the baudgeers and extract cool air through the windows from outside. This effective passive climate strategy has ensured a large number of Iranian buildings have these shape defining towers.

#### Courtyard buildings

Another shape defining, passive, climate control solution in warmer climates is the addition of a patio or courtyard in a building. Including a courtyard influences the climate by providing shading and improving natural ventilation. Shading which is created in a courtyard directly decreases solar gain for a part of the building and the courtyard. Cooler air from the courtyard is then ventilated through the rest of the building, providing comfort by ventilation and reducing the internal temperature (Al-Sallal and Rahmani, 2019). This system is shown in Figure 1.4.

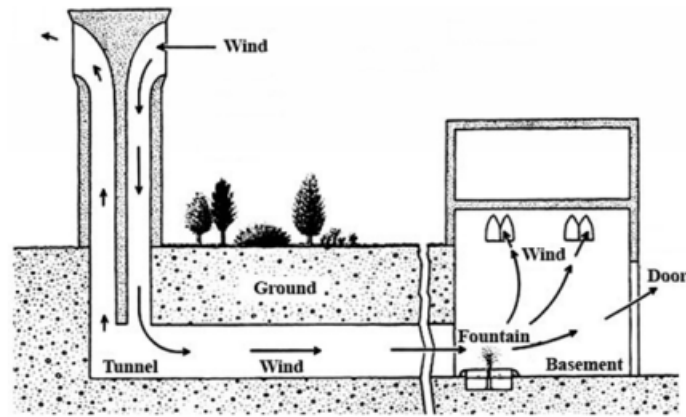


Figure 1.3: Section of an Iranian Baudgeer house (Bahadori, 1978)

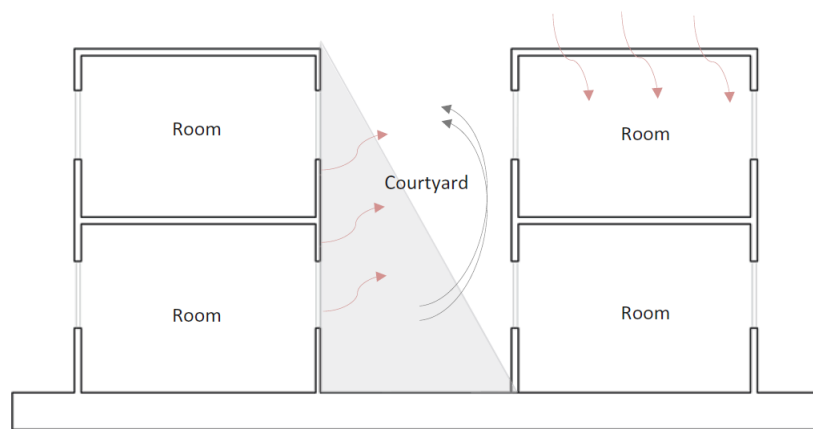


Figure 1.4: Thermal performance of a courtyard or patio (Al-Sallal and Rahmani, 2019)

#### 1.1.4. Adaptive design process

In the current industry, where a classical design strategy is followed, it is common use to design a building, then further develop it and ensure the internal climate is comfortable, which may require superfluous energy demand. In residential buildings, this can lead to the addition of cooling installations. By anticipating on the energy demand and the use of passive methods earlier in the design, the use of superfluous energy demand or installations can be avoided. Doing so makes it both easier and cheaper to have a considerable impact.

The relation between the ability to adapt a design, the moment of implementation and the costs that these adaptations entail are described by MacLeamy (2004). MacLeamy shows that changes implemented early in the design process can have a larger impact and are less expensive. Furthermore, using an integrated project design may take up more effort in the beginning, but overall make a project more efficient and reduce the total duration and costs. This idea is visualised in Figure 1.5.

Apart from the effect on the internal temperature and energy use, changing the shape of buildings will also affect the daylight entrance in a building. Since this also affect the human well being of occupants and is bound to requirements, this cannot be ignored in the analysis of building shape and energy use correlations.

#### 1.1.5. Optimisation

Inseparable from taking early design decisions following MacLeamy's theory, is the development of computational design and optimisation. Since computational power has largely increased over the last couple of decades, possibilities for performance driven design have increased. Performance driven design differs from conventional design primarily in the relation between design and performance analysis. In a conventional design, from an architects perspective, shape and and building

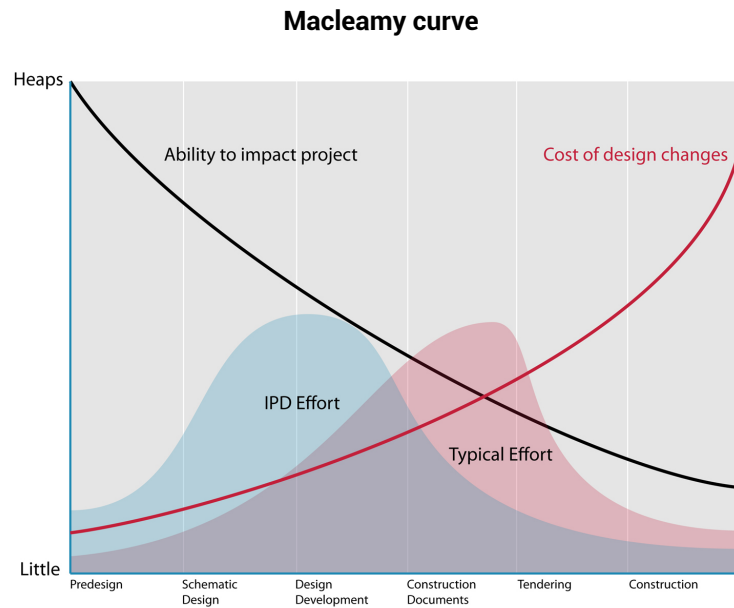


Figure 1.5: Macleamy curve, showing the relation between effort, costs and effect through the design process (MacLeamy, 2004)

volume are primary design parameters. Once an initial design is drawn, building performance is assessed, after which the design is altered. This results in an iterative process that goes through a limited amount of cycles. In performance driven design, the traditional steps of creating a shape are combined with a performance analysis. This means a number of different designs are created not primarily based on the architects aesthetic preferences, but on performance of a building shape, which can be a wide variety of parameters like energy or constructional performance. Instead of going through an iterative process from design to design, a number of designs including their performance can be generated and assessed at once. This method provides the advantage of comparing different shapes and thereby reducing the chance of overlooking a well performing design alternative.

### 1.1.6. Problem

From the developments described above, it can be concluded that there is a need to continue to change the build environment so it can help tackle the challenge to limit further climate change. From examples of vernacular architectural typologies it can be shown that shape has an impact on the internal building climate. The balance between increasing solar gain in winter and preventing solar gain in summer plays an important role. Complementary to this is the need for daylight entrance. Influencing parameters are both the shape of the building and the window-to-wall-ratio (WWR). To be able to create comfortable energy efficient buildings it is important to know how window-to-wall-ratio and shape affect energy performance, daylight entrance and thermal comfort. Ensuring no superfluous energy demand is created or installations are added it is best to determine a shape and WWR as early on in the design process as possible. Where the balance between low energy demand, sufficient thermal comfort and sufficient daylight entrance lies is the problem that will be discussed in this research. A substantial amount of research is done on the effect of these parameters for office buildings. However, because the demands and energy balance for residential buildings are different, these outcomes cannot be applied to this type of buildings.

## 1.2. State of knowledge

Knowledge about the effect of changing the WWR is available, already many studies have been conducted that assess these effects. However, a large number of these studies focuses on office buildings. The difference in climate types within these researches is large. A lot of research is focused on buildings in extreme climates, such as Alibaba (2016) who studied effect of the WWR for office buildings in hot and humid climate or Shaeri et al. (2019) who has reviewed the best WWR for office

buildings in hot-dry and cold climate in Iran. The study of Troup et al. (2019) shows that the effect of the WWR on the energy use is hard to read from the actual energy use. Troup et al. (2019) did a statistical analysis on the effect of WWR on annual energy use and on heating, cooling, lighting and ventilation energy use of existing office buildings in the USA. It was found that the WWR alone has a significant influence on the cooling, lighting and ventilation, but not the heating energy use. In 2019, the effect of the WWR was studied for office buildings in Turin and Helsinki. The WWR was the main design parameter in this study, but also the effect of changing the U-value of the building envelope and windows, the building orientation, the presence of shading devices and controlled natural ventilation were considered. For both locations the optimal WWR was found to be around 30 %. However, thermal comfort was not taken into account as an evaluation criterion by Chiesa et al. (2019). These all focus on a reduction of energy use as main objective for office buildings. Due to the difference in the distribution of energy use for residential buildings these results are not directly applicable to these buildings. The difference in energy distribution for both office and residential buildings is shown in Figure 1.6.

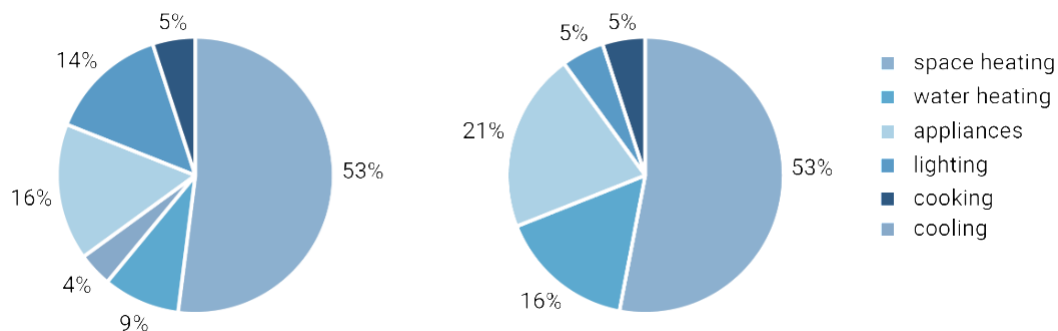


Figure 1.6: Final energy consumption in the commercial and public services (left) and residential sector (right) (IEA19)

### 1.3. Research question

From the problem definition a research question is derived. To be able to answer the main research question three sub questions are formulated. The main research question is:

- How can optimisation of building shape and window-to-wall-ratio contribute to the reduction of energy demand for mid-rise residential buildings in temperate climate, while maintaining thermal comfort and sufficient daylight entrance?

Sub questions:

1. What parameters affect the energy use for mid-rise residential buildings in a temperate climate?
2. What is the effect of shape and window-to-wall-ratio of mid-rise residential buildings in a temperate climate on energy demand, thermal comfort and daylight entrance?
3. What shapes and window-to-wall-ratios contribute to the reduction of energy demand for heating and cooling for mid-rise residential buildings in a temperate climate while maintaining thermal comfort and acceptable daylight entrance?

### 1.4. Goal

Answering the research question serves a goal, which is to enhance performance-based design early in the design process. By developing an insight in the effect of building shape and window-to-wall-ratio to the energy use in residential buildings in temperate climate. Hereby enabling easier implementation of the new nZEB requirements and contributing to creation of a more sustainable build environment.

## 1.5. Scope

### 1.5.1. Building

The focus for this research will be on mid-rise residential buildings complexes in temperate climates. The definition for mid-rise buildings is arbitrary. For this research, the aim will be at buildings between 4 storeys and 70 meters high. Four storeys are the number of floors from which a lift becomes mandatory according to the Dutch Building Decree. In the Netherlands, 70 meters is generally accepted as a point from where high rise buildings start and extra measures must be taken for fire safety (Zandbelt et al., 2008).

As a reference, a building is selected with a compact shape. This provides the opportunity to create a large variety of shapes and provides a good reference point since compact buildings are expected to perform well. The reference building should also have a simple internal layout, so realistic alternatives can be created. The selection of a reference building and its requirements are discussed in Chapter 4

For the requirements of near zero energy buildings, the Dutch BENG 1 regulation is used as a guideline. This entails the boundary condition as stated in the Dutch Building Decree is maintained, but the calculation method does not fully to the accompanying calculation NTA 8800. Moreover, not considering BENG 2 and BENG 3 means heating and cooling installation efficiency and on site energy generation are no variables in the scope of this research.

### 1.5.2. Climate

The research will focus on a temperate climate, like that of the Netherlands. This type of climate can be described by the Köppen-Geiger classification as a Cfb climate. Which stand for a temperate climate without a dry season and with warm summers (Peel et al., 2007). This type of climate is representative for a larger region of Europe as can be seen in Figure 1.7

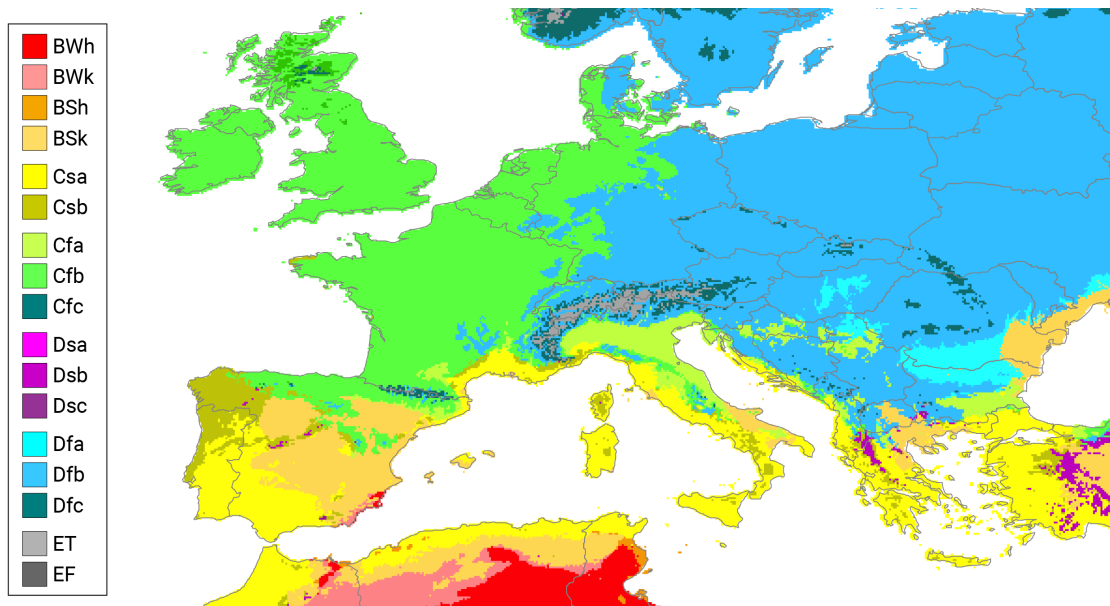


Figure 1.7: Köppen-Geiger climate type map of Europe (adapted from: Beck et al., 2018)

## Literature Review

To be able to understand what parameters should be considered in the design optimisation, the thermal balance and daylight properties of residential buildings are analysed. After this, both design variables and design objectives, that follow from these analysis are further introduced.

### 2.1. Energy in Buildings

#### 2.1.1. Energy balance for residential buildings

To be able to analyse the effect of building shape and WWR to the energy performance and thermal comfort, it is essential to understand the energy balance in a building. The energy balance describes the relation between (thermal) energy flows in a building and the heating or cooling demand that is required to keep the building at a comfortable level. This balance, is described in Equation 2.1.

$$Q_{heating/cooling} = Q_{transmission} + Q_{infiltration} + Q_{ventilation} + Q_{solar} + Q_{internal} + Q_{accumulation} \quad (2.1)$$

$Q_{heating/cooling}$	= energy demand for heating or cooling	[W]
$Q_{transmission}$	= energy flow by transmission	[W]
$Q_{infiltration}$	= energy flow through infiltration	[W]
$Q_{ventilation}$	= energy flow through ventilation	[W]
$Q_{solar}$	= energy flow through solar radiation	[W]
$Q_{internal}$	= energy flow due to internal gains	[W]
$Q_{accumulation}$	= energy accumulation in building mass	[W]

The total energy balance for a residential building consists of the different parts of the formula above. Each of these energy flows is affected by different building properties. Using Equation 2.1, it is possible to determine the heating or cooling demand for a building ( $Q_{heating/cooling}$ ). To gain equilibrium means the temperature inside the building of room is constant. Gaining an equilibrium with zero on the left hand side means no additional heating or cooling is required to maintain a constant temperature. The energy demand in Wh is calculated by summing the averages of the powers for the individual energy flows.

The amount of energy flow by transmission depends on the combination of the thermal transmission through both open and closed parts of the facade and thermal bridges. For both open and closed facade parts, the energy flow through transmission can be calculated using Equation 2.2. From this equation follows that the lowering both the U-value and the surface area (building envelope) will have an mitigating effect on the energy flows.

$$Q_{transmission} = UA(T_o - T_i) \quad (2.2)$$

$Q_{transmission}$	= energy flow by transmission	[W]
$U$	= overall heat transfer coefficient	[W/m <sup>2</sup> K]
$A$	= surface area	[m <sup>2</sup> ]
$T_o$	= outside temperature	[K]
$T_i$	= indoor temperature	[K]

The amount of energy flow through infiltration ( $Q_{infiltration}$ ) is depending on the mass flow rate of air, the heating capacity of that air and the temperature difference between inside and outside. The relation between these variables is shown in Equations 2.3. The mass flow rate of air depends on pressure differences between inside and outside the building and the air tightness of the building. Like energy flow through transmission, infiltration losses can be mitigated by reducing the surface area. Another way to decrease losses by infiltration is to improve the air tightness of the building envelope.

$$Q_{infiltration} = \dot{m}_{infiltration} c_p (T_o - T_i) \quad (2.3)$$

$Q_{infiltration}$	= energy flow through infiltration	[W]
$\dot{m}_{infiltration}$	= mass flow rate of air	[kg/s]
$c_p$	= heating capacity of dry air	[J/kgK]
$T_o$	= outside temperature	[K]
$T_i$	= indoor temperature	[K]

Similar to the infiltration losses the supply of fresh air by ventilation ( $Q_{ventilation}$ ) also has an effect on the energy balance. The difference with infiltration is that heat recovery may be included in a ventilation system and pressure differences are actively generated by ventilators. The thermal energy flow by ventilation is shown in Equation 2.4.

$$Q_{ventilation} = (1 - \eta) \dot{m}_{ventilation} c_p (T_o - T_i) \quad (2.4)$$

$Q_{ventilation}$	= energy flow through ventilation	[W]
$\eta$	= efficiency of heat recovery	[-]
$\dot{m}_{ventilation}$	= mass flow rate of air	[kg/s]
$c_p$	= heating capacity of dry air	[J/kgK]
$T_o$	= outside temperature	[K]
$T_i$	= indoor temperature	[K]

Solar gains through the windows ( $Q_{solar}$ ) are described by Equation 2.5. The energy gains from solar radiation depend on the properties of the glazing and possible shading system, the power of the radiation and the window surface area. The surface area of the glazing is dependent on the WWR of the facade.

$$Q_{solar} = \sum_i g_{glass}^i A_{window}^i g_{shade}^i P_{solar}^i \quad (2.5)$$



$Q_{solar}$	= thermal gains through solar radiation	[W]
$g_{glass}^i$	= solar factor of the glazing	[-]
$A_{window}^i$	= window surface area	[m <sup>2</sup> ]
$g_{shade}^i$	= solar factor of the shading system	[-]
$P_{solar}^i$	= power of the solar radiation on the glazing	[W/m <sup>2</sup> ]
$i$	= facade orientation	

Building mass causes a delay in exchange of energy between the building mass and the air. Energy is stored in the building mass and returned depending on the temperature difference and heating capacity of the building mass. The energy that is stored in the building,  $Q_{accumulation}$ , is calculated according Equation 2.6.

$$Q_{accumulation} = \rho V C \frac{\partial T}{\partial t} \quad (2.6)$$

$Q_{accumulation}$	= energy accumulation in building mas	[W]
$\rho$	= density of the building mass	[kg/m <sup>3</sup> ]
$V$	= Volume of the building mass	[m <sup>3</sup> ]
$C$	= heating capacity of the building mass	[J/kgK]
$\frac{\partial T}{\partial t}$	= temperature variation over time	[K/s]

The last part of the energy balance is the internal gains which is given by Equation 2.7. This is built up by the energy generation by people, lighting and other appliances. These values are calculated by the respectively Equation 2.8, 2.9 and 2.10.

$$Q_{internal} = Q_{people} + Q_{lighting} + Q_{appliances} \quad (2.7)$$

$$Q_{people} = n_{people} \times P_M \quad (2.8)$$

$$Q_{lighting} = B_{floor} A_{floor} Q_{light} \quad (2.9)$$

$$Q_{appliances} = A_{floor} Q_{appliances} \quad (2.10)$$

From the energy balance of a building it can be seen that  $Q_{transmission}$ ,  $Q_{infiltration}$  and  $Q_{solarradiation}$  are all related to the surface area of the building envelope and the size of the windows. These Properties can be encapsulated in the shape of the building, which defines the surface area of the building envelope and the orientation of the facades towards the sun, and the window-to-wall-ratio which defines what part of the building envelope is glazed.

$Q_{people}$	= internal heat gains by people	[W]
$n_{people}$	= number of people	[–]
$Q_M$	= typical heat gains by people	[W/person]
$Q_{lighting}$	= internal heat gains by lighting	[W]
$B_{floor}$	= part of floor area where the lights are on	[–]
$A_{floor}$	= total floor area	[m <sup>2</sup> ]
$Q_{light}$	= power of lighting per area	[W/m <sup>2</sup> ]
$Q_{appliances}$	= internal heat gains by appliances	[W]
$A_{floor}$	= total floor area	[m <sup>2</sup> ]
$Q_{appliances}$	= average power of appliances per area	[W/m <sup>2</sup> ]

### 2.1.2. BENG

In light of reduction of energy use another development in the Netherlands is the implementation regulations regarding near-Zero Energy Buildings (nZEB), in Dutch: Bijna Energieneutrale Gebouwen (BENG). From the first of January 2021, the current energy performance assessment system will be replaced by BENG (Ministry of the Interior and Kingdom Relations, 2020). Both the assessment criteria as the calculation method will change with these new regulations. The new BENG requirements including the calculation method for BENG, the Dutch Technical Agreement 8800 (NTA8800) will replace the NEN 7120, the "Nader Voorschrift" and the ISSO 75.3 (Ministry of the Interior and Kingdom Relations, 2019b). These new requirements will become applicable from 1 January 2021. The BENG consists of three different requirements of which the exact demands differ per building type. All three requirements have to be satisfied so no compensation between them is allowed. The different requirements are:

- BENG 1 – maximum energy demand in kWh per m<sup>2</sup> user area per year
- BENG 2 – maximum primary fossil energy demand in kWh per m<sup>2</sup> user area per year
- BENG 3 – minimum share of renewable energy as a percentage of the total energy use

Separating these three requirements ensures the trias energetica is followed up in the design. In this separation of these requirements, the BENG 1 requirement is linked to step 1 of the trias energetica, which states that energy demand should be reduced. Similarly, the BENG 2 requirement is linked to step 2, which expresses the need for renewable energy. Lastly, BENG 3 is linked to step 3 which states to use fossil fuels as efficient as possible. As these requirements are split, the possibility to compensate between these different steps of the the energy demand following from the shape of the building and the physical properties of the facade, the efficiency of the installations and the generation of renewable energy is eliminated.

As this research is focused on the relationship between building shape and energy demand, the focus lies on BENG 1. As BENG 2 and BENG 3 requirements are related to the way energy is converted and generated, these are not further discussed.

## 2.2. Daylight Entrance in Buildings

Apart from energy use, daylight entrance is an important design parameter in new buildings. Daylight entrance is strictly regulated and considered as an important factor in a healthy and comfortable living environment. Why daylight entrance is so important, how this is affected by building shape and what current Dutch regulations require are all explained in the following section.

### 2.2.1. Importance of daylight

Exposure to daylight is an important part of human beings to stay healthy. Daylight exposure is pre-dominant in maintaining a good daily rhythm. When people are exposed to daylight, the production of

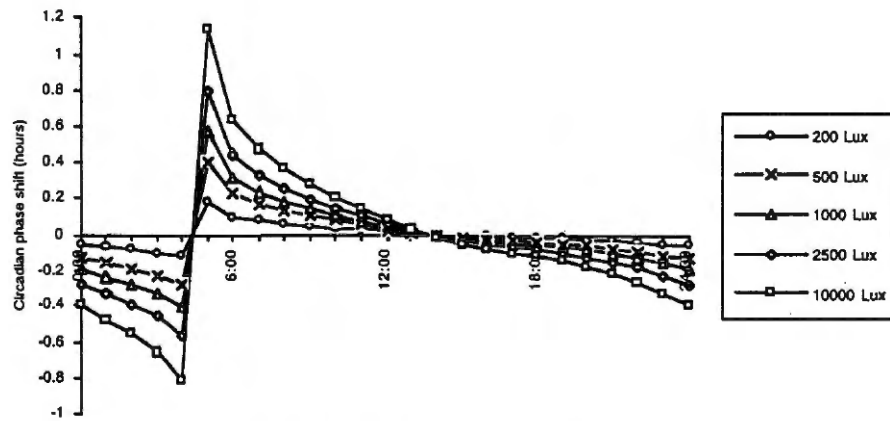


Figure 2.1: Human sensitivity to daylight (Cawthorne, 1995)

melatonin is being limited. This ensures people to feel awoken, thus affecting the sleep-wake rhythm. Apart from maintaining a proper sleep-wake rhythm, mental and physical health issues can be related to a disturbed circadian rhythm.

Without daylight exposure, the circadian cycle would slow down, causing a phase shift between the circadian rhythm and people's daily routine. To be able to prevent this shift, it is important to receive high levels of daylight. Especially early morning exposure to daylight is important since at that moment the brain is most sensitive. This sensitivity to daylight is shown in Figure 2.1. Because of the high sensitivity to daylight in the morning and the fact that most people are still at home around that time, sufficient daylight entrance in their homes plays an important role.

## 2.3. Design Variables

The design variables that are found to have an influence on the building's energy demand are defined here. The first set of parameters are the design variables. These are the variables that will be changed in the optimisation process to obtain an optimal result. The preset parameters are all parameters that are set for this research and shape the boundary conditions for which the results will be valid. The Optimisation objectives are the thresholds that form the minimal requirements the results should comply with.

### 2.3.1. Window-to-wall-ratio

The WWR is defined as the relation between the glazed surface area of the facade and the total facade area ( $A_{gl}/A_{fs}$  [-]). An example of this is given in Figure 2.2.

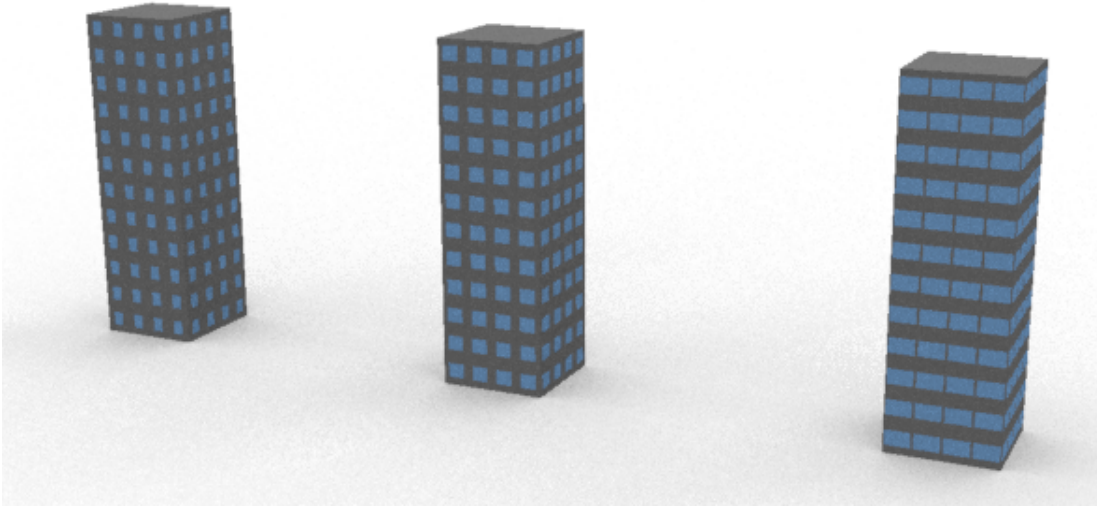


Figure 2.2: Buildings with WWR 0.2, 0.3 and 0.45

### 2.3.2. Shape

As seen in section 1.1.3, the ratio between building volume and the building envelope is an important parameter to steer internal climate. This ratio can be described as the compactness of a building, as shown in Section 2.1.2, by the characteristic length ( $L_c$ ), which is also a shape factor for the compactness of the building. The calculation of the characteristic length is given by Equation 2.11.

Assuming straight walls, a perfect cube is the most compact form a building can get. Presenting the shape of a building relative to this form gives a good impression how compact the building is. This relative compactness is given by Equation 2.12 (Pessenlehner and Mahdavi, 2003).

Figure 2.3 illustrates how buildings with equal volumes can have different shape factors. The six different building masses are all built up out of 27 cubes of 10x10x10 m and therefore all have an identical volume (27000 m<sup>3</sup>). Figure 2.3a shows the most compact form possible, for each shape the relative compactness is given with respect to this mass.

As can be seen in Figure 2.3, it is possible to have different shapes with equal shape factors (Figure 2.3b and 2.3e, 2.3c and 2.3f). Therefore it is important also to consider what the orientation of the building envelope is (e.g. 9000 m<sup>2</sup> for 2.3b east and 6000 m<sup>2</sup> for 2.3e east).

$$L_{c,i} = \frac{V}{A} \quad (2.11)$$

$$RC_i = \frac{L_{c,mc}}{L_{c,i}} \quad (2.12)$$

$L_{c,i}$	= characteristic length (shape factor for compactness)	[m]
$RC_i$	= Relative compactness of i <sup>th</sup> shape to the most compact building shape	[-]
$L_{c,mc}$	= characteristic length for the most compact shape	[m]
$V$	= total (climatised) volume	[m <sup>3</sup> ]
$A$	= total building envelope	[m <sup>2</sup> ]

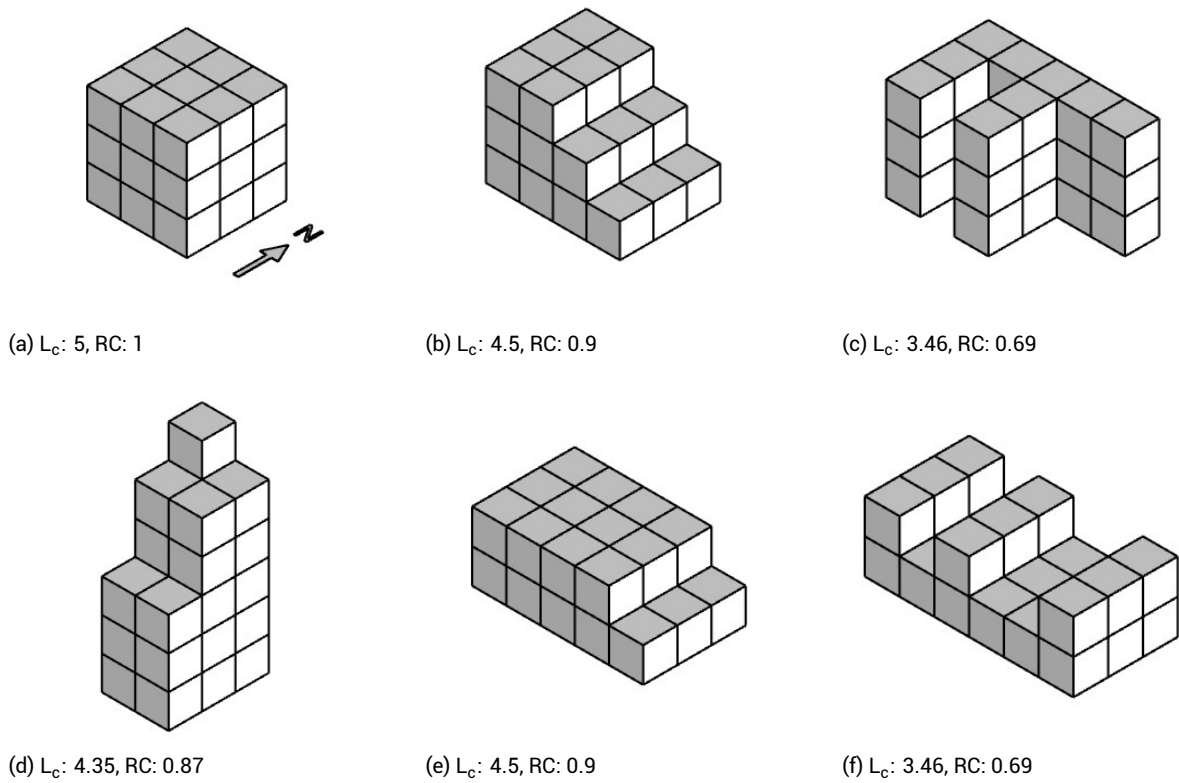


Figure 2.3: Building shapes with equal volume (27000 m<sup>3</sup>), but different shape factors ( $L_c$  and (relative) compactness (RC))

### 2.3.3. Orientation

The orientation of the entire building is partially incorporated into the massing. As seen in Figure 2.4, three different shapes are actually the same building but differently orientated. This shows by only considering shape, building orientation in four orientations (north, east, south and west) can be incorporated.

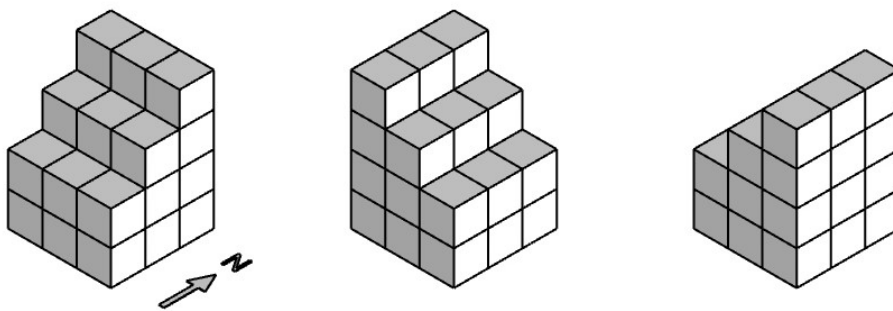


Figure 2.4: Different building orientations

## 2.4. Design Objectives

### 2.4.1. Energy demand

Energy demand is determined by the demand for both heating and cooling demand similar to BENG 1. In this calculation lighting energy demand is therefore not considered. However, the heating energy created by lighting is included in the energy demand calculation, see Equation 2.9. The design objective for energy demand is to minimise the demand and satisfy to the boundary conditions for energy demand for BENG 1. The energy performance indicator for the new nZEB regulation (BENG1) is defined as the summation of the heating demand and the cooling demand per square meter of usable floor area per year for a standard ventilation system in kWh. By including a standard ventilation system in the calculation the effect of the ventilation is excluded from the assessment of the building performance. The standard ventilation system that is included in BENG1 is c1. This is a system with natural supply and mechanical exhaust, all manually operated.

#### BENG requirements

The requirements for the new BENG regulation are shown in Table 2.1. In this research only BENG 1 will be assessed, for which the requirement is depending on the compactness of the building, which is visualised in Figure 2.5.

Table 2.1: BENG requirements for residential buildings (Ministry of the Interior and Kingdom Relations, 2019a)

Compactness [-]	Energy demand (BENG 1) [kWh/m <sup>2</sup> ·yr]	Primary fossil fuel use (BENG 2) [kWh/m <sup>2</sup> ·yr]	Share renewable energy (BENG 3) [%]
$A_{Is}/A_g \leq 1.83$	$\leq 65$	$\leq 50$	$\geq 40$
$1.83 < A_{Is}/A_g \leq 3.0$	$\leq 55 + 30 \cdot (A_{Is}/A_g - 1.5)$	$\leq 50$	$\geq 40$
$A_{Is}/A_g > 3.0$	$\leq 100 + 50 \cdot (A_{Is}/A_g - 3.0)$	$\leq 50$	$\geq 40$

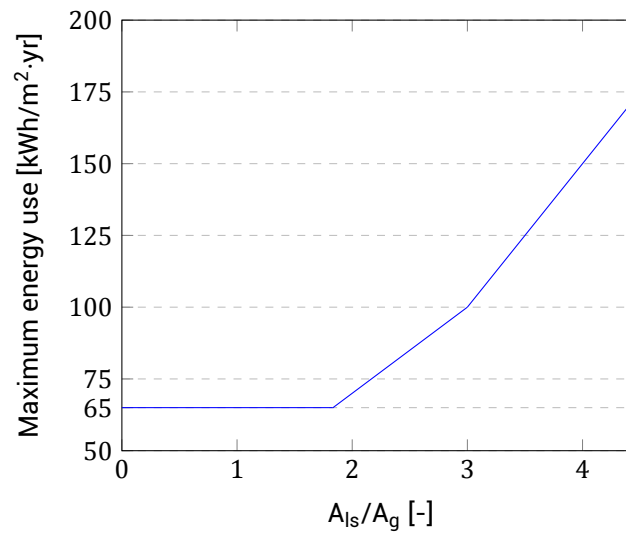


Figure 2.5: BENG1 requirement, maximum energy use depending on compactness ( $A_{Is}/A_g$ )

### 2.4.2. Thermal comfort

The most simple way to assess the thermal comfort in a building is to assess the number of hours the internal temperature exceeds a certain boundary value, better known as the TO-criterion (temperature exceeding criterion). For this method generally the number of hours is counted when the temperature is higher than 25 or 28 °C.

However, thermal comfort can not be captured in a single boundary value such as a maximum temperature. Next to the indoor air temperature, thermal comfort is influenced by a large set of parameters such as radiant temperature of the floor, walls and ceiling, the amount of clothing people wear, the activity level of the occupants and the outdoor temperature.

Much research has been conducted to try and capture all of these parameters in a single assessment criterion. An important study in this research is the comfort theory developed by Fanger (1970). In his research Fanger describes the PMV-model (Predicted Mean Vote). This model is based on three conditions under which thermal comfort is obtained. These conditions are: equilibrium in the human thermal balance and skin temperature and evaporation of sweat should be equal to the thermal energy production per square meter of body surface. These three conditions, combined with experimentally gathered data, Fanger set up the basic equation for thermal comfort of an average person as seen in Equation 2.13. The results from this formula are given on a seven point scale shown in Table 2.2.

$$f(H, l_{cl}, \theta_a, \theta_{mrt}, p_a, v_{ar}) = 0 \quad (2.13)$$

$H$	= intrinsic thermal energy production per square meter body surface	$[W/m^2]$
$l_{cl}$	= intrinsic thermal resistance of clothing	$[clo]$
$\theta_a$	= air temperature	$[^\circ C]$
$\theta_{mrt}$	= average radiation temperature	$[^\circ C]$
$p_a$	= partial vapour pressure in the air	$[Pa]$
$v_{ar}$	= relative air speed	$[m/s]$

$$PPD = 100 - 95 \times e^{-0.03353 \times PMV^4 - 0.2179 \times PMV^2} \quad (2.14)$$

By using the Fanger comfort equation (Equation 2.14), the predicted percentage of people that is dissatisfied (PPD) can be calculated. The relation between the PMV and PPD is shown in Figure 2.6.

Table 2.2: Seven point thermal sensation scale (Fanger, 1970)

+3	hot
+2	warm
+1	slightly warm
0	neutral
-1	slightly cool
-2	cool
-3	cold

The PMV-mode by Fanger is used as principle for the NEN-EN-ISO 7730 and ISO 74. The ISO norm is focused on office buildings and therefore less applicable for this research. NEN-EN-ISO 7730 is also applicable for residential buildings and therefore of better use in this case.

Most research in thermal comfort is executed for office buildings. Because the conditions and activities in residential buildings differ from those in offices, the results of this research are not entirely representative for residential buildings. What can be said about the difference between these two types is that a larger range of temperatures can be accepted in residential buildings. The reason for this larger acceptance is explained through mechanisms that can be divided into three categories.

The first category is expectation. Due to the lower availability of air conditioning in residential buildings, people expect higher temperatures in summer. These expectations contribute to a greater acceptance to higher temperatures. The second category is influence that residents have on the internal climate. In their homes, people have more influence on the internal climate, they are able

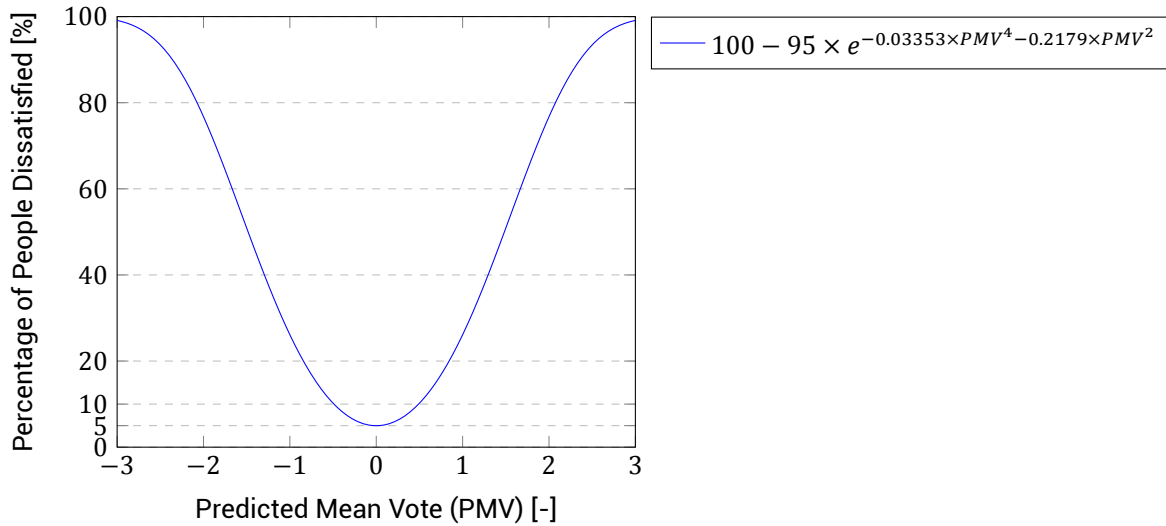


Figure 2.6: PMV vs PPD (Fanger, 1970)

to easily change the heating set-back temperature or open windows to increase natural ventilation. This directly influences the temperature and gives people the feeling of being in control. The feeling of being in control has the psychological effect of creating larger acceptance (Bluyssen, 2009). The last category is the behavioural adaptations by residents. People are more likely to change clothes or move to another location or room when they are at home than at work (Kurvers et al., 2012).

The ISO 74 describes a method that is more elaborate, but still easy to implement. Boundary conditions are set for both the minimum and maximum temperature depending on the outdoor temperature. These requirements are based on a combination of the PMV-model by Fanger and concept of the adaptive thermal comfort by Nicol and Humphreys (2002). The requirements consider an expected amount of people that will be dissatisfied (PPD) under certain conditions. Different classes are defined based on the PPD (ISO, 2014).

Comfort is determined based on the running mean outdoor temperature. This is the calculated average outdoor temperatures over the past 7 days according to Equation 2.15. The daily average temperatures are determined by the average of the daily minimum and maximum temperature.

$$\theta_{rm} = 0.253(\theta_{ed-1} + 0.8\theta_{ed-2} + 0.8^2\theta_{ed-3} + 0.8^3\theta_{ed-4} + 0.8^4\theta_{ed-5} + 0.8^5\theta_{ed-6} + 0.8^6\theta_{ed-7}) \quad (2.15)$$

$\theta_{rm}$  = running mean temperature [°C]

$\theta_{ed-i}$  = average temperature of the  $i^{\text{th}}$  day before [°C]

### Thermal comfort requirements

For the analysis of the thermal comfort the class B requirements for adaptive thermal boundary conditions are used as shown in Figure 2.7. Based on the flowchart shown in Figure A.1 in Appendix A, the  $\beta$  upper boundaries are maintained. Since this research focuses on the preliminary design phase, local discomforts are left out of scope.



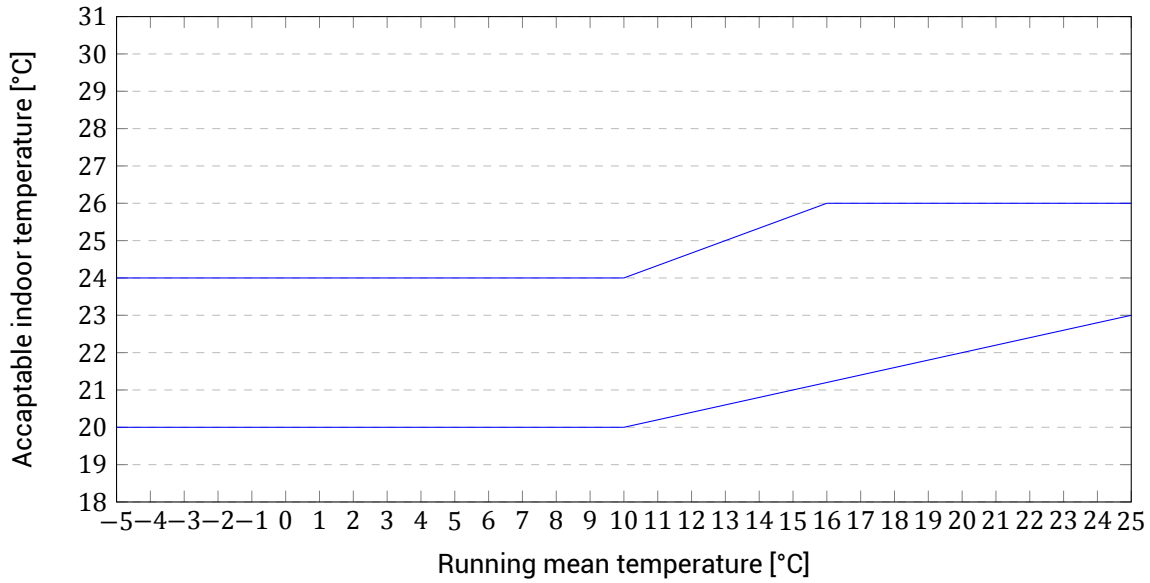


Figure 2.7: Class B thermal comfort operative temperature requirements (adapted from (ISSO, 2014))

### 2.4.3. Daylight entrance calculations

According to the Dutch Building Decree (DBD), the sufficiency of daylight is assessed by calculating the "equivalent daylight surface area" according to the NEN 2057. This code is expected to be replaced by NEN 17037 shortly after 2021 (NEN, 2019). In this new code, daylight entrance is assessed by calculating the daylight factor instead of an equivalent daylight surface. The implementation of the daylight factor has two large advantages. The first advantage is that a daylight factor calculation is better suited to be implemented into computer models. As the calculation of an equivalent daylight surface area is based on designing buildings in 2D, the daylight factor calculation method better suits current practise. The second advantage is that the daylight factor gives a more intuitively interpretable result.

Based on these two advantages, it is decided to use the daylight factor calculation and the accompanying advised requirements, as described hereafter, to determine the conditions regarding daylight entrance in the building.

The daylight factor is defined as the relation between the illumination in the free field, so outside without any obstructions, and the illumination at a reference plane inside the room that is assessed. This relation is shown in Equation 2.16.

$$DF = \frac{E_{room}}{E_{freefield}} \times 100\% \quad (2.16)$$

$DF$  = daylight factor [%]

$E$  = (horizontal) illuminance [lux]

The daylight factor needs to be calculated on a grid, which should comply with the size according to Equation 2.17.

$$p = 0.5 \times 5^{\log_{10}(d)} \quad (2.17)$$

$p$  = grid size ( $\leq 10$ ) [m]

$d$  = the longest distance in the calculated area (width or depth of the room) [m]

### Daylight factor requirements

The daylight factor should be assessed on a reference plane 0.85 m above the floor area. The minimum daylight factor used as a requirement in this research is based on the recommendation of the working group for the NEN 17037 norm (van der Horn et al., 2019). This group advises to maintain a minimum requirement for DF for at least 50% of the rooms floor area ( $DF_{50\%}$ ) of 2.1%. To pass and prevent compensation between better and worse performing rooms all assessed rooms should comply with this requirement.

The DF should be calculated for a CIE overcast sky, which is a completely clouded sky with changing luminance over the height. An example of the daylight distribution for a CIE overcast sky is shown in Figure 2.8, showing the luminance distribution over the sky at noon on 20 June.

Calculating the DF, internal reflection factors are 0.2 for floors, 0.5 for walls and 0.7 for the ceiling. External reflection factors are 0.2 for both the ground surface as for external walls. These numbers are all based on the new Dutch national standard for daylight analysis, NEN 17037.

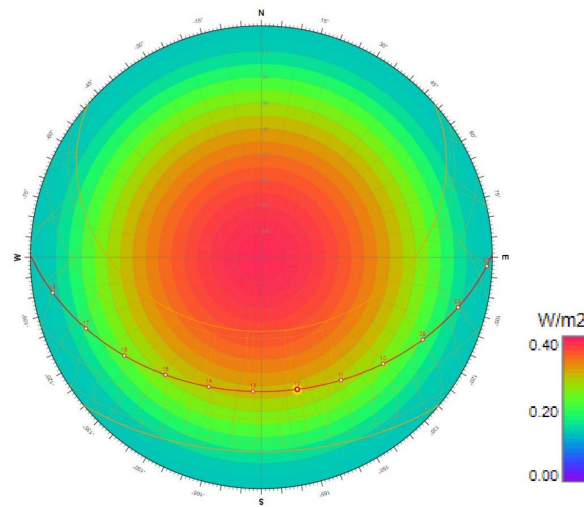


Figure 2.8: CIE overcast sky at 20 June 12:00 (Marsh, 2018)

### Additional requirements

Apart from building and objective requirements, there are also requirements for the environment. Most important requirement for the environment is the weather data for the energy and daylight factor analysis. The weather data that is used is a standardised weather file for the Netherlands according to NEN-5060-2018. For this norm, the weather data is selected per month as a representative month for the local climate. Each month is selected from the period 1966-2015. This has resulted in the selection shown in Table 2.3.

Table 2.3: Selected months for reference climate year for energy calculations

Month	1	2	3	4	5	6	7	8	9	10	11	12
Year	2001	2004	2004	2002	2000	2011	2008	2001	2011	2010	2003	2003

# Methodology

This chapter will discuss the way data is collected and reviewed, allowing to create an answer on the research question. First the framework for the model is explained in section 3.1. After that, the three components from the framework are treated in section 3.2, 3.3 and 3.4.

## 3.1. Framework

The framework that is used for the generation of data is given by Sariyildiz (2012) and consists out of three parts:

- Form generation
- Performance evaluation
- Optimisation

An interpretation of that framework, adapted for this research is shown in Figure 3.1. To create data first building shapes are created, which is the first part of the information. Each analysed building consist of a set of parameters that together create a building shape. All those shapes are then analysed to check their performance, this is the second step in the framework and enables it to quantify the performance of that shape. Based on objectives of the building performance, the next step in the framework is to optimise the input parameters to increase the performance and thereby creating new shapes. This way multiple shapes are tested and adapted in order to generate shapes that converge to optimal solutions within the given boundary conditions. This way a range of solutions will be created with increasing performance. This should then lead to information about the performance related to the input.

The three steps in this framework can be roughly linked to three types of parameters or boundary conditions. In the first step, the form generation, the variable parameters are important. These define the shape and WWR and are the parameters that are of interest in this research.

In the second step a large number of other parameters is required to conduct a performance analysis. These are all set parameters and are not varied during the optimisation process in contrast to the parameters that are used to determine the design in step 1. In Table 3.1 an overview is presented of the most important set parameters that are related to the energy performance calculation. Table 3.2 shows an overview of the set parameters that affect the daylight calculation. For a complete overview of the input parameters see Section 4.4 and Appendix A.

There are a number of other parameters that can be of influence on design choices which are not listed Table 3.1 and 3.2. Examples of these parameters are: aesthetics, costs and BENG 2/3 requirements. As stated in the scope, these parameters will be left out of the optimisation process in this research.

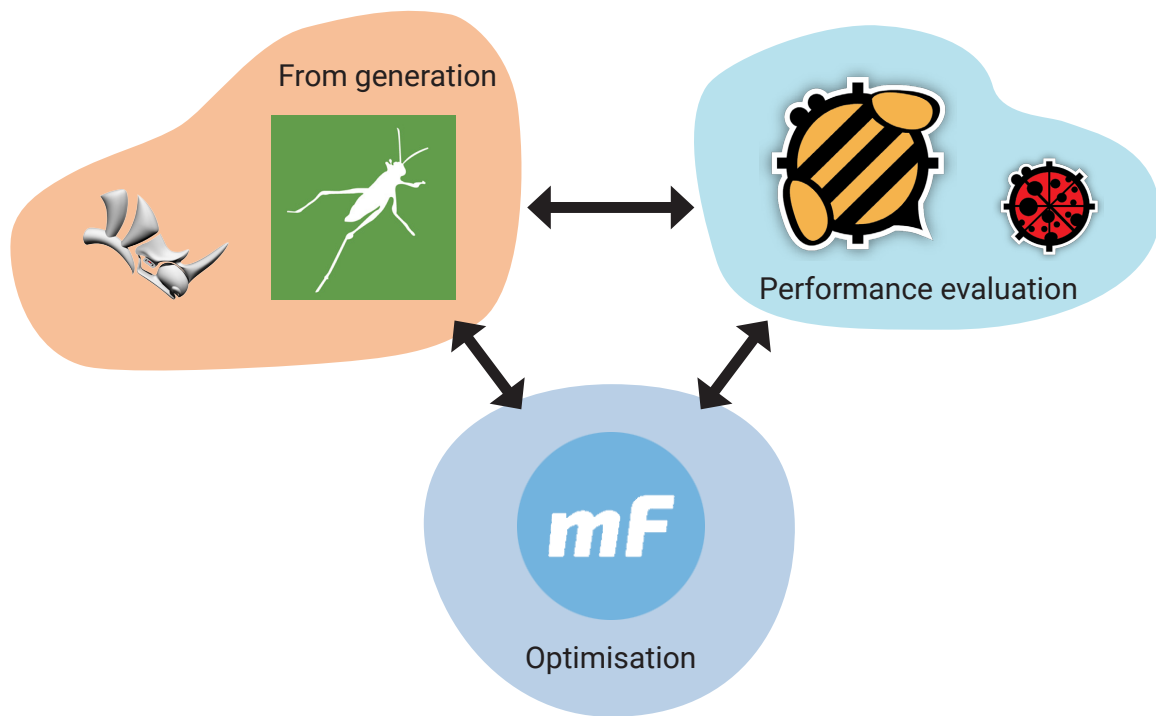


Figure 3.1: Framework performance driven design applied for this research (adapted from Sariyildiz, 2012)

Table 3.1: Building requirements

Parameter	value	unit
U-value glazing	1.1	$[W/m^2 K]$
SHGC glazing	0.33	$[-]$
Thermal insulation facade	4.5	$[m^2 K/W]$
Thermal insulation roof	6.0	$[m^2 K/W]$
Thermal insulation ground floor	3.5	$[m^2 K/W]$
Heating set back temperature	see Fig. 2.7	$[^{\circ}C]$
Cooling set back temperatures	see Fig. 2.7	$[^{\circ}C]$
Occupancy	0.02	$[people/m^2]$
Mechanical ventilation rate	0.001	$[m^3/s * m^2]$
Natural ventilation rate	variable	$[m^3/s * m^2]$
Infiltration rate	0.00042	$[m^3/s * m^2]$
Lighting power	2	$[W/m^2]$
CoP heating system	1	$[-]$
CoP cooling system	1	$[-]$

Table 3.2: Building requirements

Parameter	value	unit
Visible transmittance glazing	0.6	[-]
Reflection coefficient walls	0.5	[-]
Reflection coefficient ceiling	0.7	[-]
Reflection coefficient floor	0.2	[-]
Reflection coefficient exterior	0.2	[-]

## 3.2. Form Generation

To generate a selection of different buildings, all with different shape, WWR and orientation, a parametric design model will be created. The model should be constructed in such a way that only the parameters that are studied can vary within set limits. This means the rest should be fixed and not changed in the optimisation process. The form generation will take place in Rhinoceros (Rhino). Using the built-in plug-in Grasshopper (GH) which enables parametric design of the building shapes. A variety of shapes will be created, based on a reference model. The same plot will be used as a starting point. On that plot different shapes will be created with similar floor areas to make a fair comparison in the end results. How the form generation is shaped will be explained in Section 4.3. Apart from a minimum and maximum requirement for the gross floor area, no criteria will be set for the compactness of the building to ensure the best possible insight in the effect of shape on energy demand.

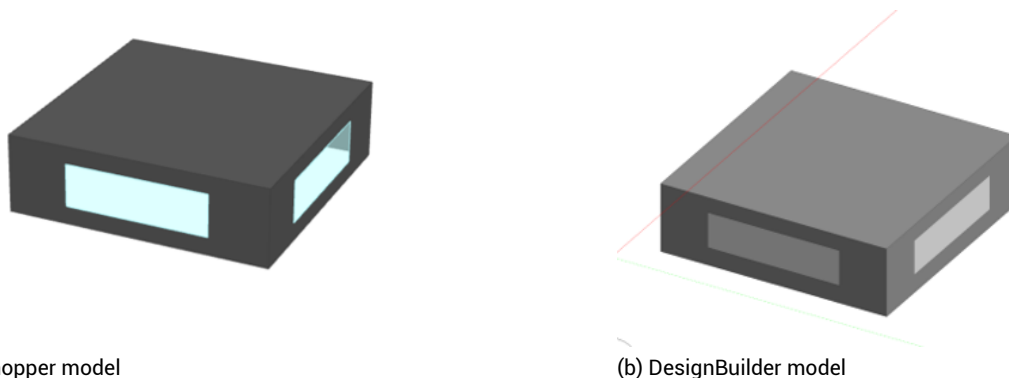
## 3.3. Performance analysis

### 3.3.1. Energy performance

The performance analysis of the different building configurations will be executed using Honeybee, a plugin package for GH that uses EnergyPlus as calculation software. Environmental data for those analyses is loaded into GH by Ladybug. Before optimisation the performance analysis is validated. By creating a similar building in DesignBuilder for different building configurations, the performance assessment of the GH model is validated. DesignBuilder is chosen as validation software since it also runs on the EnergyPlus calculation software. This way the validation process is focused on the correct application of the Honeybee components in the Grasshopper model.

To validate the Grasshopper model, a simple building is constructed in both grasshopper (Figure 3.2a) and DesignBuilder (Figure 3.2b). The building dimensions are 10m x 10m x 3m (LxWxH) and have the same properties as shown in Table 3.1 and 3.2. For both buildings the energy demand for heating and cooling is calculated for the months of July, January and April.

Due to the complexity of the energy modelling a deviation is allowed. The maximum allowable deviation between the two models is 10%. Table 3.3 shows the results of the validation process. The deviation is below 10% for all three months and therefore acceptable.



(a) Grasshopper model

(b) DesignBuilder model

Figure 3.2: Buildings used in validation process

Table 3.3: Validation of Energy demand [kWh] for months January, April and July

		January	April	July
<b>Grasshopper</b>	<b>Heating</b>	2011.11	635.65	0.44
	<b>Cooling</b>	0	3.65	95.06
	<b>Total</b>	2011.11	639.30	95.50
<b>DesignBuilder</b>	<b>Heating</b>	1883.52	582.47	0
	<b>Cooling</b>	0	0	103.97
	<b>Total</b>	1883.52	582.47	103.97
	<b>Deviation</b>	6.34%	8.37%	8.57%

### 3.3.2. Daylight entrance

As described in Section 2.4.3. daylight factor calculations suit the current practice of assessing daylight entrance in 3d computer models and give more intuitive results than the equivalent daylight surface method. However, daylight factor calculations are computationally heavier and therefore increase calculation time. These long computation times are inefficient in an optimisation research when hundreds of design alternatives are assessed. For this reason the daylight assessment in this study will be based on a visible part of the sky factor assessment (VSF). The VSF will then be linked to daylight factor values through an assessment of the relation between these two methods. The results of this assessment is shown in Section 4.2.1. Using this method can save 1 - 3 minutes of time per design evaluation.

The calculation of the visible part of the sky seen by each window surface is expressed as the visible part of the sky factor. The surface area of each window is divided into different segments which are all analysed. For each segment the part of the sky dome that is visible for that segment is determined.

In the assessment a part of the sky is reckoned as not visible when it is blocked by either a part of the analysed building itself or neighbouring buildings. The sky dome is centred above the analysed segment and since the analysis is made for one side of each plane, facing outwards. This results in a maximum value of 50% VSF, as 50% of the dome is always on the other side of the plane. Each visible part of the sky is weighted by the area they project on the analysed surface. Meaning, horizontal views are weighted heavier than parts of the sky seen that are closer to the zenith. This results in higher values for visible parts of the sky on the same height as the windows than parts of the sky that are closer to the zenith. For this calculation the sky is modelled as a CIE overcast sky, similar as for DF calculations.

The disadvantage of this method is that glazing properties, and reflection coefficients considered as constants in the daylight analysis and cannot be optimised. The advantage of this method is that it requires less calculation time, which enables a greater amount of shape variations and faster optimisation of the building shape and WWR.

For the assessment of daylight entrance the requirements for DF calculations, as discussed in Section 3.3.2, are maintained. To be able to assess the DF criteria using VSF calculations, a relation between these two parameters is required. For this both the  $DF_{50\%}$  and the VSF have to be calculated for a standard room. Comparing  $DF_{50\%}$  and VSF values, multiplied by the WWR, should lead to a relationship between these two methods. VSF results should be multiplied by the WWR since this also has an effect on the daylight entrance. This is illustrated by a situation where windows without obstructions have a VSF of 50% independent of the size of the windows. The size of the window will then be determining the actual daylight entrance in the building. The relation between  $DF_{50\%}$  and  $VSF \cdot WWR$  for this research are presented in Section 4.2.1

## 3.4. Optimisation

When the form generation and the performance evaluation are combined, optimisation can take place. Based on the input variables for the the shape generations and the outcomes of the performance

evaluation, the building design is optimised. This section describes the concept of optimisation and what software and algorithms are used.

In the optimisation process, a set of designs is created, using the form generation step in the framework. Each of these designs will be tested to both constraints and objectives in the performance evaluation step. In the third step of the framework, the actual optimisation, all test results are used to determine the next set of designs, iterating until an optimum design, or set of optimum designs is found.

In this research, building shape is optimised to reduce the energy demand for heating and cooling while maintaining sufficient daylight entrance. Here, a minimum energy demand is the objective, with an energy demand of 0 kWh as highest achievable goal. Daylight entrance in the building is a constrained since no optimum value is required but only a boundary value needs to be met. Besides energy demand and daylight entrance, there are three other boundary conditions that are incorporated into the model as constraints. These constraints are for windowless zones, floor area and compactness.

To ensure only feasible designs are assessed, a constraint is incorporated into the design that will check for zones without any windows. If more than 16 zones are windowless, the analysis is aborted and no performance calculation will be executed. The boundary value for this constraint is determined by the analysis of the reference building, which has an equal amount of floor area that is not exposed to any daylight. By performing a floor area check, it is made sure only buildings of equivalent size are considered. Each design should include a gross floor area (GFA) within 10% of the GFA of the reference building.

When all constraints are met, the energy demand for heating and cooling is calculated for both winter and summer period. The total of these values is then used by the optimisation software to determine the values for the input variables for the next iteration of designs. This process continues until little to no improvements in the design can be found. The software used in this research for the optimisation process is modeFRONTIER, a software package developed by Esteco. This software package can adopt grasshopper as a calculator for which it decides the values of the variable input parameters. As seen in Figure 3.3, different variables serve as input for the Grasshopper node, which performs the energy and daylight calculations. The results of those calculations are used to analyse the performance corresponding to the input variables. This data is then used by modeFRONTIER to decide on the input variables for the next iteration cycle.

The way in which modeFRONTIER selects designs, and converges to an optimum, depends on the optimisation algorithm. Depending on; the model, which can be computationally light or heavy; the objective, either one or multiple and required accuracy or robustness of the optimisation, different algorithms are best suited. Figure 3.4 shows an overview of the different algorithms available in modeFRONTIER.

In choosing an algorithm, three important considerations are to be made. First, is the goal of the optimisation to find either a global optimum, or to find a local optimum in an already known area of design. For this research, it is important to focus on finding a global optimum since this research is targeted at the early design stage and further optimisation will be possible. This is related to the second consideration, robustness. A robust algorithm will not be likely to linger in a local optimum but is able to search through the entire design space. The downside of an algorithm with high robustness is that accuracy, the third consideration, is often reduced.

For this research the pilOPT algorithm is selected. The performance analysis in this model is a moderate to heavy calculation which is the target group of the pilOPT algorithm. Since the goal of this research is to optimise for an early design stage a more robust algorithm is required. Although, if a very robust algorithm is chosen, chances are no real optima are found. Therefore pilOPT suits the optimisation in this research as it implements both strategies for local and global optimisation. Besides that, an accurate algorithm would require a large amount of time and would pose the risk of not finding the global optimum. The last advantage of pilOPT is that it is autonomous, which means it can pick the best suited strategy for finding optima automatically. A downside of the pilOPT algorithm is that it is a black box, because it is a proprietary algorithm by Esteco, it is not possible to exactly uncover what choices the algorithm made in the optimisation process (Esteco, 2018).



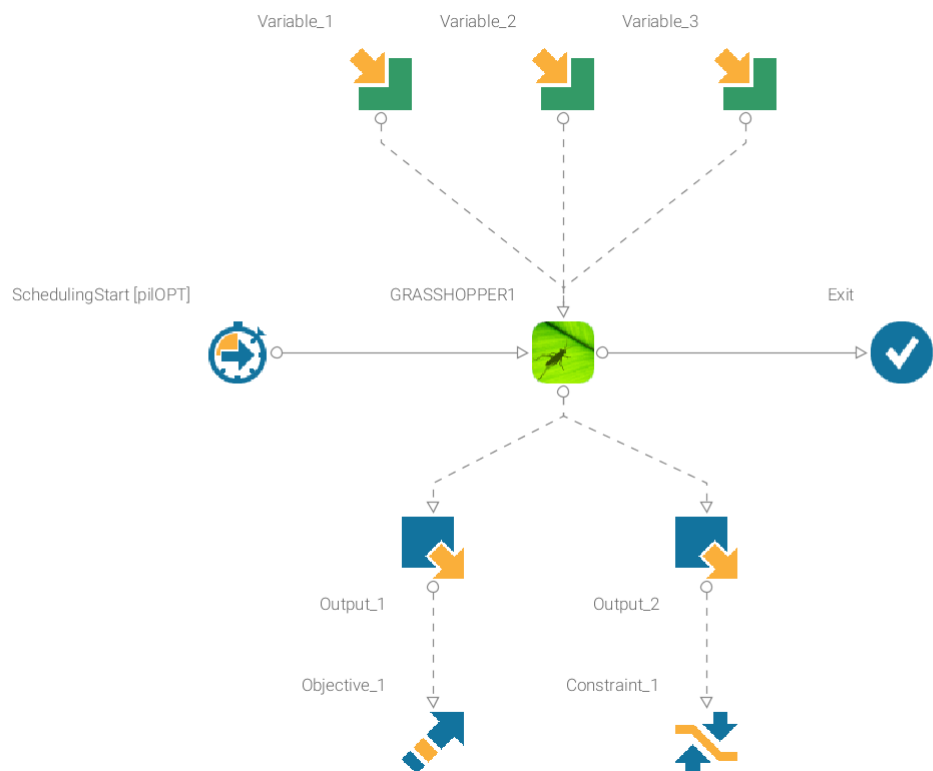


Figure 3.3: Exemplary modeFRONTIER optimisation set-up

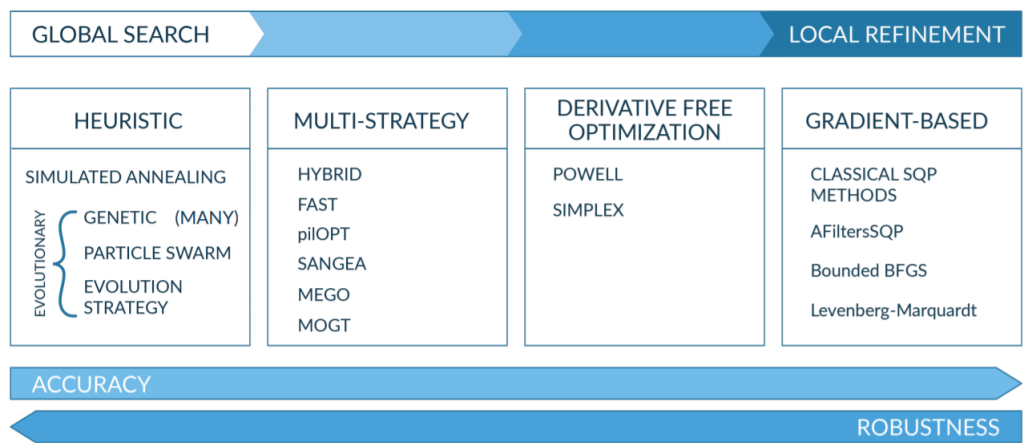


Figure 3.4: Classification of different optimisation algorithms within modeFRONTIER (Esteco, 2018)

## Reference Project

### 4.1. Building information

To create useful results and to be able to make a comparison in the performance of the building, a reference building is selected. This building will also assist in the demarcation of certain boundary conditions such as the plot, floor area and local environment. The building that is selected as a reference building is a student housing complex on the campus of the Erasmus University of Rotterdam, designed by Mecanoo (Figure 4.1). The building consists of 281 studio units, which means each apartment consists of only two zones, a combined living room, bedroom and kitchen and a bathroom. The total gross floor area of the building is 9000 m<sup>2</sup> and the building was completed in 2018 (Mecanoo architecten, 2020).



Figure 4.1: Erasmus Student housing by Mecanoo (Mecanoo)

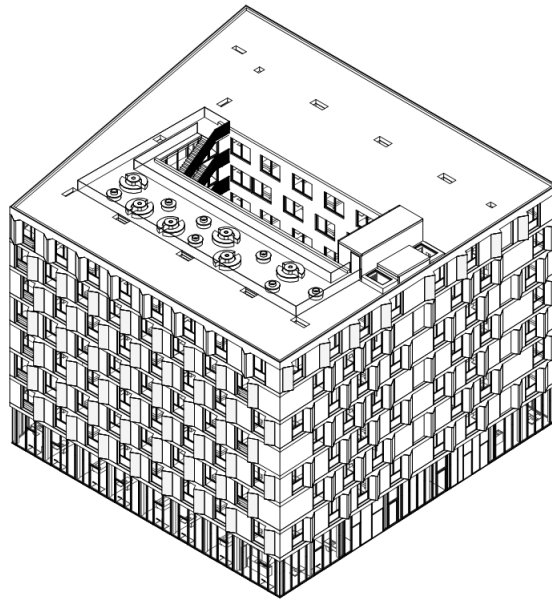


Figure 4.2: Axonometry of Erasmus Student housing (Mecanoo)

#### 4.1.1. Building selection

The Mecanoo Erasmus student housing complex is selected as a reference building for three main reasons. First, the building has a compact shape with a high shape factor  $L_c = 3.94$ . This is close to the maximum shape factor of 5.0, or RC of 1.0. Therefore it is hard to create buildings more compact and most shape variations will cause a less compact shape. This is therefore a good example to see if more compact buildings are possible whilst complying to daylight entrance regulations on the one hand and to explore if less compact buildings can perform better on energy demand. The building has a simple shape, that is a common typology. This makes sure that it serves as a valuable comparison and makes it easier to link performance results to shape alterations. Secondly, the apartments are all studios, which reduces the total amount of zones. This way a realistic model can be created, while keeping computation time low because of the low amount of different zones in the reference building. The compact shape of the reference building can clearly be seen in the axonometric drawing of the building in Figure 4.2.

#### 4.1.2. Layout

The layout of the apartment building is, apart from the ground floor, identical for each floor. All floors are divided into 37 apartments as seen in figure 4.3. The window to wall ratio differs per facade orientation, being similar for north/south and east/west orientations. The north facade has a WWR of 0.22, the south facade of 0.20, the east facade of 0.26 and the west facade has a WWR of 0.27. These numbers are calculated for the entire facade, from the 1st floor up. The ground floor has a WWR of 0.8 for all orientations.

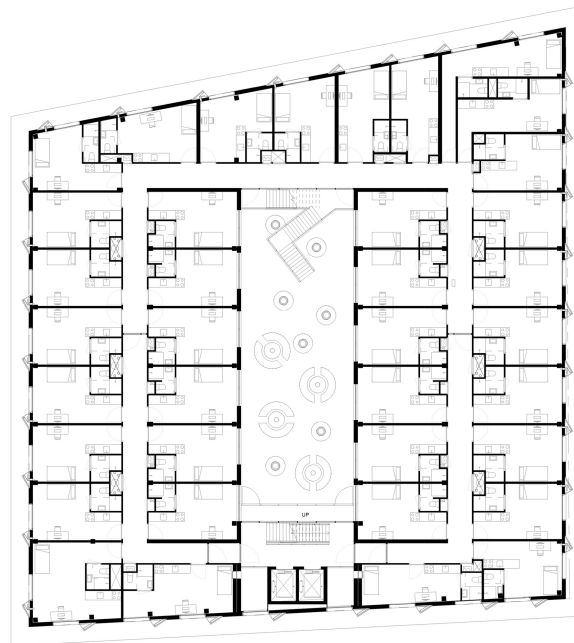


Figure 4.3: Floor plan Erasmus Student Housing 1<sup>st</sup> floor (Mecanoo)

## 4.2. Reference building data

To be able to compare the optimised building shape to the current building, both the daylight entrance and the energy performance of the reference building are assessed. For daylight the daylight factor is calculated, this value is then converted to the visible part of the sky. The energy performance of the reference building is calculated by both the heating and cooling demand.

### 4.2.1. Daylight analysis of the reference building

The daylight entrance in the reference building is assessed for two critical rooms. The studios on the first floor in the north east and south west corner of the patio are selected as most critical. These rooms are selected because they are the lowest studios on the courtyard side of the building, on the ground floor no studios are present towards the patio. For the selected rooms daylight is blocked both by the building itself, opposite to the room on the other side of the courtyard, and close to one side. Apart from the two other inner corner rooms on the first floor, all rooms are more exposed to daylight. Since all other affecting parameters, such as window size and visible transmittance of the glazing are equal for the courtyard rooms, it is assumed the selected rooms will perform worst on daylight entrance assessment. Figure 4.4 shows the courtyard of the reference building, in which the obstruction of daylight into the studios by the building itself is visible. From the daylight entrance assessment for the selected rooms, using a daylight factor calculation in Grasshopper it can be seen that the rooms have an average daylight factor of 0.27% and 0.32% and a daylight factor for 50% of the room of 0.51% to 0.58%, shown in Figure 4.5.

The daylight analysis that is tested here is for a room that does not have the exact same measurements as the real rooms do. This is due to the simplifications made in the design of the building. Where the room dimensions are equally divided over the floor plan.

To test the daylight entrance in these critical rooms another check is made following the current requirements from the Dutch Building Decree. According the Building Decree (3.11), the equivalent daylight surface of a room, calculated according NEN 2057, should be at least 10% of the surface of the space surface area and at least 0.5 m<sup>2</sup>.



Figure 4.4: View on the patio of the Erasmus Student Housing (Xior)

These analyses show an equivalent daylight surface of  $1.29 \text{ m}^2$  for the room in the north east corner of the patio on the first floor and  $1.25 \text{ m}^2$  for the room in the south west corner of the patio on the same floor. Both rooms have a floor surface of  $18.2 \text{ m}^2$ , which means the minimum requirement is a equivalent daylight surface of  $1.82 \text{ m}^2$ . This shows the requirements are not met for both of the two rooms. The full input and results of the NEN 2057 analysis can be seen in Appendix A

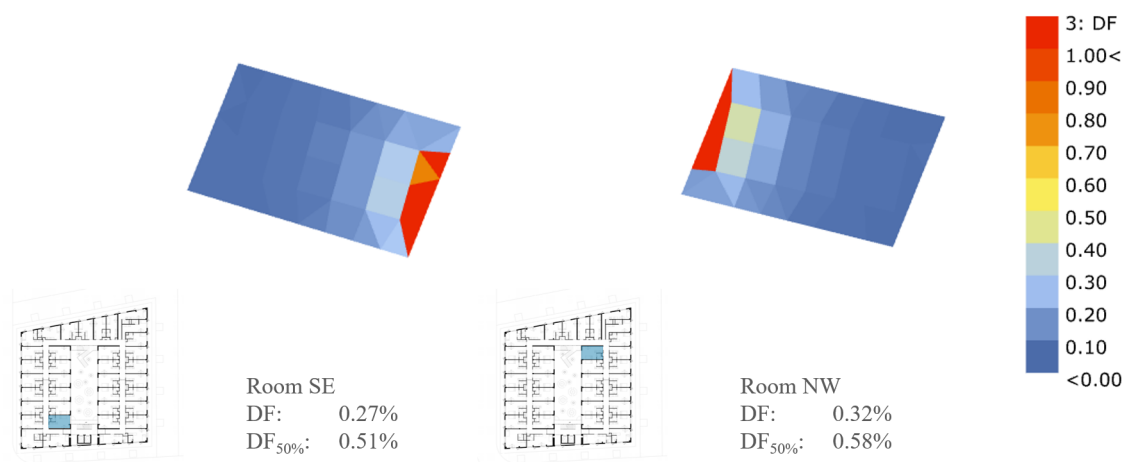


Figure 4.5: Daylight factor calculation for critical rooms

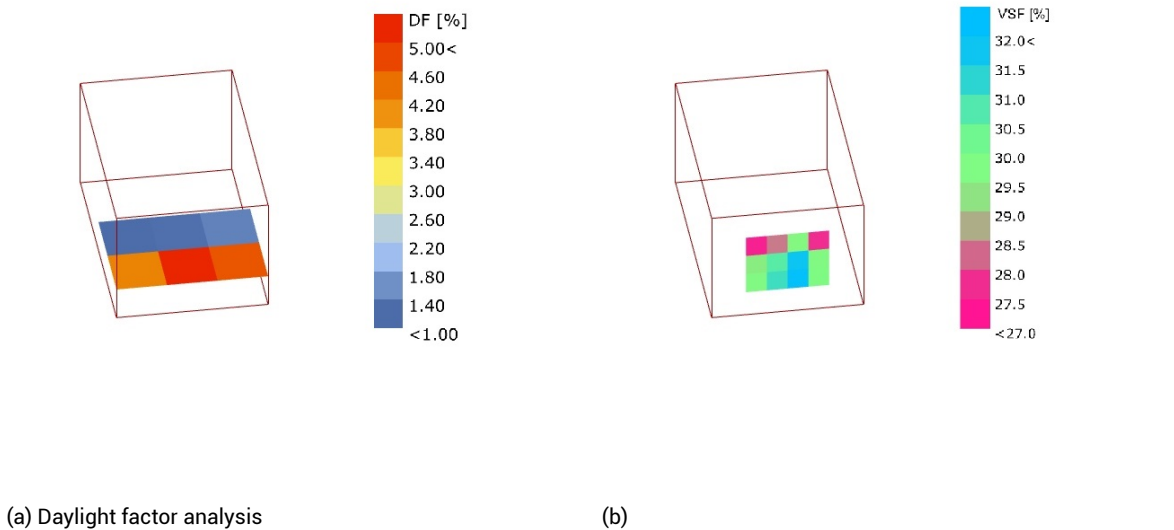


Figure 4.6: Daylight analysis of a representative room by daylight factor analysis (a) and Visible part of the sky analysis (b)

#### Relation daylight factor and visible part of the sky

To be able to use a VSF analysis to assess the DF in the building, an assessment is made comparing these methods for a standard room of the reference building. Such a standard room is based on the dimensions of the most occurring studio size, which is the same room used in the DF analysis of the reference building in Figure 4.5. These rooms measure 5.9x3.8x3.0 m (l<sub>x</sub>w<sub>x</sub>h).

For such a room both the daylight factor for 50% of the space ( $DF_{50\%}$ ) and the visible part of the sky are calculated as shown in Figure 4.6. This is repeated for a evenly distributed set of WWRs and a random variation of obstructions in front of the facade. Afterwards, the results are analysed to determine the relationship between the daylight factor ( $DF_{50\%}$ ) and the visible part of the sky for different WWRs. The relation that is derived from this analysis, with  $r^2 = 0.9898$ , is shown in Equation 5.1. The results of this analysis and the regression line are shown in Figure 5.1 and the input data can be found in Appendix A. In accordance with to Equation 5.1 and the minimum daylight factor requirement of 2.1% for at least 50% of the space, as mentioned in Section 2.4.3, the minimum requirement for  $WWR * VSF = 4.39\%$ .

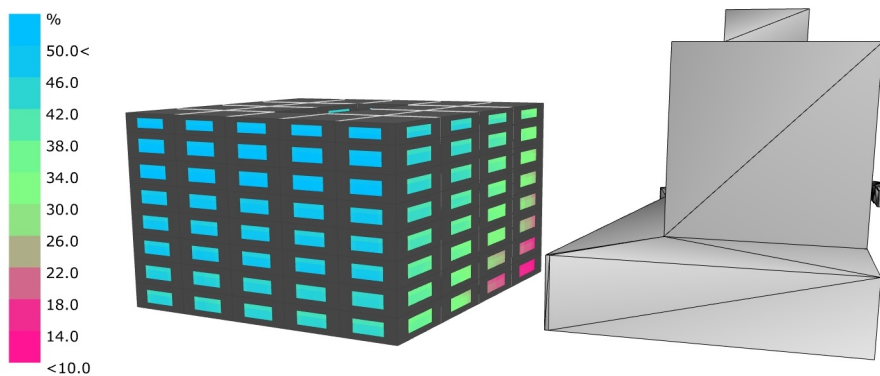


Figure 4.7: Daylight analysis (VSF) for reference building view on south and east facade

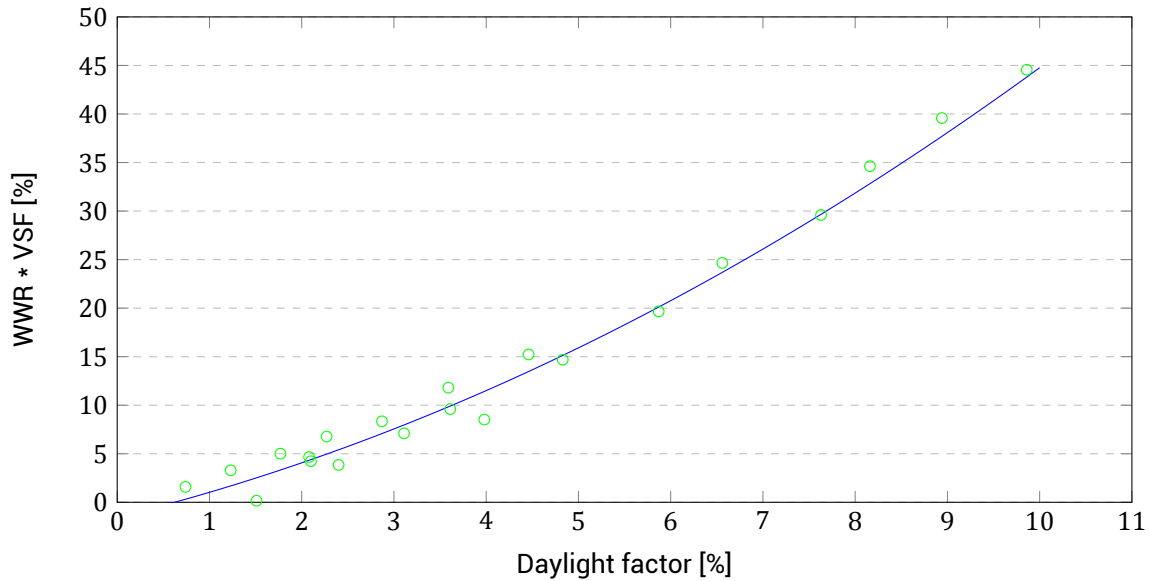


Figure 4.8: Daylight factor ( $DF_{50\%}$ ) [%] versus the window-to-wall ratio times the visible part of the sky (WWR\*VSF) [%]

$$WWR \times VSF = 0.2279 \times DF_{50\%}^2 + 2.3527 \times DF_{50\%} - 0.5524 \quad (4.1)$$

$WWR$	= window-to-wall ratio	[-]
$VSF$	= visible part of the sky	[%]
$DF_{50\%}$	= daylight factor for 50% of the space	[%]

### 4.3. Massing model

To create a 3d massing for the shape creating the floor plans of the reference building are analysed. As can be seen in Figure 4.9, first the floor plan is divided into horizontal and vertical strokes. Both the horizontal and vertical distribution are then approximated by even distributed spaces as shown in Figure 4.10. This results in a distribution as shown in Figure 4.11. The distribution is made in such a way the original floor plan can be approximated and a large variety of shapes can be created. For the energy performance assessment this means two rooms are assessed together as no further internal layout is added.

This 4 x 5 grid is extended throughout the entire height of the building. Each grid cell is connected over four floors and the entire building is then doubled in height, enabling large shape variation and staying within the limits for building height in the area which is 50m in this area of Rotterdam (Zandbelt et al., 2008). This results in an building consisting of four layers each divided into 20 (4x5) building blocks. The complete model, consisting of 80 building blocks, is shaped as seen in Figure ??.





Figure 4.9: Analysis of reference building floor plans



Figure 4.10: Even distribution of reference building floor plans





Figure 4.11: Final distribution of spaces for massing

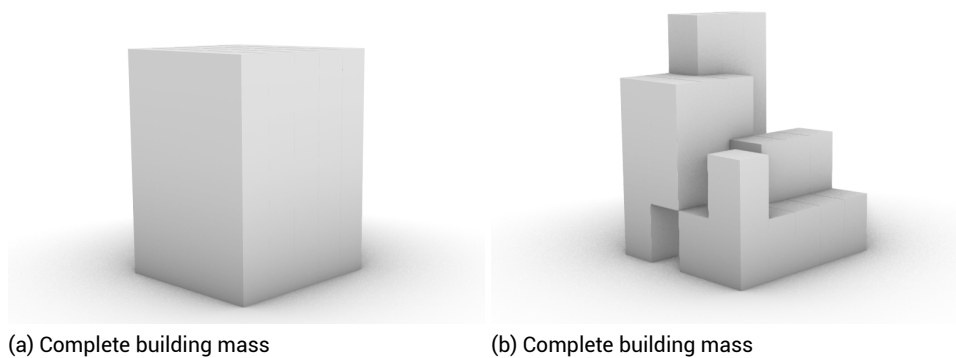


Figure 4.12: Massing based on the reference building, when all masses are selected (a) and when a design is created (b)

## 4.4. Grasshopper model

This section shows the Grasshopper model made for the building design and the performance analyses for energy demand and daylight entrance.

### 4.4.1. Building design

Building designs are created by assigning a 1 or 0 to each of the possible building blocks. This selection is shown in Figure 4.14. Based on the massing this selection created floors are added to the building designs and zones are created as shown in Figure 4.15.

To restrict calculation time, the created building shapes are checked on windowless zones. The model allows for 4 windowless zones, as they could be used for storage, installation rooms etc. This amount of blind zones is based on the area of blind zones in the reference building. If the tested building shape has more than 4 windowless zones, the building shape is discarded and the calculation for that shape is ended (Figure 4.13).

Following up on the zoning, glazing is added to the design, based on the WWR per facade orientation as shown in Figure 4.16. After this, Materials properties are assigned and materials are assigned to the building (see Appendix A, Figures A.1, A.2, A.3, A.4, A.5 and A.6).

Based on the model described above, building parameters are calculated, such as the relative facade area per orientation. This is shown in Appendix A Figure A.7.

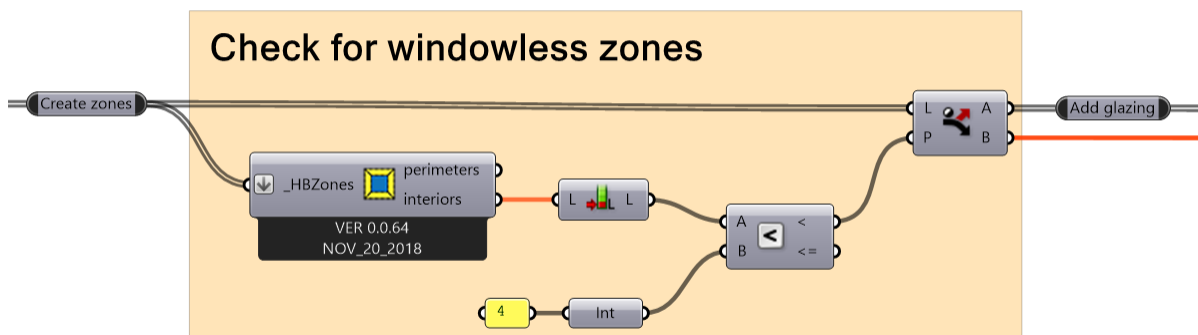


Figure 4.13: Grasshopper model check and dispatch for windowless zones

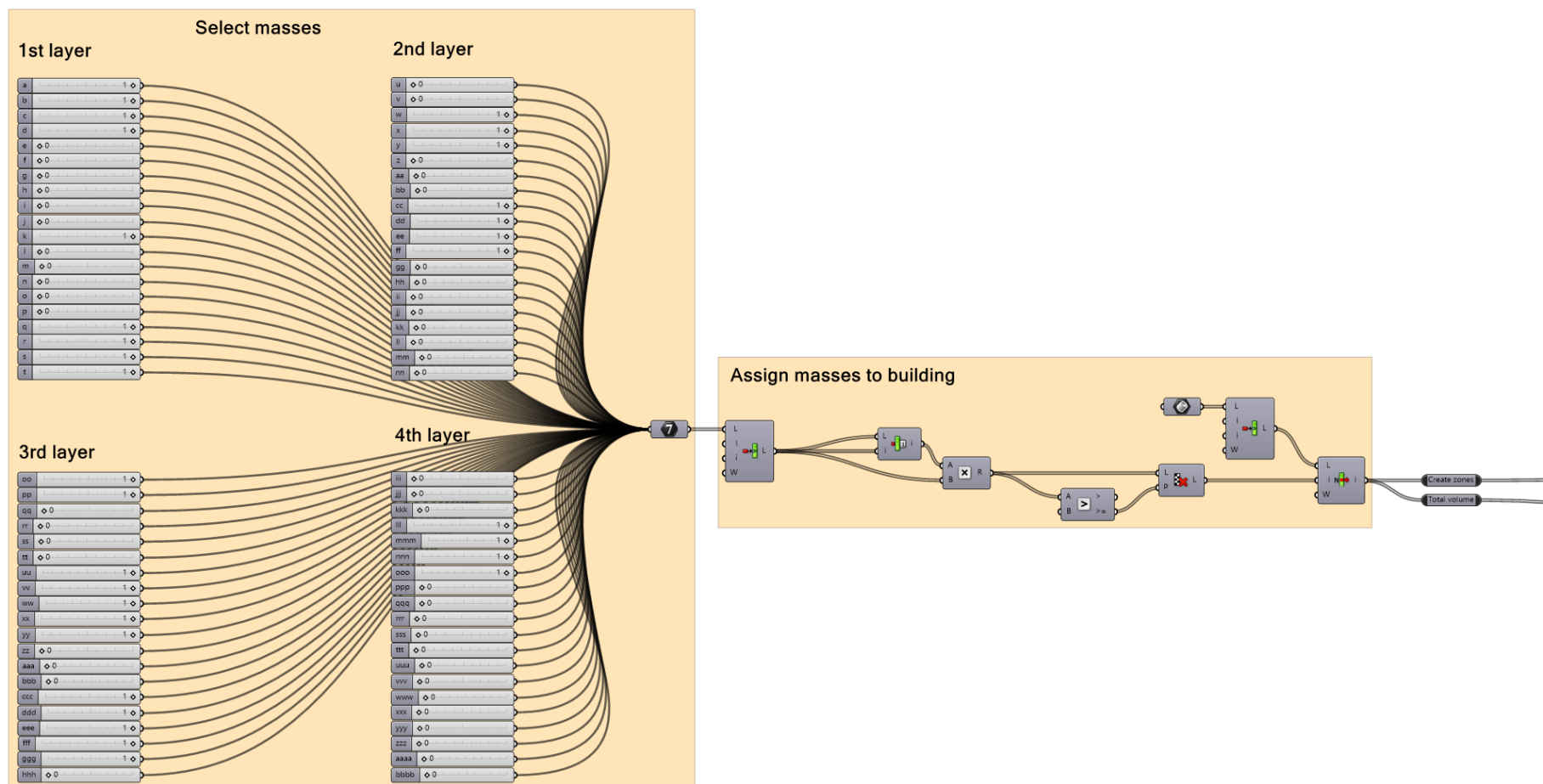


Figure 4.14: Grasshopper model building block selection

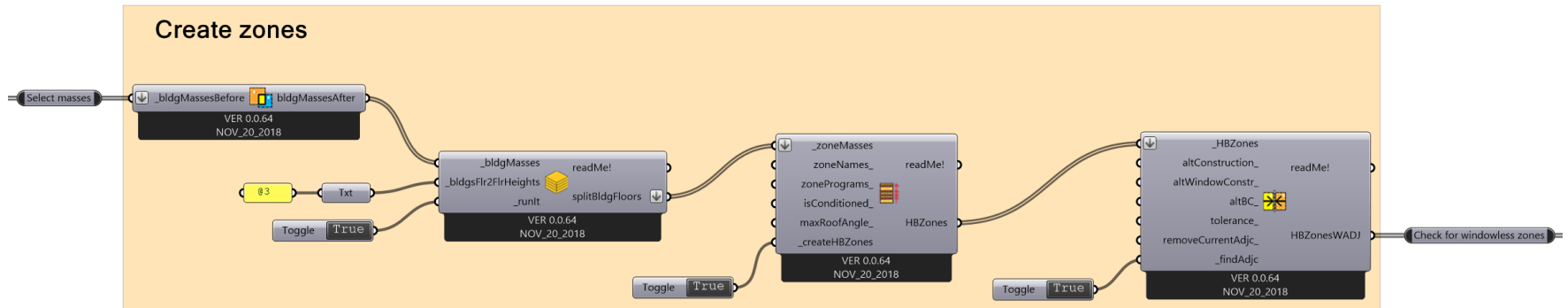


Figure 4.15: Grasshopper model creation of floors and zones

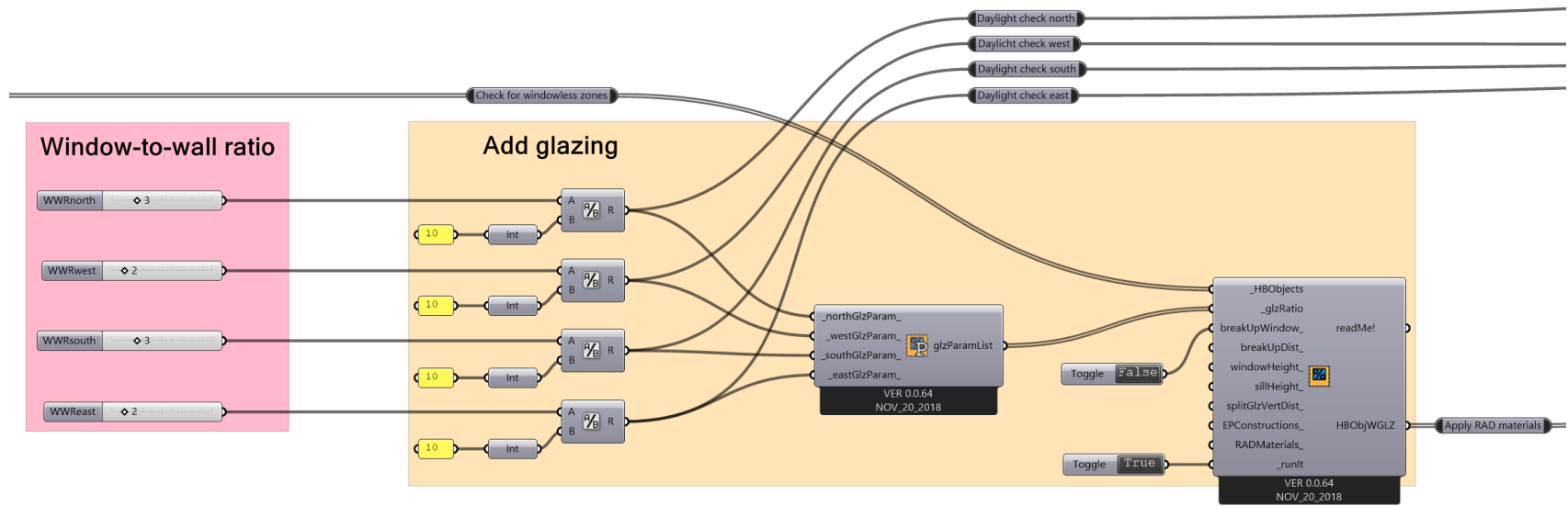
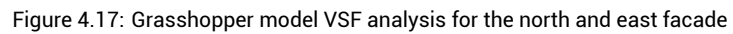


Figure 4.16: Grasshopper model addition of glazing based on WWR per facade orientation

#### 4.4.2. Performance analysis

When the building is created and all materials are assigned, each building is assessed on daylight entrance by a VSF calculation. This calculation is performed for each facade orientation independently. All four orientations should comply with the VSF boundary conditions. If one of the orientations does not comply, the design is discarded. The VSF calculation is shown in Figure 4.17 for the north and east orientation. The VSF calculation for the south and west orientation and the comply check can be seen in Appendix A Figure A.8 and A.9.

If the design complies with the daylight requirements, an energy calculation is made for a winter and summer situation. The energy performance calculation is based on the input of the HVAC details (Figure 4.18), the zone details (Figure 4.19), and the zone thresholds (Figure 4.20). The Energy calculation and the calculation properties are shown in Figure 4.21. Finally the energy demands are normalised and the output data for modeFRONTIER is selected which can be seen in Appendix A Figure A.10.



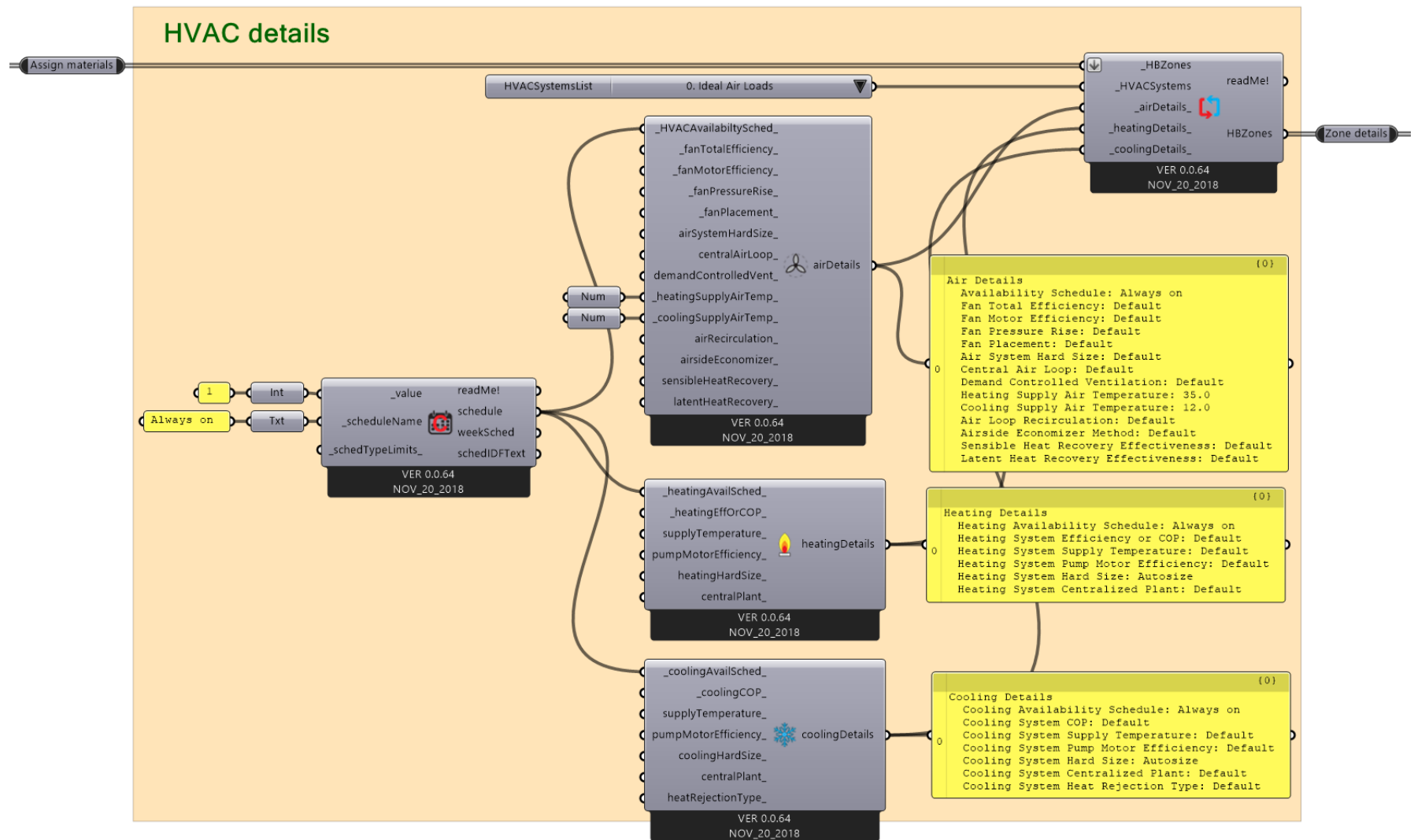


Figure 4.18: Grasshopper model HVAC details

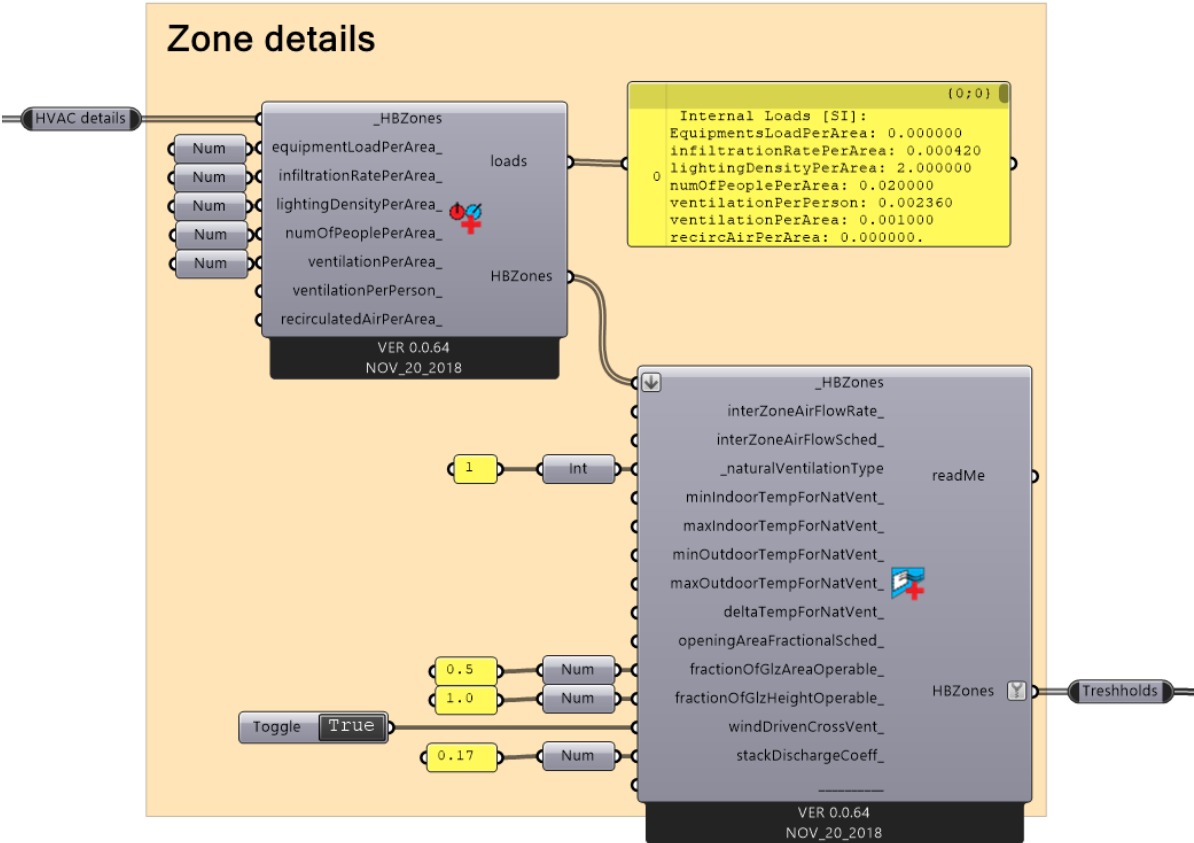


Figure 4.19: Grasshopper model zone details



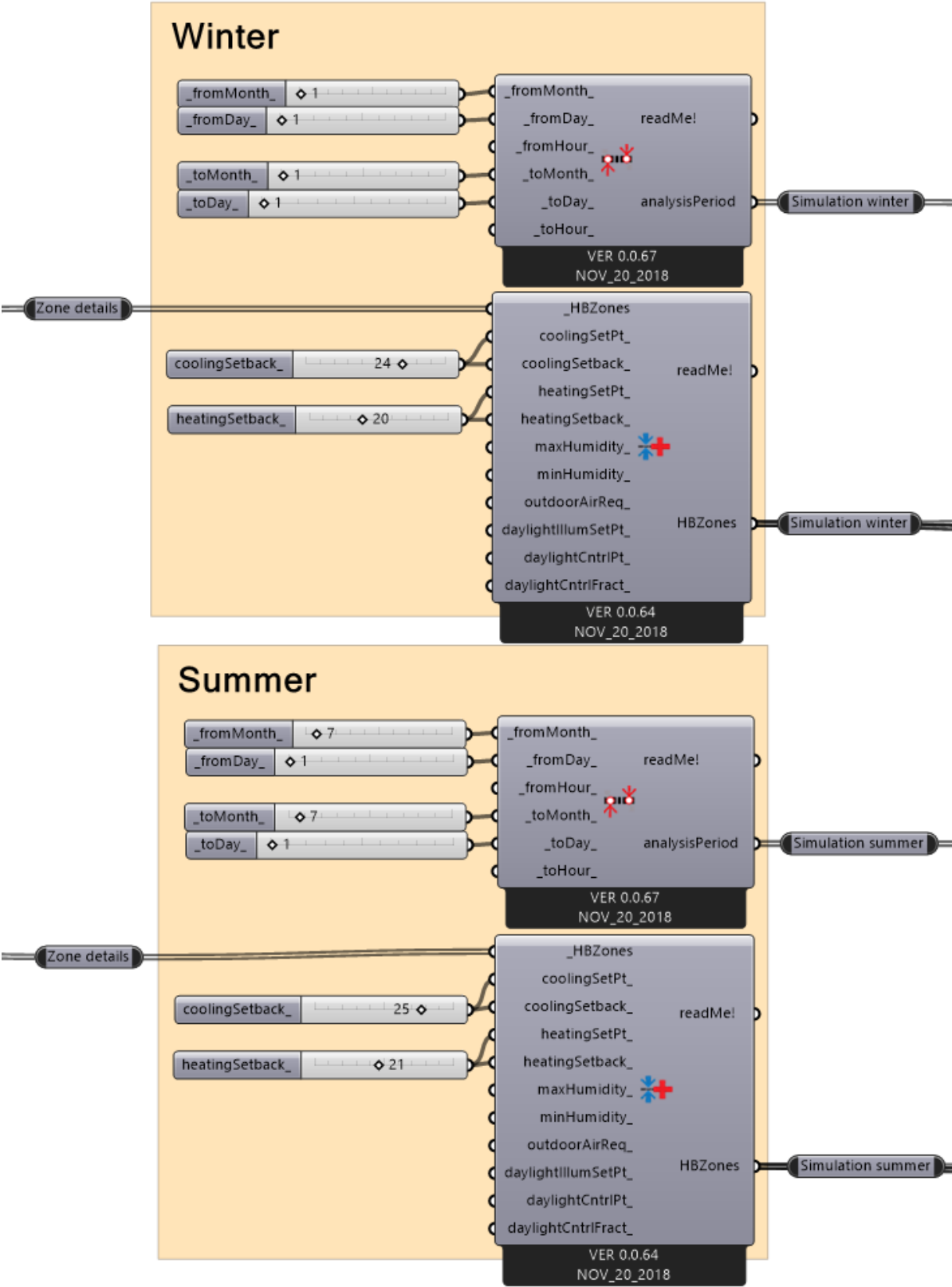


Figure 4.20: Grasshopper model zone thresholds and analysis period selection

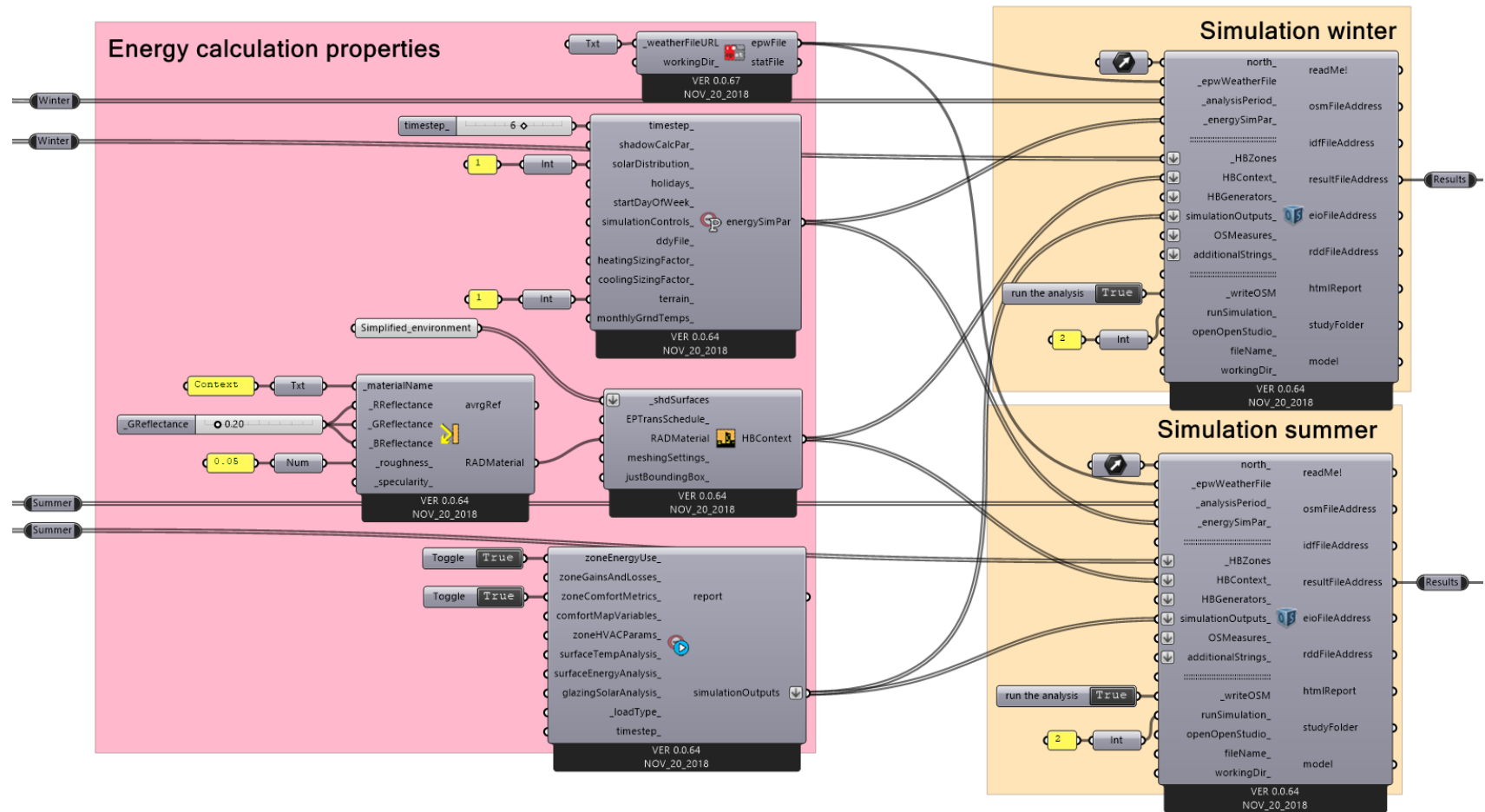


Figure 4.21: Grasshopper model energy calculation properties and summer/winter energy performance calculation

## 4.5. Optimisation model workflow

The grasshopper massing and performance evaluation model described above acts as a design producer and performance calculator in the optimisation workflow. Figure 4.22 shows the optimisation workflow. In the top half of the workflow four rows of input parameters are shown which represent the building block required to create the different building designs. Each variable, a - bbbb, can become either 1 or 0 indicating if a building block is selected for the design or not. Variables a - t, represent the bottom layer of building blocks, u - nn represents the second layer. oo - hhh represents the third layer and iii - bbbb represents the top layer of building blocks.

On the left side of the workflow the WWR input values are shown. For each facade an input value can be given between 1 - 9, resulting in a WWR of 0.1 to 0.9, with steps of 0.1. The floor\_area\_upper and floor\_area\_lower, shown on the mid right of the workflow, are the top and bottom constraint for the  $A_g$  test. At the bottom right of the workflow diagram, output values are shown which are used in the analysis of the different building shapes, such as the relative part of the facade per orientation. On the bottom left the shape factor ( $L_c$ ) is shown, which is one of the key output values for the analysis of the results. Next to the shape factor the output for heating and cooling energy demand in both summer and winter situation are shown. The summation of these energy demands results in the total normalised energy demand. Minimising this value is the objective in this research.

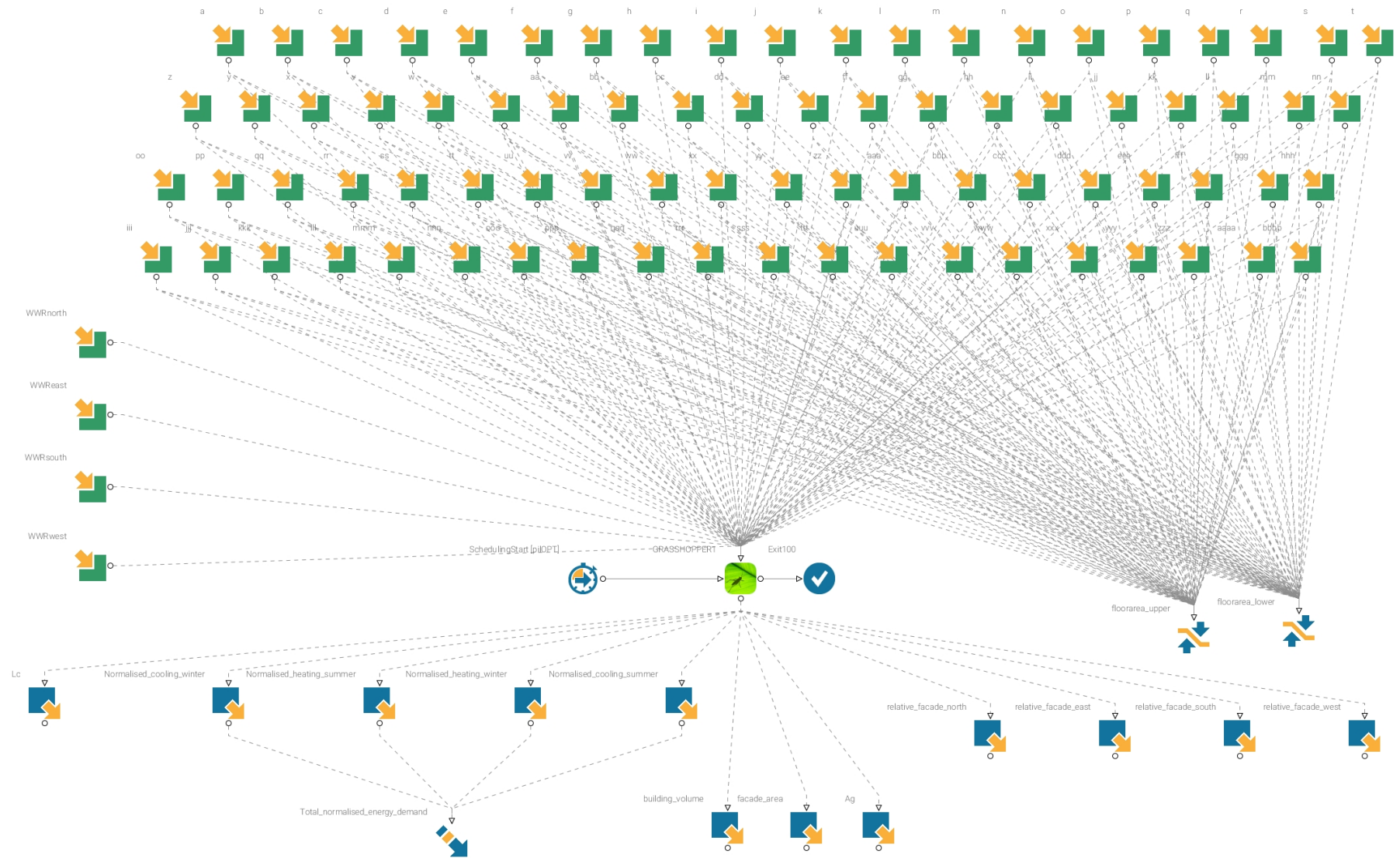


Figure 4.22: modeFRONTIER optimisation workflow, showing all input variables, output variables, objective and constraint

## Results

This chapter treats the outcome of different (sub)analyses which have been conducted to answer the research question. First the results concerning daylight entrance analysis are shown. After that, results regarding the WWR are given and lastly the results regarding building shape are presented.

### 5.1. Daylight analysis

Daylight entrance is assessed for standard reference rooms, based on the a representative room in the reference building, measuring 5.9 x 3.8 x 3.0 m (L x W x H). For these rooms a daylight factor of 2.1% was set as boundary value for 50% of the room, based on recommendations by a working group for implementation of new regulation (half of the room nearest to the window). Full explanation of the chosen room size, calculation method and boundary conditions are described in Section 3.3.2.

An overview of the results is shown in Figure 5.1. Plotting the daylight factor against the WWR\*visible part of the sky and analysing the relation resulted in a correlation with an  $R^2$  of 0.9898, given by Equation 5.1.

This results in both a minimum requirement for the WWR and VSF, dependant on a  $DF_{50\%} = 2.1\%$ , are given in respectively Table 5.1 a and b.

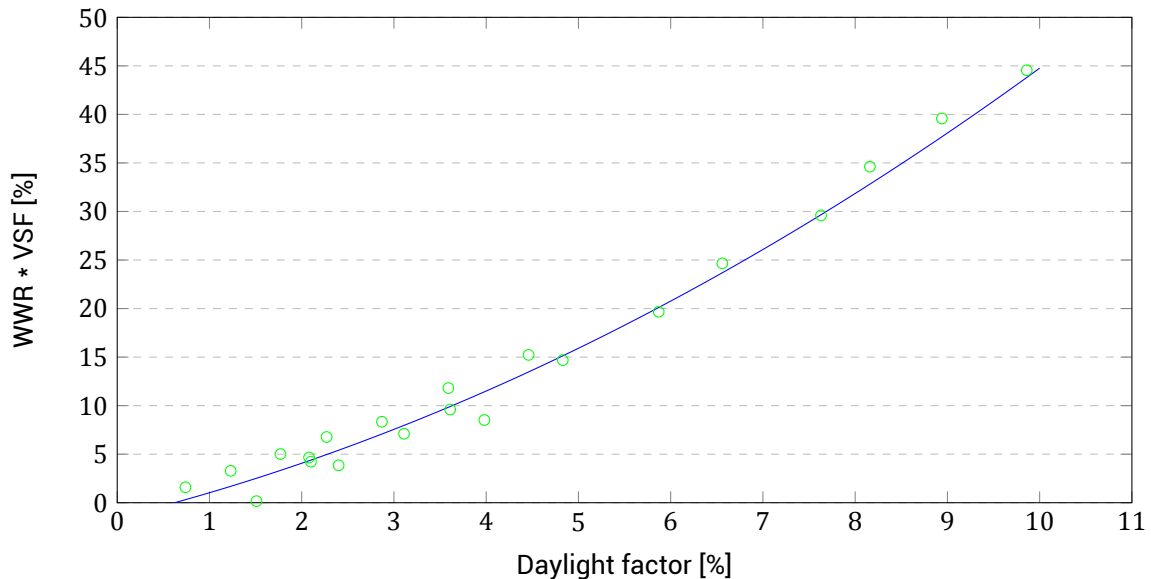


Figure 5.1: Daylight factor ( $DF_{50\%}$ ) [%] versus the window-to-wall ratio times the visible part of the sky (WWR\*VSF) [%]

$$WWR \times sky\% = 0.2279 \times DF_{50\%}^2 + 2.3527 \times DF_{50\%} - 0.5524 \quad (5.1)$$

$WWR$	= window-to-wall ratio	[-]
$sky\%$	= visible percentage of the sky	[%]
$DF_{50\%}$	= daylight factor for 50% of the space	[%]

Table 5.1: Required WWR for a certain VSF (left) and required VSF for en certain WWR (right) to reach a  $DF_{50\%}$  of 2.1 %

(a)		(b)	
$SVF[\%]$	$WWR[-]$	$WWR[-]$	$SVF[\%]$
5.0	0.88	0.10	43.93
10	0.43	0.20	21.97
15	0.29	0.30	14.64
20	0.22	0.40	10.98
25	0.18	0.50	8.79
30	0.15	0.60	7.32
35	0.13	0.70	6.28
40	0.11	0.80	5.49
45	0.10	0.90	4.88
50	0.09	0.95	4.62

## 5.2. Optimisation study

The optimisation study is performed in two parts. The first part uses the summer situation based on the first week of July of the representative year, assessing 2129 design variations. The second part used the warmest week of the representative year, the second week of August, for the summer energy demand calculation. The second part analysed 1257 design variations. In the rest of this chapter, both optimisations will be referred to as optimisation July and optimisation August for the first and the second optimisations respectively.

A requirement which is incorporated into the modeFRONTIER model is the gross floor area check. Based on the number of building blocks that is selected, modeFRONTIER will assess if  $A_g$  deviates maximum 10% of that of the reference building as discussed in Chapter 4. All designs within this range are assessed in Grasshopper, all other designs are discarded as error designs. In Figures 5.2 and 5.3 a random number of building designs is shown. These are all designs which passed the  $A_g$ -test and are therefore considered in the performance analysis. This Figure gives an overview of the variety in shapes the model provides.

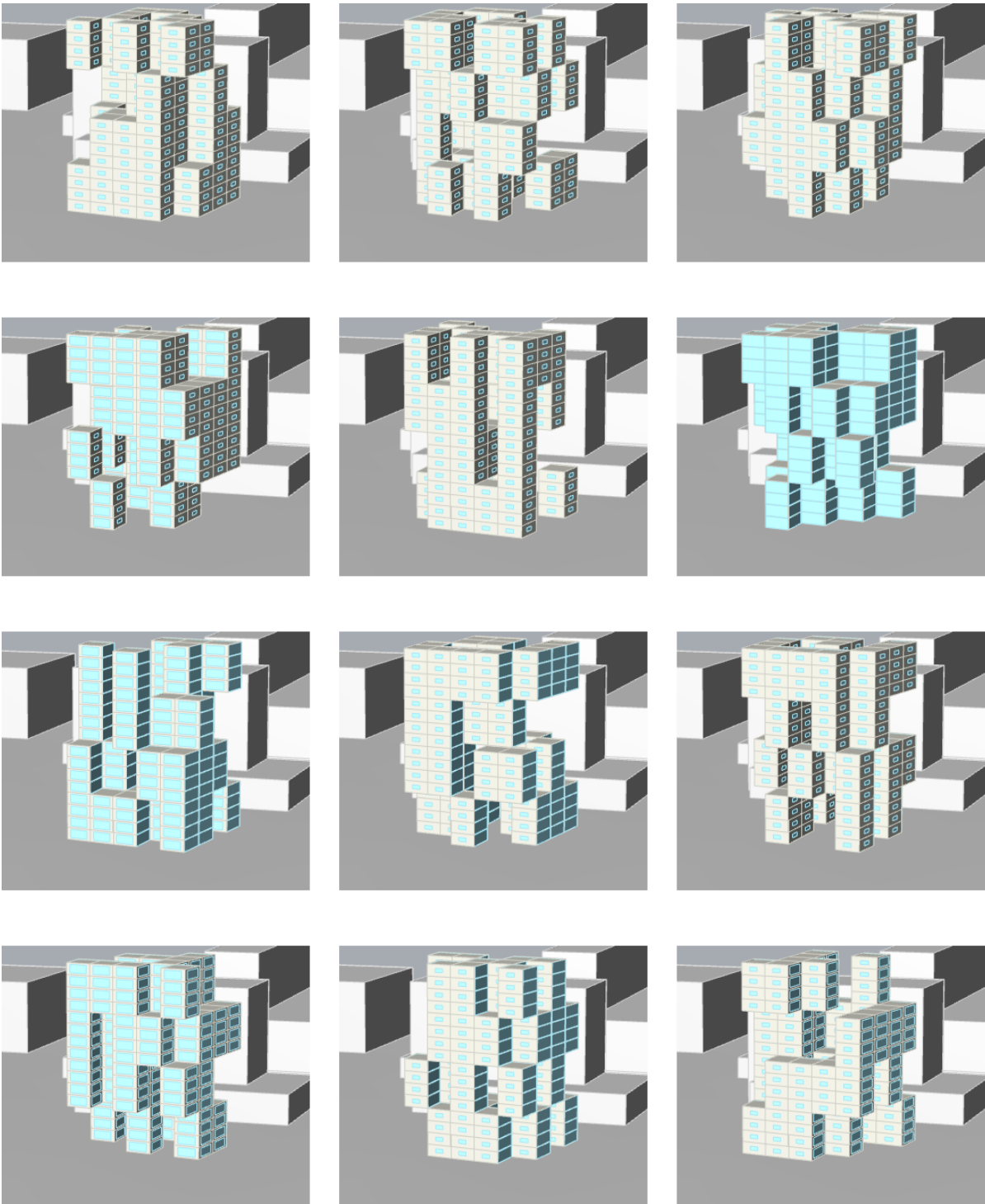


Figure 5.2: Overview of randomly selected building designs generated by the pilOPT algorithm (part I)

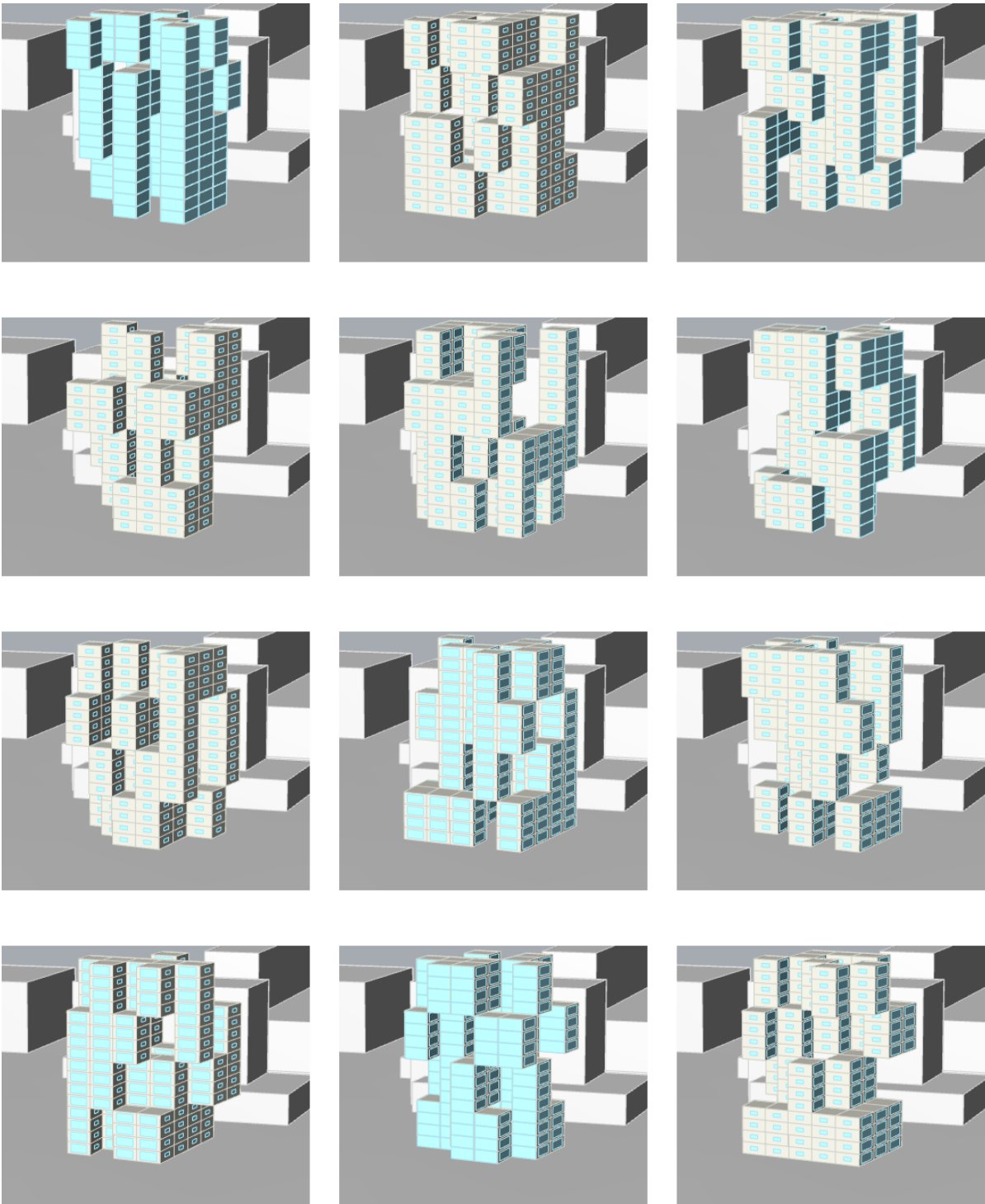


Figure 5.3: Overview of randomly selected building designs generated by the pilOPT algorithm (part II)



### 5.2.1. Effect of window-to-wall ratio

Before the start of the optimisation the effect of WWR on the energy demand has been analysed. The WWR is varied per facade for the reference building. This analysis is made for both the heating season and cooling season.

From this analysis, correlations are derived. All correlations shown in this Chapter are Pearson correlations. A Pearson correlation measures to what extent two variables have a linear dependence, ranging from -1 to +1. Correlations in the range of  $\pm 0.6$  to 1.0 can be regarded as having a high correlation,  $\pm 0.3$  to 0.6 shows a moderate correlation and  $\pm 0.1$  to 0.3 shows a low to no correlation (Esteco, 2019). The Pearson correlation is calculated according to Equation 5.2.

$$\rho_{X,Y} = \frac{cov(X,Y)}{\sigma_X \sigma_Y} = \frac{E[(X - \mu_X)(Y - \mu_Y)]}{\sigma_X \sigma_Y} \quad (5.2)$$

$\rho_{X,Y}$	= correlation between parameter X and Y	[-]
$\sigma_i$	= standard deviation of i	[-]
$\mu_i$	= mean value of i	[-]
$E$	= expected value	[-]

From this analysis of the building used in the validation process (Figure 3.2a), where only the WWR was changed and no natural ventilation was applied, the correlations between the WWR and the energy demand for heating and cooling are presented in Table 5.2. For the cooling season, it can be seen that there is correlation of 0.577, 0.534 and 0.606 between the energy demand and the WWR for east, south and west orientation respectively. For the north orientation there is a correlation of 0.192 between the energy demand and the WWR. In the heating season, there is correlation between the energy demand and the WWR of 0.613, 0.517 and 0.571 for the north, east and west orientation respectively and a correlation of 0.311 for the south orientation.

In the optimisations, both the WWR and the shape of the building are changed and in this assessment natural ventilation is considered as shown in Section ???. From the first and the second optimisation the correlation between the WWR and the energy demand is presented in Table 5.3. Since no cooling energy was used by the buildings in either optimisation process this table shows the correlation between the WWR and the heating energy demand.

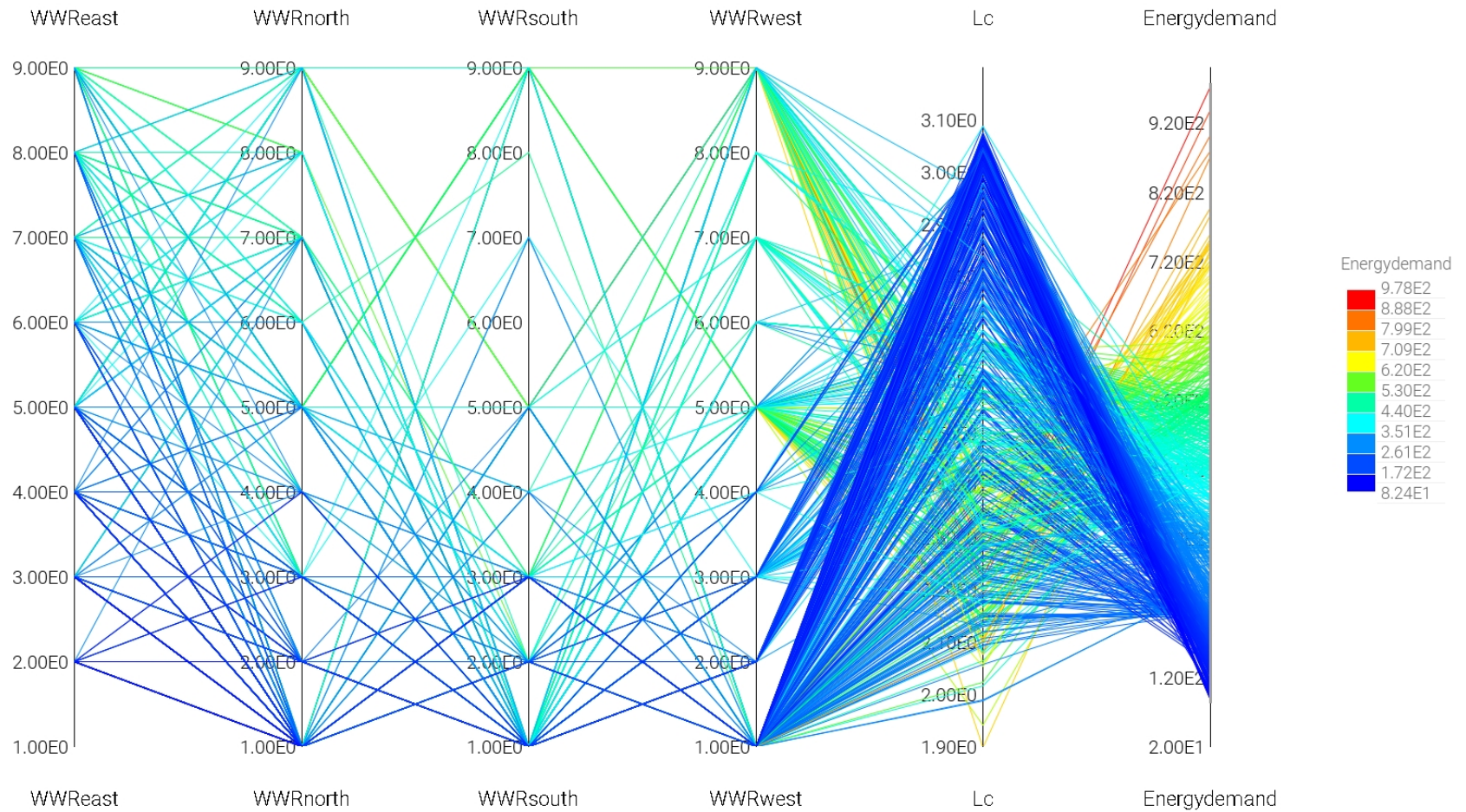
The spread of WWR per facade, related to the shape factor and the normalised energy demand is shown in Figure 5.4 for optimisation July and in Figure 5.5 for optimisation August.

Table 5.2: Correlation matrix between the WWR [-] per orientation and the normalised energy demand for heating and cooling [kWh]

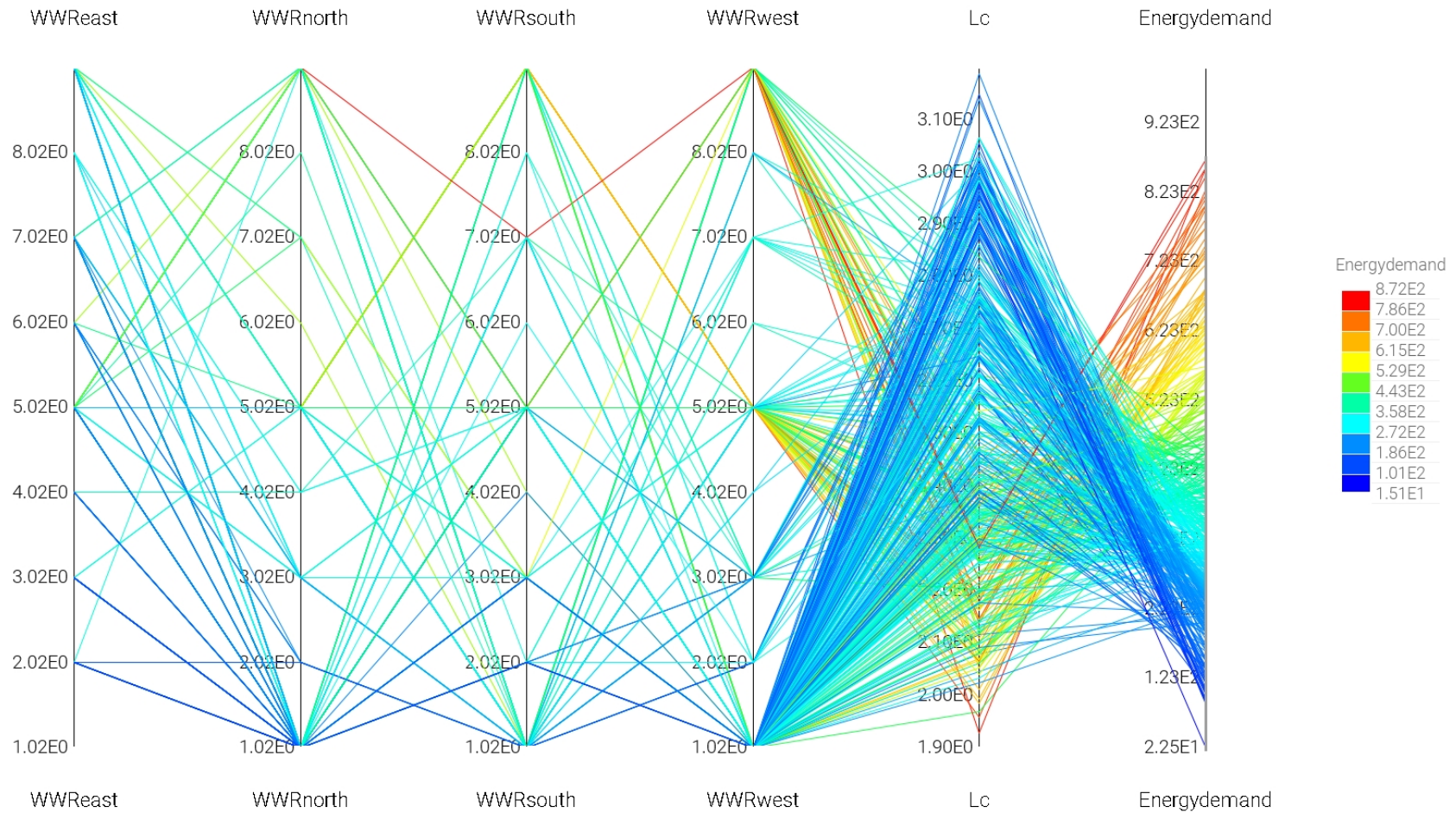
Orientation	Summer		Winter	
	Cooling	Heating	Cooling	Heating
North	+0.192	-	-	+0.613
East	+0.577	-	-	+0.517
South	+0.534	-	-	+0.311
West	+0.606	-	-	+0.571

Table 5.3: Correlation matrix between the WWR [-] per orientation and the normalised energy demand for heating and cooling [kWh]

<b>Orientation WWR</b>	<b>Correlation optimisation July</b>	<b>Correlation optimisation August</b>
North	+0.721	+0.655
East	+0.679	+0.267
South	+0.585	+0.621
West	+0.725	+0.630

Parallel Coordinates - WWR east, WWR north, WWR south, WWR west  $L_c$  and Energy demand, optimisation 1Figure 5.4: WWR [-] for each facade orientation in relation to the shape factor ( $L_c$ ) [m] and the total normalised energy demand [kWh/m<sup>2</sup>] for the first optimisation, coloured based on the energy demand

Parallel Coordinates - WWR east, WWR north, WWR south, WWR west, Lc and Energy demand, optimisation 2

Figure 5.5: WWR [-] for each facade orientation in relation to the shape factor ( $L_c$ ) [m] and the total normalised energy demand [ $\text{kWh}/\text{m}^2$ ] for the second optimisation, coloured based on the energy demand

### 5.2.2. Effect of shape

Here the results from the shape optimisation are presented. Figure 5.6 and 5.7 show an overview of all non error analysed designs. This means all designs which fulfil the daylight requirement and have limited windowless zones as is described in Chapter 4.

From the optimisation it can be seen that most feasible designs for both optimisations, having a  $L_c$  higher than 2.8, have a total normalised energy demand below 300 kWh/m<sup>2</sup>.

From these designs, the correlation between the shape factor and the energy demand is calculated. There is a correlation between the shape factor and the energy demand of -0.624 derived from optimisation July and a correlation of -0.632 derived from optimisation August.

Apart from the shape factor, the relative part of the facade is evaluated per orientation. These relative facade areas are presented in Figure 5.8 for optimisation July (1st) and in Figure 5.9 for optimisation August (2nd).

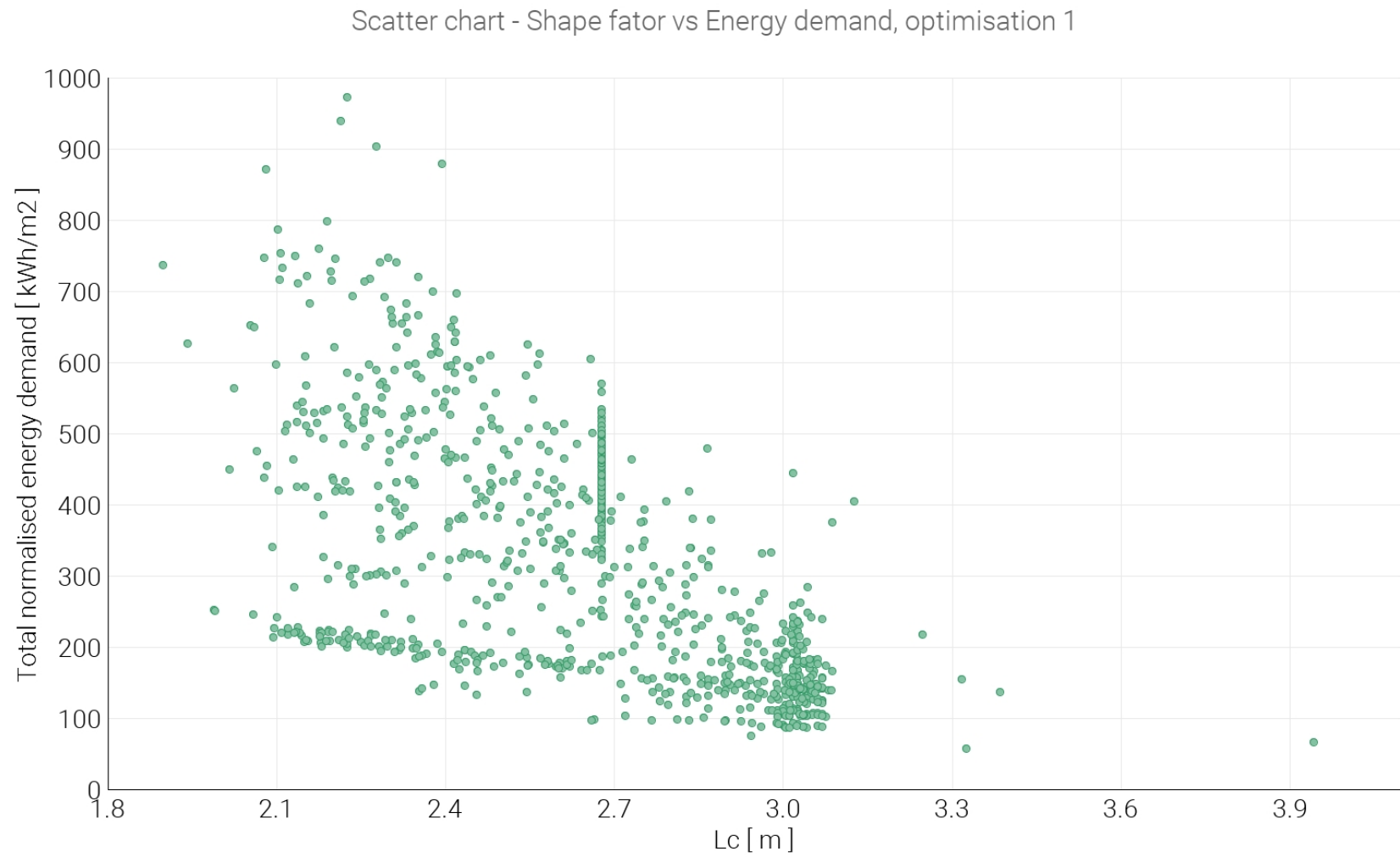


Figure 5.6: Overview of all building designs of the first optimisation, showing the relation between the shape factor ( $L_c$ ) and the normalised energy demand for heating and cooling



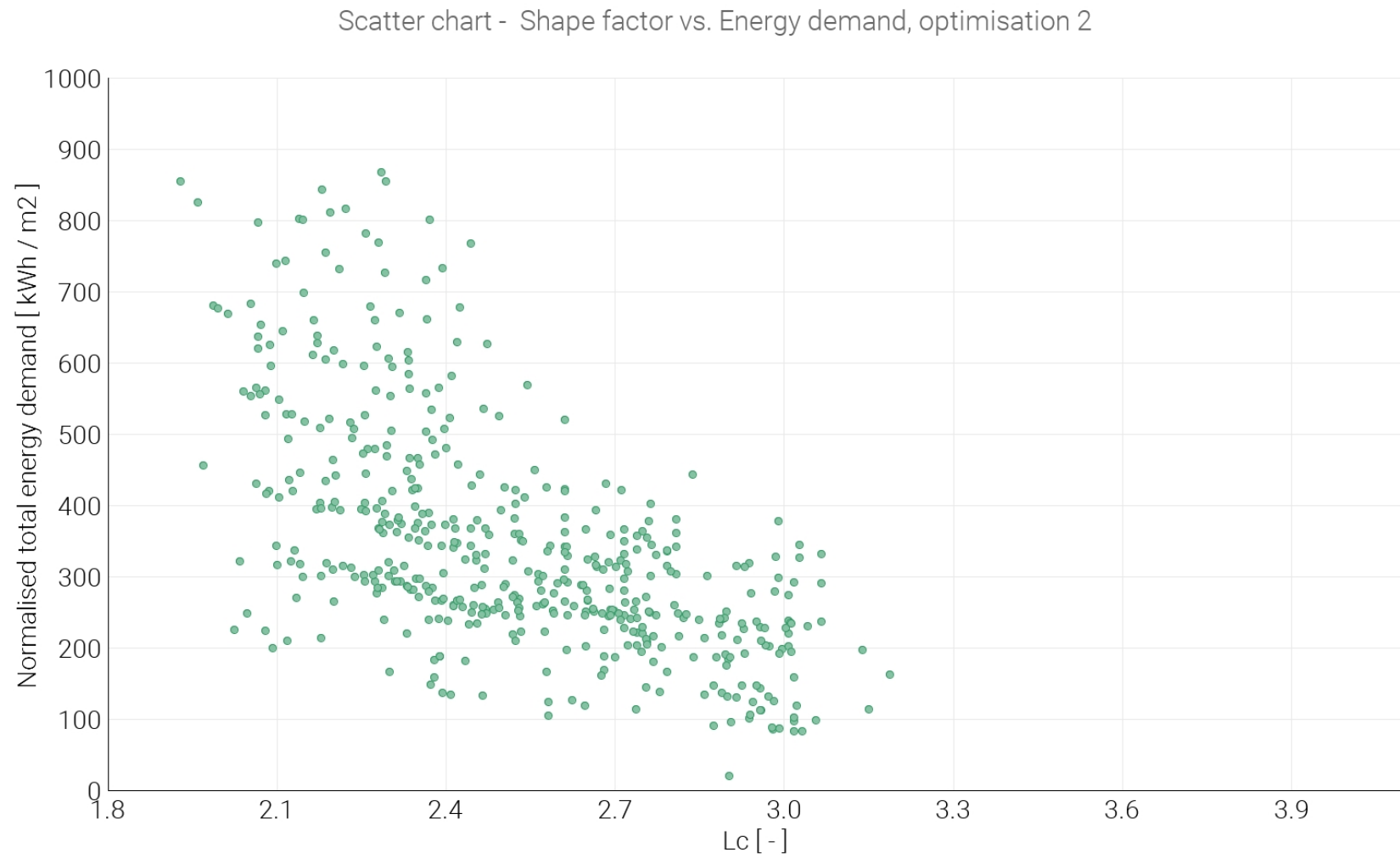


Figure 5.7: Overview of all building designs of the second optimisation, showing the relation between the shape factor ( $L_c$ ) and the normalised energy demand for heating and cooling

Parallel Coordinates -  $L_c$ , Relative facade east, Relative facade north, Relative facade south, Relative facade west and Energy demand, optimisation 1

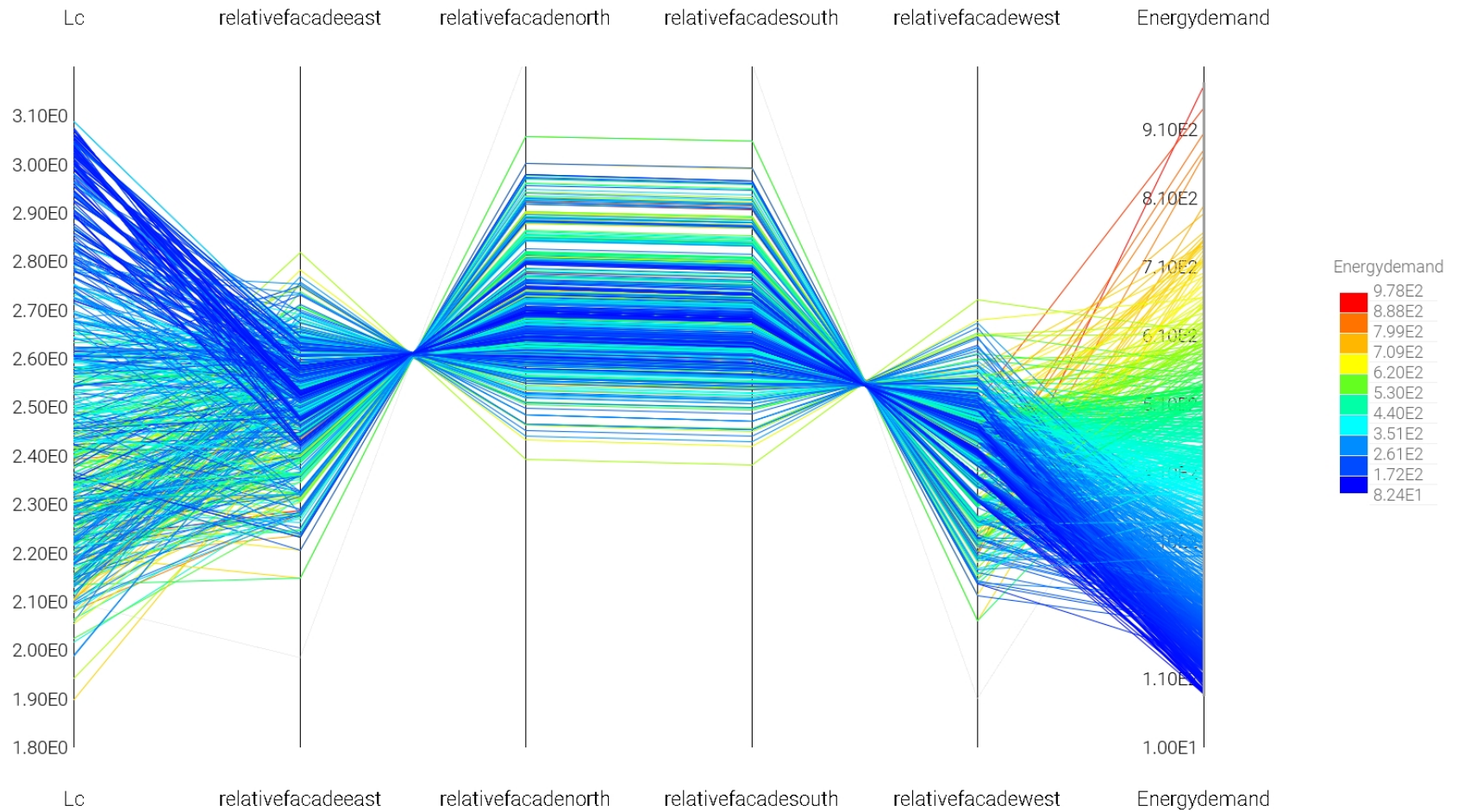


Figure 5.8: Showing the relative part of the total facade for each orientation [-] in relation to the shape factor ( $L_c$ ) [m] and total normalised energy demand [ $\text{kWh/m}^2$ ] for the first optimisation, coloured based on energy demand



Parallel Coordinates -  $L_c$ , Relative facade east, Relative facade north, Relative facade south, Relative facade west and Energy demand, optimisation 2

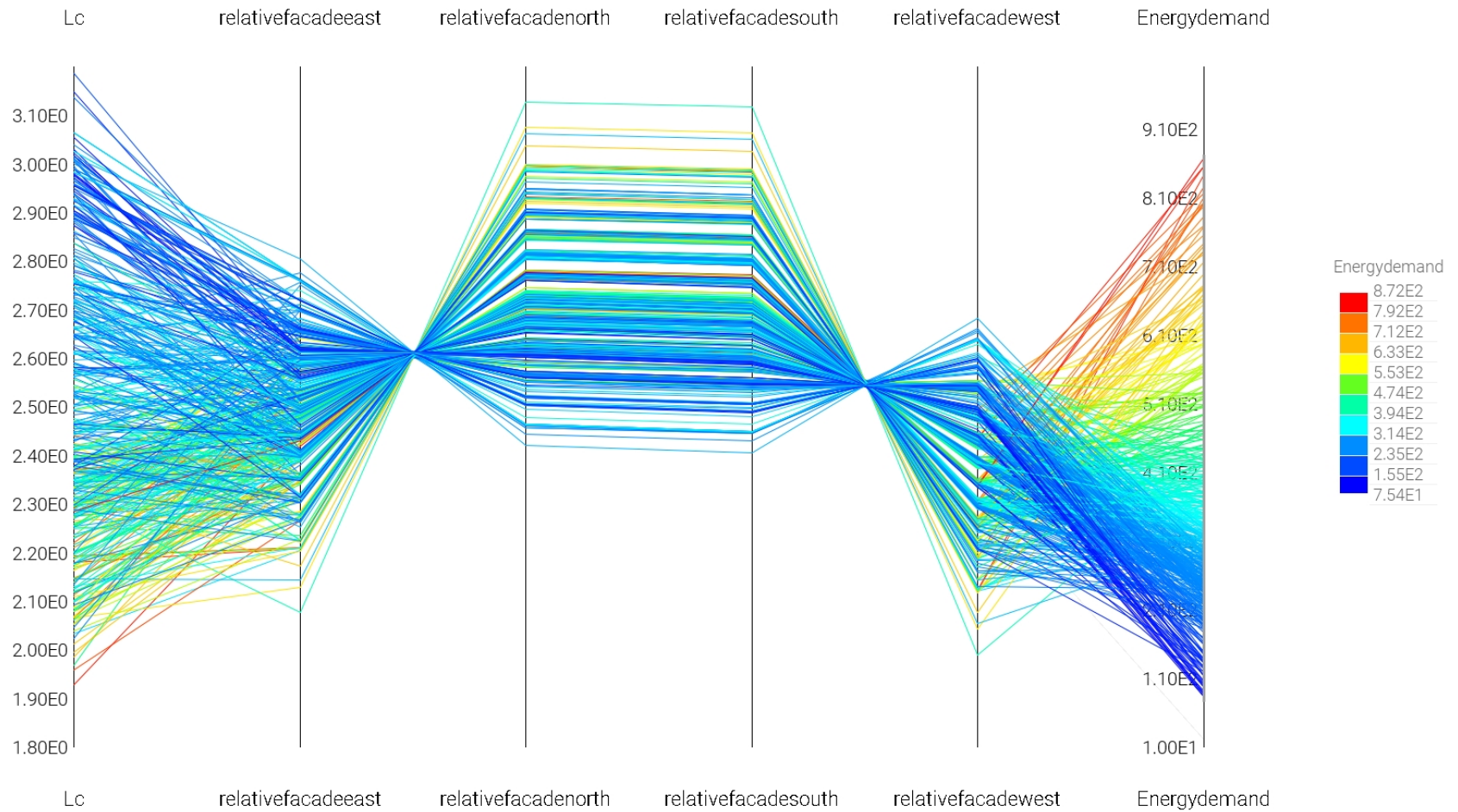
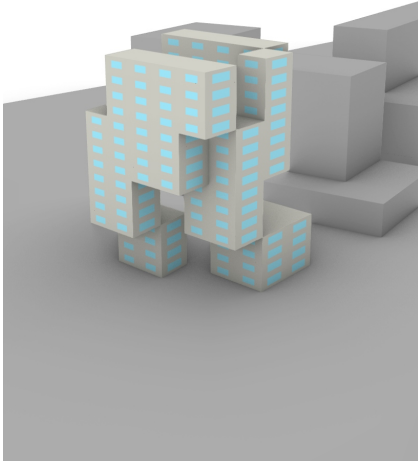


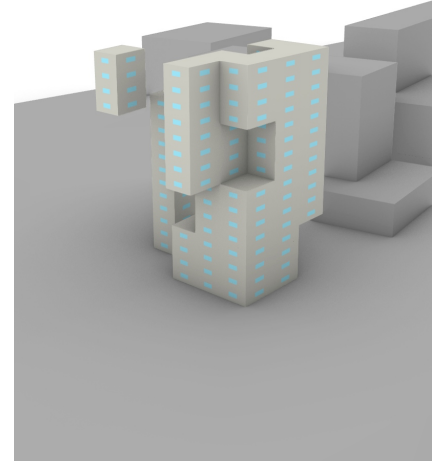
Figure 5.9: Showing the relative part of the total facade for each orientation [-] in relation to the shape factor ( $L_c$ ) [m] and total normalised energy demand [ $\text{kWh}/\text{m}^2$ ] for the second optimisation, coloured based on energy demand

### 5.2.3. Visualisation

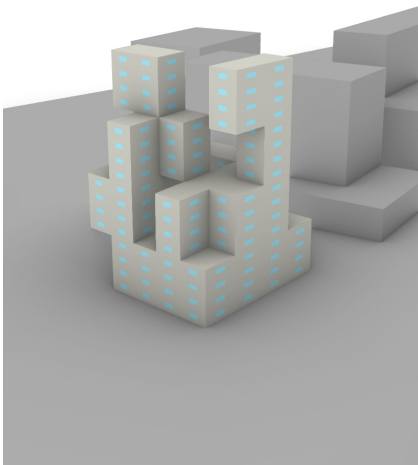
To give an idea of what the shape factors mean for the building shape, what possible directions of optimal building shapes could be according the optimisation, four buildings designs are presented in Figure 5.10. These designs are marked in Figure 5.11



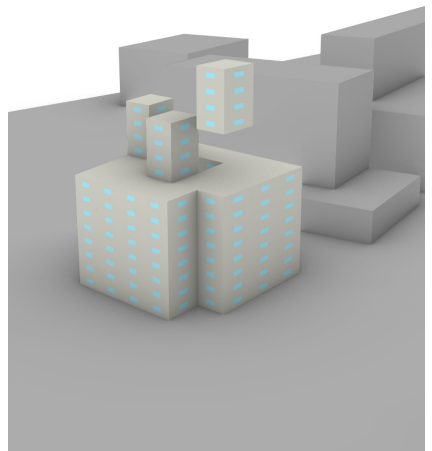
(a) Design 693



(b) Design 1382



(c) Design 1883



(d) Design 1900

Figure 5.10: Visualisation of building designs 693 (a), 1382 (b), 1883 (c) and 1900 (d)

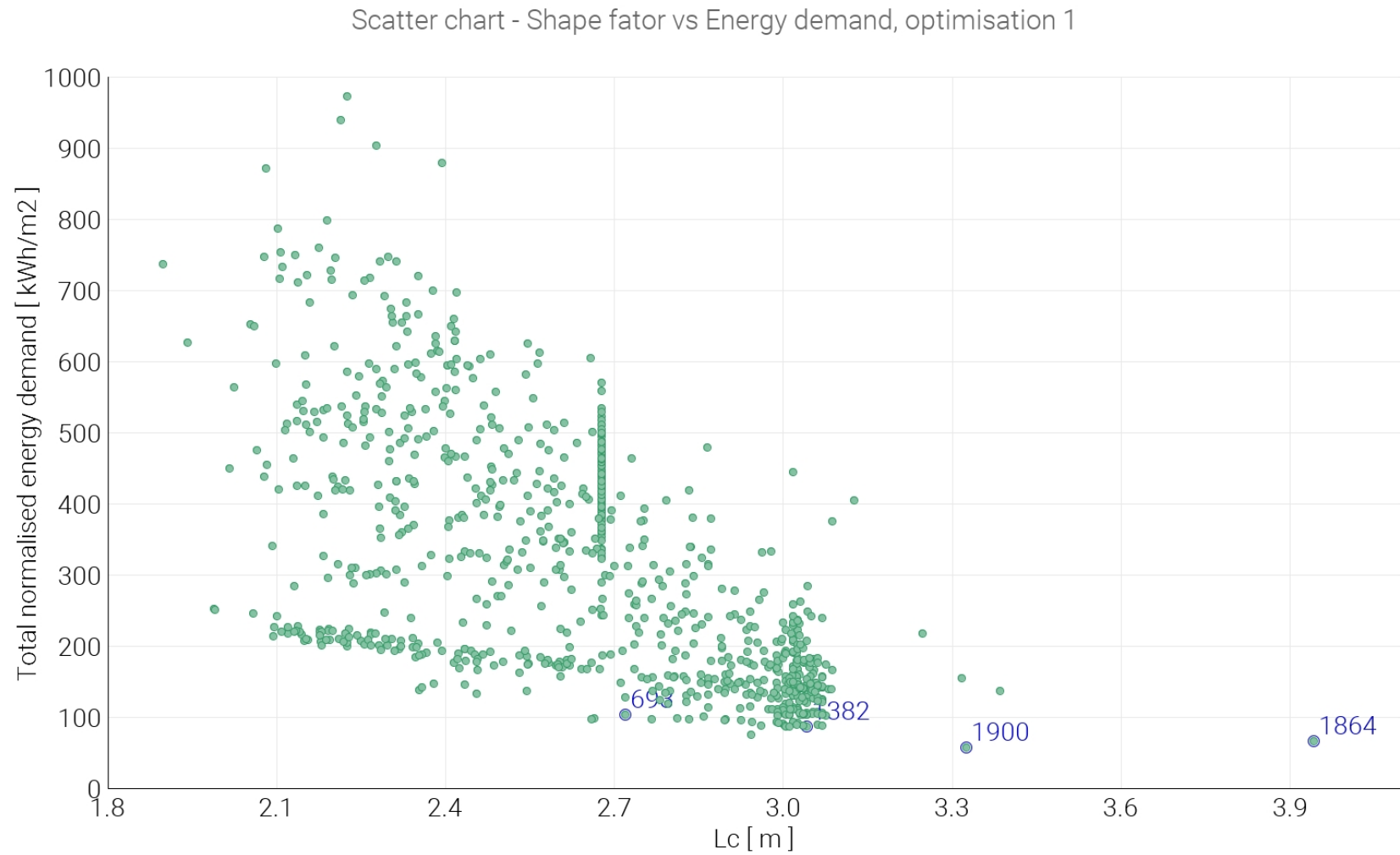


Figure 5.11: Overview of all building designs of the first optimisation, showing the relation between the shape factor ( $L_c$ ) and the normalised energy demand for heating and cooling including marked designs

# 6

## Discussion

This chapter will discuss the analysis of the results presented in Chapter 5. Here, a reflection is presented what the results mean, how they can be interpreted and to what extent they can be related to the reference project or seen more in general. First the results from the literature study are discussed. After that the daylight analysis results are discussed and lastly the results of the optimisation study are described.

### 6.1. Effect of WWR before optimisation

As shown in Table 5.2, the scatter chart for optimisation 1, and 5.3, the scatter chart for optimisation 2, WWR has a different effect on the energy use depending on the orientation. Results presented in Table 5.2, show that in summer there is a large positive correlation between the east, south and west orientated WWR and the energy demand for cooling. In winter there is a larger positive correlation between the WWR on the north, east and west orientation with the energy demand for heating. From these correlations it can be seen that adjusting the WWR for both east and west orientation will not have a great effect because it will either increase or decrease the energy demand in both summer and winter. This makes sense since the angle of attack on windows facing east and west is more constant over the year.

Therefore, aiming for a low WWR on both the south and north facade would help lowering the energy demands for heating and cooling. WWR on both east and west facade can be relatively larger than on the north/south orientation, because they will have a smaller effect on the energy demand.

Results shown in Table 5.3 show a more uniform correlation between the different orientations. Here the orientation shows a less strong correlation between the WWR and the energy demand is east. It seems like the optimisation model here has stuck to the a WWR of 0.6. Because of this, most feasible designs have a WWR of 0.6, the small variation in WWR then causes a low correlation. Because of the adjacent buildings on this side, a WWR of 0.1 is not feasible. This most likely is the reason the the optimisation model had trouble finding a correct WWR and when it did it held on to it for a large number of building designs.

The absence of cooling in the optimisation studies can possibly be explained by the addition of natural ventilation, which was turned off when only the WWR was assessed, as discussed in Section 5.2.1. In both optimisations natural ventilation was turned on, which could have increased the cooling capacity by (night time) ventilation and therefore make additional cooling redundant.

### 6.2. Daylight analysis

From the daylight analysis a correlation is found between the  $DF_{50\%}$  and the  $WWR * VSF$ , having a  $R^2 = 0.9898$ . This shows daylight factor analysis can be substituted in a building optimisation process by the  $WWR * VSF$  method maintaining a realistic approach of the daylight entrance. This is important to notice since substituting the daylight factor analysis can save a large amount of time during the optimisation process due to faster analysis. Both the daylight factor analysis and the VSF are methods that are already found in the literature. However, combining these two methods to indirectly assess

the daylight factor and reduce computation time has been seen in other literature.

Although this method has proven for the current reference project, for new projects the relation between  $DF_{50\%}$  and  $WWR * VRF$  should be verified. This is required since the current relation, as presented in Equation 5.1 is determined for a standard room of the Erasmus campus student housing complex.

### 6.3. Optimisation study

From the optimisation studies a Pearson correlation is found of -0.624 and -0.632 between the shape factor  $L_c$  and the total normalised energy demand. This implies more compact buildings use less energy for both heating and cooling which can be related to the reduction of energy losses through the building envelope as described in Equation 2.2 in Chapter 2. The fact that the cooling energy demand is 0 for all building designs can be related to a low solar heat gain coefficient (SHGC) of 0.33. Efficient natural ventilation can have contributed to this.

From the building shape optimisation study a similar correlation is found between the WWR and the total energy demand as for the reference building. From this it can be seen that reducing the WWR has a positive effect on the reduction of energy demand for the building on all orientations (see Table 5.3. Limiting factor in this will be the daylight requirements. For standard rooms this cannot go as low as 0.1, since in that case a SVF of 43.93% is required as seen in Table 5.1. This means almost no blocking of entering daylight is allowed to reach sufficient daylight entrance. What is interesting to this finding is that, from an energy perspective and respecting regulations, WWRs can be lower than commonly used in practice. As discussed in Section 4.1.2, the WWRs of the reference building lay between 0.2 and 0.3. Looking at other research, as discussed in Section 1.2, WWRs can be lower according to this study. It is important to note that in this study only amount of daylight entrance is assessed and other visual comfort parameters, such as sufficient view are out of scope for this study.

#### 6.3.1. Effect of shape

From the optimisation study, and the results presented in Figures 5.6 and 5.7, a preference for more compact buildings can be seen. Overall, buildings with a higher  $L_c$  perform better as they have a lower energy demand. Two things should be noted here. First, for both optimisations no cooling energy was recorded. Secondly, the weather file that is used is slightly dated, since it is based on the typical climate in the years 1966 - 2015 from which only months are selected up to 2011 as shown in 2.3. When looking at the future, when temperatures are expected to rise this may not be representative.

Because heating is the major driver for the shape definition (while restricted by the daylight requirements) it comes as no surprise a more compact shape is preferred. When linked to the vernacular architectural typologies and based on existing knowledge on the effect of shape this outcome was expected.

Four regions in Figure 6.1 should be pointed out. Designs in area A show a similar shape factor, but still have different energy demands, ranging from 300 to 600 kWh/m<sup>2</sup>. This is a stage in which modeFRONTIER searched for a relation between the WWR and the energy demand, as these are all similar buildings, only varying in WWR.

The second region that requires attention is region B from Figure 6.1. Here a number of good performing building designs are visible. However, these buildings are very slender and some of these designs may therefore be hard to realise in practice or have inefficient plans. Building design 693, shown in Figure 5.10(a) is an example of this.

The building at location C is the best performing design from the first optimisation, which is shown in Figure 5.10(d). The design at location D is the reference building. As can be seen here the reference building is one of the best performing building designs.

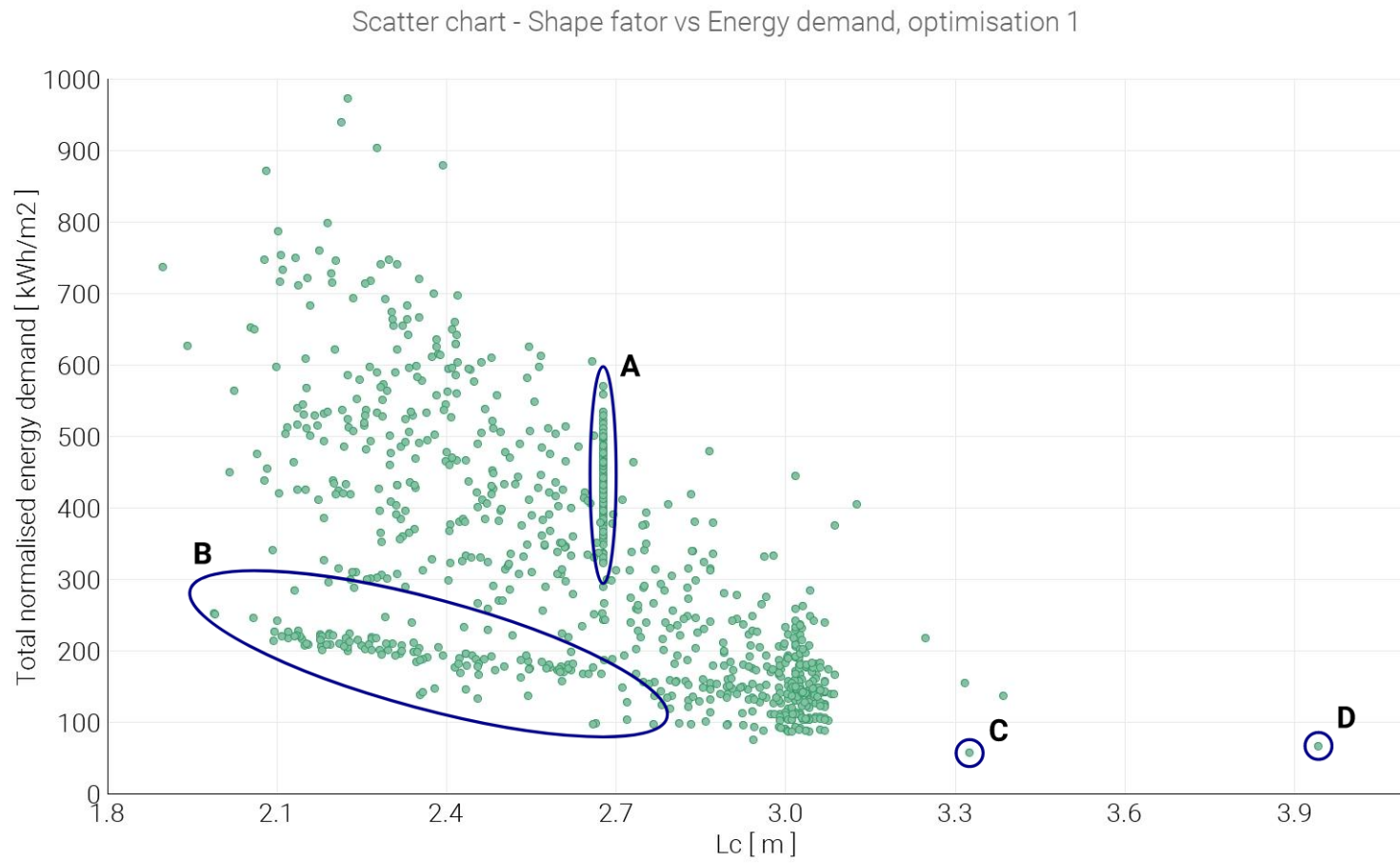


Figure 6.1: Overview of all building designs of the first optimisation, showing the relation between the shape factor ( $L_c$ ) and the normalised energy demand for heating and cooling, highlighting interesting areas

### 6.3.2. Effect of window-to-wall-ratio

From Figure 5.4, it is visible WWRs for north, south and west orientations for the most energy efficient buildings range, apart from one design, from 1 to 5, where the WWR for the east facade varies between 2 and 9. One important reason for this difference can be sought in the daylight requirements. The east facade is the only orientation directly facing other buildings. Already in the daylight analysis of the reference building shown in Figure 4.7 this orientation shows lower VSF values. Opposed to this, daylight values on other facade orientations are similar to values shown on the south orientation. Apart from affecting daylight entrance requirements, neighbouring buildings also have an effect on the thermal balance of a building. In case of the reference building, the WWR should be higher on the east facade to allow enough daylight to enter. However, direct solar radiation is blocked, which affects the heating and cooling need for the apartments on this side of the building. This will lead to less direct heat accumulation in the east facing apartments, decreasing the cooling demand in summer, but increasing the heating demand in winter.

Since the neighbouring buildings on the east side of the reference building are typical for this situation, a larger WWR on the east facade should also be seen as a building typical optimum. What this does show more in general, is that neighbouring buildings have a large effect on the optimal WWR.

The large effect of neighbouring buildings on the daylight entrance and therefore WWR, shows the importance of including shading effects of off-property mass. In current daylight regulation NEN 2057 and the new NEN-EN 17037 only building part are considered on the assessed plot. As this research shows, this leaves out a large influencing parameter, the effect of neighbouring buildings. This effect is important to consider for newly built buildings, but the effect of newly built neighbouring buildings should also be taken into account.

### 6.3.3. Effect of facade orientation

From Figure 5.8 it can be seen that in general, the building shapes are more east-west orientated. Since relatively more of the facade is faced east and west than north and south. From the more compact and more energy efficient buildings, this preference is even stronger as for buildings with an  $L_c$  higher than 3.0 all have larger east/west orientated facades than north/south facing facades.

The overall tendency of buildings having more east-west orientated facades may be an effect of the specific massing the designs are bound to. Since all building blocks are not square, but rectangular, a preference for east-west orientated buildings is embedded in the design. However, north-south orientated buildings are still possible within this design. The preference shown from the results for east-west orientated buildings therefore can be seen as a guiding principle for design of this type of buildings.

# Conclusion

In this chapter the conclusions which answer to the main research question and to the different sub questions are discussed. First all sub questions are answered and finally the main research question is answered.

## 7.1. Sub-research questions

- What parameters affect the energy use for mid-rise residential buildings in a temperate climate and what is the effect of WWR and shape, of mid-rise residential buildings in a temperate climate, on energy demand and daylight entrance?

From literature study and analysis of the energy balance of buildings a number of parameters is found which affect the energy use for heating and cooling. For this study, three parameters are most important. These are  $Q_{transmission}$ ,  $Q_{infiltration}$  and  $Q_{solarradiation}$  which are all related to the surface area of the building envelope and the size of the windows. These three parameters can be translated into the WWR and the shape factor of a building. WWR affects both transmission losses and the incoming solar radiation as thermal resistance of the building envelope changes with these parameters. For larger WWRs transmission losses are higher and so is the incoming solar radiation. Infiltration is linked to the shape factor, as a lower compactness increases the infiltration losses through the building envelope.

As shown in Table 5.2, WWR has a different effect on the energy use depending on the orientation. In summer there is a large positive correlation between the east, south and west orientated WWR and the energy demand, while in winter there is a larger positive correlation between the WWR on the north, east and west orientation and the energy demand. From these correlations it can be seen that adjusting the WWR for both east and west orientation will not have a great effect since they are both positively correlated to the heating and cooling energy demand. This makes sense since the angle of attack on windows facing east and west is more constant over the year.

Therefore, aiming for a low WWR on both the south and north facade would lower energy demands, whereas WWR on both east and west facade can be larger due to the smaller effect on the energy demand.

- What is an acceptable range for WWR (I), shape(II) and orientation(III) of mid-rise residential buildings in a temperate climate in which they contribute to low energy demand while maintaining thermal comfort and acceptable daylight entrance?
- I From the results it is seen that buildings with a high shape factor ( $L_c$  above 2.8), which means they are more compact, are more likely to achieve all constraints and demands and are therefore preferred over less compact buildings with lower shape factors ( $L_c$  below 2.8).
  - II Buildings with low WWRs also more likely to have lower energy demand through the year. Without adjacent buildings, WWRs can be as low as 0.1. Although, a optimal WWRs are largely affected by the presence of adjacent buildings, causing optimal WWRs to become higher than 0.1, depending on the size and the distance of the adjacent building.



- III For minimising the energy demand, a slight preference for east/west orientations has been found. It is also been found that the changing the window to wall ratio on the north and south orientation has a large effect on the energy demand through the entire year.

## 7.2. Main research question

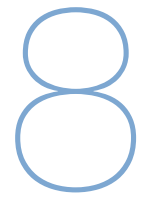
- How can optimisation of building shape and window-to-wall-ratio contribute to the reduction of energy demand for mid-rise residential buildings in temperate climate, while maintaining thermal comfort and sufficient daylight entrance?

From this study, building shape and window-to-wall-ratio prove to be important design parameters when designing residential buildings. For mid-rise buildings in a temperate climate, compact buildings with low window-to-wall-ratios are preferred. Considering this early on in the design process can help reducing energy demand and can prevent cooling installations from being required, saving both costs, energy and reducing the impact on the environment.

This study confirms the knowledge and current practice to make buildings as compact as possible to reduce the energy demand. By assessing a large number of design variations, the aim for compact buildings as a way to reduce the energy demand is confirmed.

Introducing a combined daylight entrance analysis between the daylight factor analysis and the visible part of the sky factor analysis prove to be an efficient way to assess daylight for optimisation studies. This method reduced the assessment time by 1 - 3 minutes per design variation, saving several days of optimisation time.

This study has also shown the large effect adjacent buildings have on the optimal WWR. Since adjacent buildings are not considered in daylight calculation according NEN 2057 and the new NEN-EN 17037, situations may occur where buildings will obtain legal daylight entrance requirements are in reality show poor daylight entrance.



# Recommendations

Based on the knowledge that is gained during this research a set of recommendations will be given in this chapter. These recommendations are divided over two main categories, recommendations for further or extended research into the subject of this thesis and recommendations for building designers e.g. architects or building engineers.

## 8.1. Recommendations for further research

The recommendations for further research are split up into two groups, first recommendations are presented that are aimed at research projects using a similar methodology to optimise building shapes. After that a number of recommendations is presented aimed at additional research following up on this thesis.

### 8.1.1. Other optimisation studies

Because of the vast amount of possible variations the optimisation software requires a large amount of time to converge to the optimum solution. Apart from a slow optimisation process, this could result in missing well performing options. Starting the optimisation process by running a DOE that is well distributed over the complete range of options (e.g. making use of a latin hypercube DOE) could help creating an insight of what designs are possible and how they perform. This might speed up the process of optimisation.

Another option would be to include designs which align to shapes which are expected to perform well, or are in a range that would be preferred based on other criteria (e.g. aesthetics). However, too much of this type of input might steer the optimiser in a certain direction, possibly missing better performing designs.

Additionally, when assessing building shapes, it is important to consider off site buildings in the daylight analysis.

### 8.1.2. Follow up research

During the execution of this research a large number of choices was made, narrowing down the variation and thereby also limiting the scope. There are four important limitations of this research, suitable to be incorporated in further research.

First, an addition of multiple case studies could strengthen the results found in this research. By analysing more case studies, results from this research can be further underpinned or alleviated. In both cases more insight will be gained into the effect of shape and WWR for residential buildings in temperate climate.

Secondly, in this thesis a wide variety of building shapes has been allowed in the optimisation process, although the variation in WWR was limited to only 9 options per facade. Allowing for smaller steps in the adjustment of the WWR could create more insight in the effect of this parameter. This could also lead to a more specific advise for building designers as the steps now were quite large.

As a third limitation, no variation in installations is considered. By doing so, the results only reflect the performance of the building shape, but in a real situation the lowest energy demand for heating

and cooling based on the shape only does not have to be the best option. An example of this could be the situation where an ATEs (aquifer thermal energy storage) is applied and there is a need for equal demand for heating and cooling throughout the year. This is one example, but more variations of installations could have different effects on the desired shape and are therefore an interesting subject for further research.

The fourth recommendation for further research is to look into the effect of considering on site energy production, since the type of installations is related to the BENG 2 requirement and the third step of the trias energetica, how efficiently fossil fuels are used in buildings. Investigating the effect of on site energy production would relate to the BENG 3 requirement or the third step of the trias energetica, to use as much renewable energy as possible. The most obvious choice would be to consider the installation of PV-panels on the roof and facade. In such a research different shape factors and WWRs may be preferred since more space for energy production can finally result into a lower fossil fuel demand.

## **8.2. Recommendations for building designers**

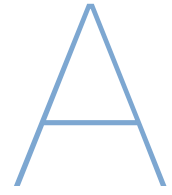
Recommendations for Building Designers mainly follow from the conclusions stated in the previous Chapter.

When using an optimisation process to determine building shape in an early design stage there are two important recommendations to be made. First recommendation is to make use of visible part of the sky analysis (VSF) in the assessment of daylight criteria. The analysis in this research between the daylight factor (DF) and the VSF shows there is a strong correlation between these two which makes VSF a suitable substitution for DF analysis. Using VSF can save minutes of computation time per building analysis thereby speeding up the optimisation process. However, it should be noted this method would be effective only if equally sized building blocks are used in the shape generation since the relation between VSF is based on one typical space. This is important to consider in an early stage, while setting up the massing model.

# Bibliography

- Al-Sallal K. A. and Rahmani M. Vernacular Architecture in the MENA Region: Review of Bioclimatic Strategies and Analysis of Case Studies. In Sayigh A., editor, *Sustainable Vernacular Architecture*, chapter 3, pages 23–53. Springer, 2019. ISBN 9783030061845. doi: 10.1007/978-3-030-06185-2\_{\\_}15.
- Alibaba H. Determination of optimum window to external wall ratio for offices in a hot and humid climate. *Sustainability*, 8(2):187–208, 2016. ISSN 20711050. doi: 10.3390/su8020187.
- Bahadori M. N. Passive Cooling Systems in Iranian Architecture. *Scientific American*, 283(2):144–145, 1978. ISSN 0036-8733. doi: 10.1038/scientificamerican0278-144.
- Bahadori M. N. and Dehghani-sanij A. *Towers*. Springer, 2014. ISBN 9783319058764.
- Beck H., Zimmermann N., McVicar T., Vergopolan N., Berg A., and Wood E. Present and future Köppen-Geiger climate classification maps at 1-km resolution, 2018.
- Bluyssen P. *The Indoor Environment Handbook*. Earthscan, London, 2009. ISBN 9781844077878. doi: 10.4324/9781849774611.
- Cawthorne D. *Daylighting and occupant health in buildings*. PhD thesis, University of Cambridge, 1995.
- CBS . *Hernieuwbare elektriciteit; productie en vermogen*, 2019. URL <https://opendata.cbs.nl/statline/#/CBS/nl/dataset/82610ned/table?ts=1576852629567>.
- Chiesa G., Acquaviva A., Grosso M., Bottaccioli L., Floridia M., Pristeri E., and Sanna E. M. Parametric optimization of window-to-wall ratio for passive buildings adopting a scripting methodology to dynamic-energy simulation. *Sustainability*, 11(11), 2019. ISSN 20711050. doi: 10.3390/su11113078.
- Duijvestein K. *Ecologisch bouwen*. Publikatieburo Bouwkunde, Delft, 1998.
- Esteco . *Effective Optimization Driven Design*, 2018. URL [https://www.esteco.com/system/files/BROCHURE\\_numerics\\_2018\\_R2\\_web.pdf](https://www.esteco.com/system/files/BROCHURE_numerics_2018_R2_web.pdf).
- Esteco . *modeFRONTIER User Guide*, 2019.
- European Commission . *The Energy Performance of Buildings Directive*, 2019.
- Fanger P. O. Thermal comfort. Analysis and applications in environmental engineering. *Copenhagen: Danish Technical Press*, 1970.
- van der Horn A., Verbaan G., and Vreeken M. Daglichtfactoren. *Bouwfysica*, 30(2):2–5, 2019.
- ISSO . *Publicatie 74*, 2014.
- Kurvers S., van der Linden K., and Cauberg H. Literatuurstudie thermisch comfort. Technical report, RVO, Den Haag, 2012.
- MacLeamy P. There are lessons in manufacturing, 2004. ISSN 08919526.
- Marsh A. CIE Sky generator, 2018. URL <https://drajmarsh.bitbucket.io/cie-sky.html>.
- Masson-Delmotte V., Zhai P., Pörtner H.-O., Roberts D., Skea J., Shukla P. R., Pirani A., Moufouma-Okia W., Péan C., Pidcock R., Connors S., Matthews J. B. R., Chen Y., Zhou X., Gomis M. I., Lonnoy E., Maycock T., Tignor M., and Waterfield T. Global Warming of 1.5°C An IPCC Special Report. Technical report, Intergovernmental Panel on Climate Change, 2018.

- Mecanoo architecten . Erasmus Campus Student Housing, 2020. URL <https://www.mecanoo.nl/Projects/project/215/Erasmus-Campus-Student-Housing?t=3>.
- Ministry of the Interior and Kingdom Relations . Besluit van 13 december 2019, houdende wijziging van het Bouwbesluit 2012 en van enkele andere besluiten inzake bijna energie-neutrale nieuwbouw. *Staatsblad van het Koninkrijk der Nederlanden*, (501), 2019a.
- Ministry of the Interior and Kingdom Relations . Nadere informatie over energiezuinige nieuwbouw (BENG), 2019b.
- Ministry of the Interior and Kingdom Relations . Invoeringsdatum BENG-eisen/ NTA 8800 / vernieuwing energielabel naar 1 januari 2021, 2020.
- NEN . Persbericht - Nieuwe norm belangrijke factor voor daglicht in gebouwen, 2019.
- Nicol J. F. and Humphreys M. A. Adaptive thermal comfort and sustainable thermal standards for buildings. *Energy and Buildings*, 34(6):563–572, 2002.
- ODYSSEE-MURE . Sectoral Profile - Households, 2015.
- Peel M., Finlayson B., and McMahon T. Long-term rates of mass wasting in Mesters Vig, northeast Greenland: Notes on a re-survey. *Hydrogen and Earth System Sciences*, 11:1633–1644, 2007. ISSN 10456740. doi: 10.5194/hess-11-1633-2007.
- Pessenlehner W. and Mahdavi A. Building Morphology, Transparency, and Energy Performance. In *8th International IBPSA Conference*, pages 1025–1032, Eindhoven, Netherlands, 2003.
- Rijksoverheid . Klimaatakkoord, 2019.
- Sariyildiz S. Performative computational design. In *Architecture and Technology*, number 15-17 November 2012 in Iconarch, pages 313–344, Konya, Turkey, 2012. URL <http://repository.tudelft.nl/assets/uuid:b637bb68-7e90-44f7-9c45-74a05e29a69d/289840.pdf>.
- Shaeri J., Habibi A., Yaghoubi M., and Chokhachian A. The optimum window-to-wall ratio in office buildings for hot-humid, hot-dry, and cold climates in Iran. *Environments*, 6(4), 2019. ISSN 20763298. doi: 10.3390/environments6040045.
- van Straalen I. J., de Winter P. E., Coppens E. G. C., and Vermande H. M. Eindrapport historisch onderzoek technische bouweisen. Technical report, TNO, Utrecht, 2007. URL <http://www.bouwbesluitinfo.nl/media/download/ExternetoetsenenbeoordelingenBouwbesluit2012/Eindrapporthistorischonderzoektechnischebouweisen-TNO070917.pdf>.
- Troup L., Phillips R., Eckelman M. J., and Fannon D. Effect of window-to-wall ratio on measured energy consumption in US office buildings. *Energy and Buildings*, 203, 2019. ISSN 03787788. doi: 10.1016/j.enbuild.2019.109434.
- United Nations . Paris Agreement, 2015.
- Whitsett D., Silver P., and McLean W. *Introduction to Architectural Technology*. Laurence King, London, 2 edition, 2013. ISBN 9781780672946.
- Zandbelt D., van den Berg R., Bokkers T., and Witteman B. Een studie naar Nederlandse hoogbouw-cultuur. Technical report, Stichting Hoogbouw and Zandbelt&vandenBerg, Rotterdam, 2008. URL [www.hoogbouw.nl](http://www.hoogbouw.nl).



## Appendix A - ISSO 74

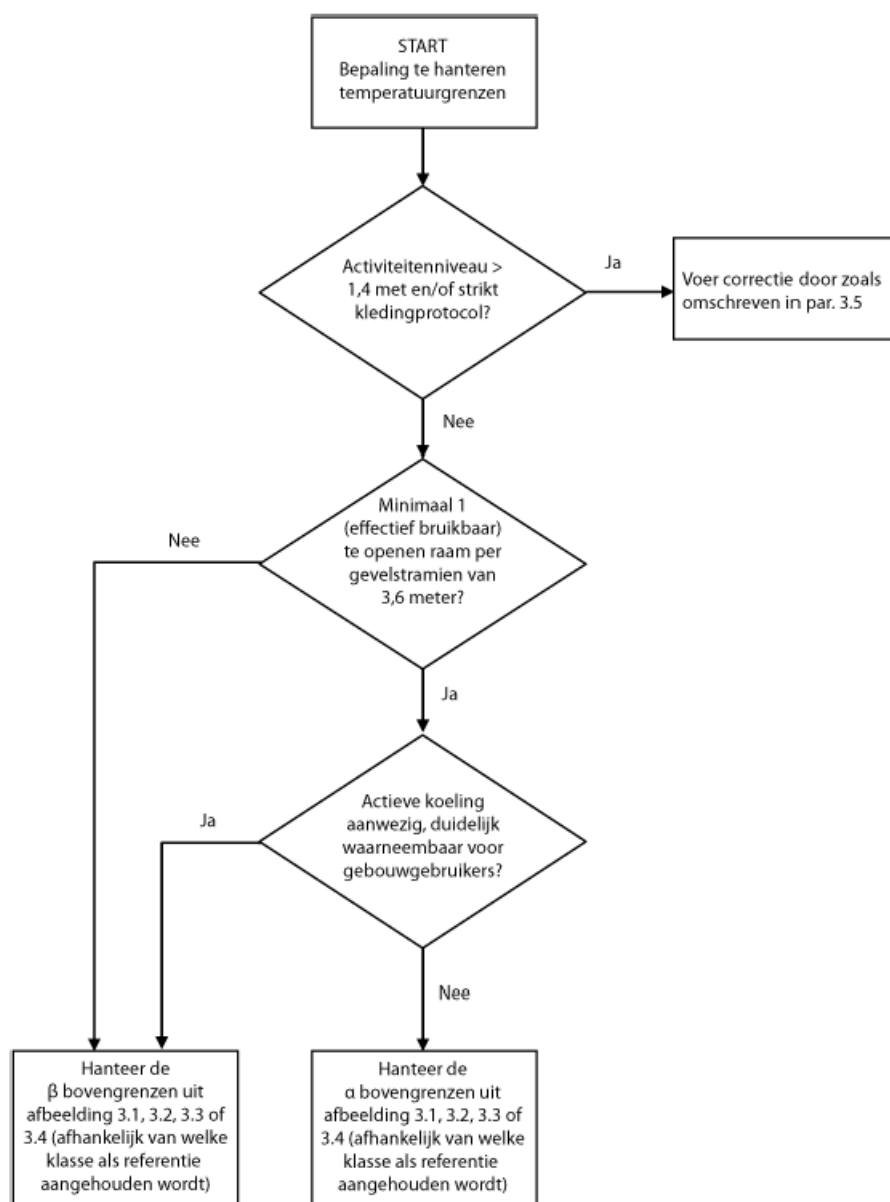
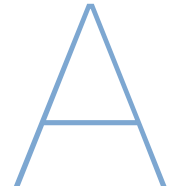


Figure A.1: Flowchart to determine upper temperature boundaries for comfort (ISSO, 2014)



## Appendix B - Daylight Factor to visible part of the sky



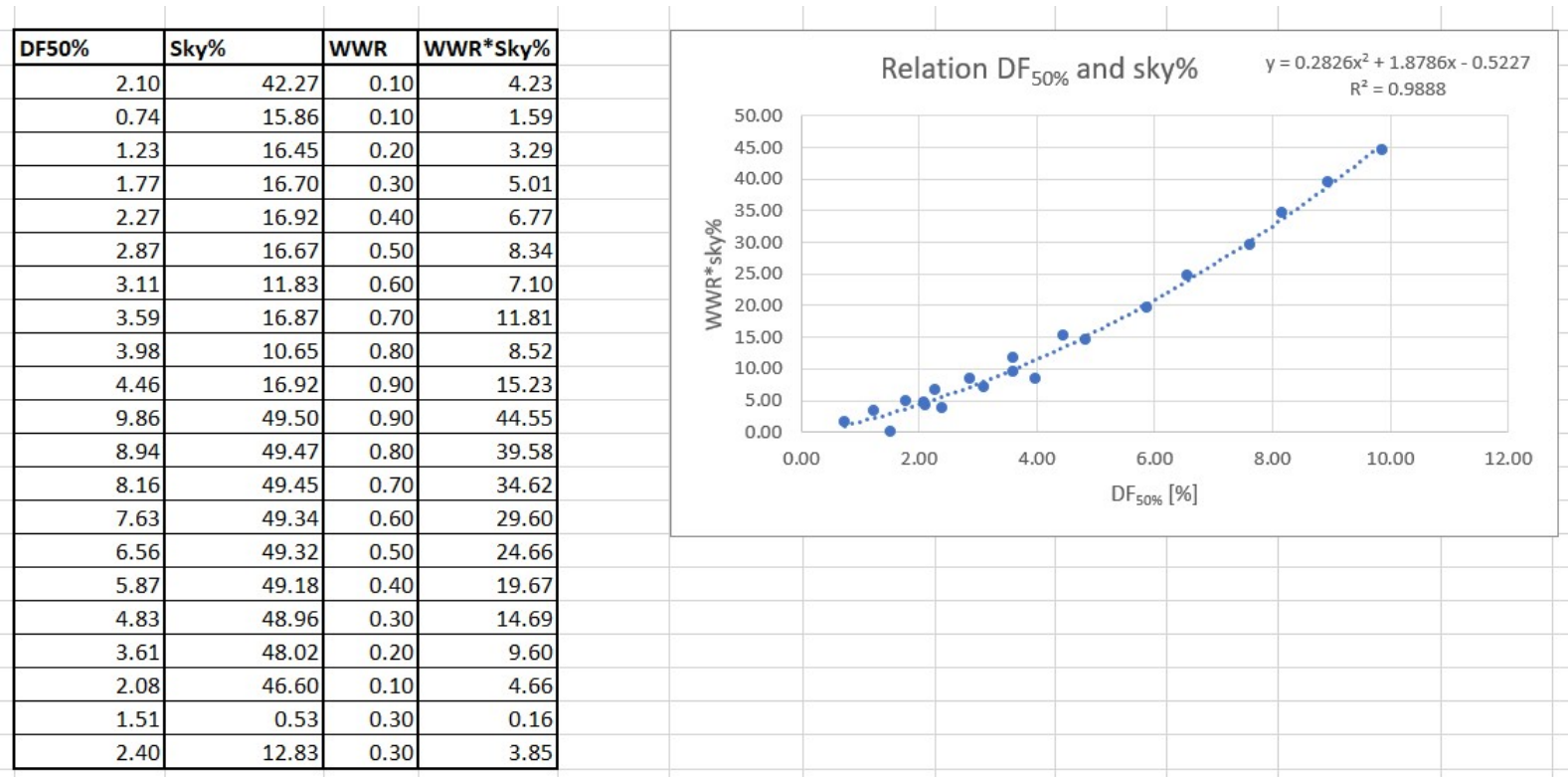
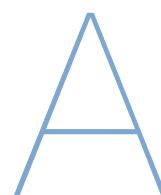


Figure A.1: Data and relation between  $DF_{50\%}$  and window-to-wall ratio times the visible part of the sky (Sky%)



## Appendix C - NEN 2057

GEBIED A - ruimte 1				
<b>Tabel gelinkt aan:</b>		Ruimte 1	$\alpha$ min [°]	20
		Opening 1	$\alpha$ max [°]	80
<b>Verdieping:</b>		[..]		
$\alpha$ per sector	hoogte verschil belemmering en onderzijde raam mm	diepte belemmering mm	hoek °	hoek alfa (min 20°, max 80°) °
-50	19,800	7,800	68	68
-40	19,800	7,800	68	68
-30	19,800	7,800	68	68
-20	19,800	7,800	68	68
-10	19,800	7,800	68	68
+10	19,800	7,800	68	68
+20	19,800	7,200	70	70
+30	19,800	4,500	77	77
+40	19,800	3,200	81	80
+50	19,800	2,200	84	80
alfa gemiddeld				72

Figure A.1: Input data NEN 2057 check reference building room 1

GEBIED A - ruimte 2				
<b>Tabel gelinkt aan:</b>		Ruimte 2	$\alpha$ min [°] 20	
		Opening 1	$\alpha$ max [°] 80	
<b>Verdieping:</b>		[..]		
$\alpha$ per sector	hoogte verschil belemmering en onderzijde raam mm	diepte belemmering mm	hoek °	hoek alfa (min 20°, max 80°) °
-50	19,800	7,800	68	68
-40	19,800	7,800	68	68
-30	19,800	7,800	68	68
-20	19,800	7,800	68	68
-10	19,800	7,800	68	68
+10	19,800	6,400	72	72
+20	19,800	3,100	81	80
+30	19,800	2,100	84	80
+40	19,800	1,400	86	80
+50	19,800	1,000	87	80
alfa gemiddeld				73

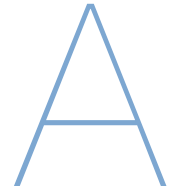
Figure A.2: Input data NEN 2057 check reference building room 2

GEBIED A - ruimte 3				
Tabel gelinkt aan:		Ruimte 3	$\alpha$ min [°]	20
		Opening 1	$\alpha$ max [°]	80
Verdieping:		[..]		
$\alpha$ per sector	hoogte verschil belemmering en onderzijde raam mm	diepte belemmering mm	hoek °	hoek alfa (min 20°, max 80°) °
-50	8,200	7,800	46	46
-40	8,200	7,800	46	46
-30	8,200	7,800	46	46
-20	8,200	7,800	46	46
-10	8,200	7,800	46	46
+10	8,200	7,800	46	46
+20	8,200	7,800	46	46
+30	8,200	7,800	46	46
+40	8,200	7,800	46	46
+50	8,200	7,800	46	46
alfa gemiddeld				46

Figure A.3: Input data NEN 2057 check reference building room 3

Bepalen equivalent daglichtoppervlak																		
GEBIED A																		
Verblijfsruimte		oppervlakte A [m <sup>2</sup> ]	A <sub>reductie</sub> [m <sup>2</sup> ]	Oppervlakte van de doorlaat i, in m2				overstaande belemmering α [°]	Belemmeringshoek β			Uitwendige reductiefactor		A <sub>eq</sub> [m <sup>2</sup> ]	Eis verblijfsruimte		Eis verblijfsgebied	
				daglicht opening nr.	hoogte [glas] (excl. 600mm) [m]	breedte [glas] [m]	A <sub>d,i</sub> [m <sup>2</sup> ]		diepte belemme ring [m]	1/2 * hoogte glas [m]	β [°]	C <sub>b</sub> [-]	C <sub>u</sub> [-]		Eis [m <sup>2</sup> ]	Beoordeling	Eis [%]	Beoordeling
Ruimte 1	Room NE	18.2												1.29	0.50	Voldoet	10%	Voldoet niet
				1	1.5	2.2	3.3	72	0.300	0.75	22	0.39	1.00	1.29	1.29		7%	
Ruimte 2	Room SW	18.2												1.25	0.50	Voldoet	10%	Voldoet niet
				1 5	1.5	2.2	3.3	73 -	0.300	0.75	22	0.38	1.00	1.25	1.25		7%	
Ruimte 3	Room middle	18.2												1.91	0.50	Voldoet	10%	Voldoet
				1	1.5	2.2	3.3	46	0.300	1	22	0.58	1.00	1.91	1.91		10.5%	
		m2 54.6	m2 44.6											m2 4.46	m2 1.50	Voldoet		

Figure A.4: Results equivalent daylight surface area calculation critical rooms reference building



## Appendix D - Grasshopper model and input

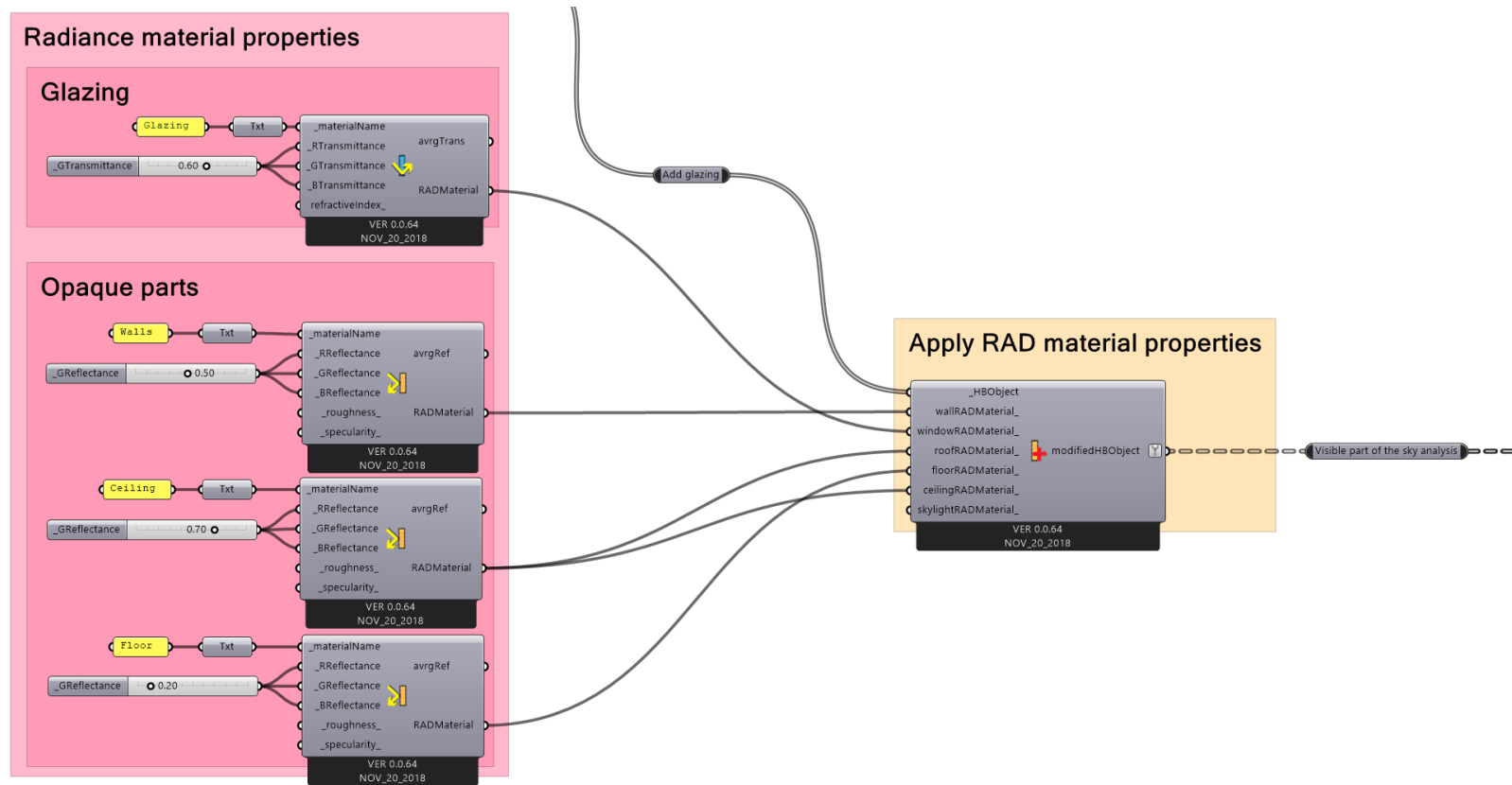


Figure A.1: Grasshopper model assigning RAD material properties



## Apply Energy+ material properties

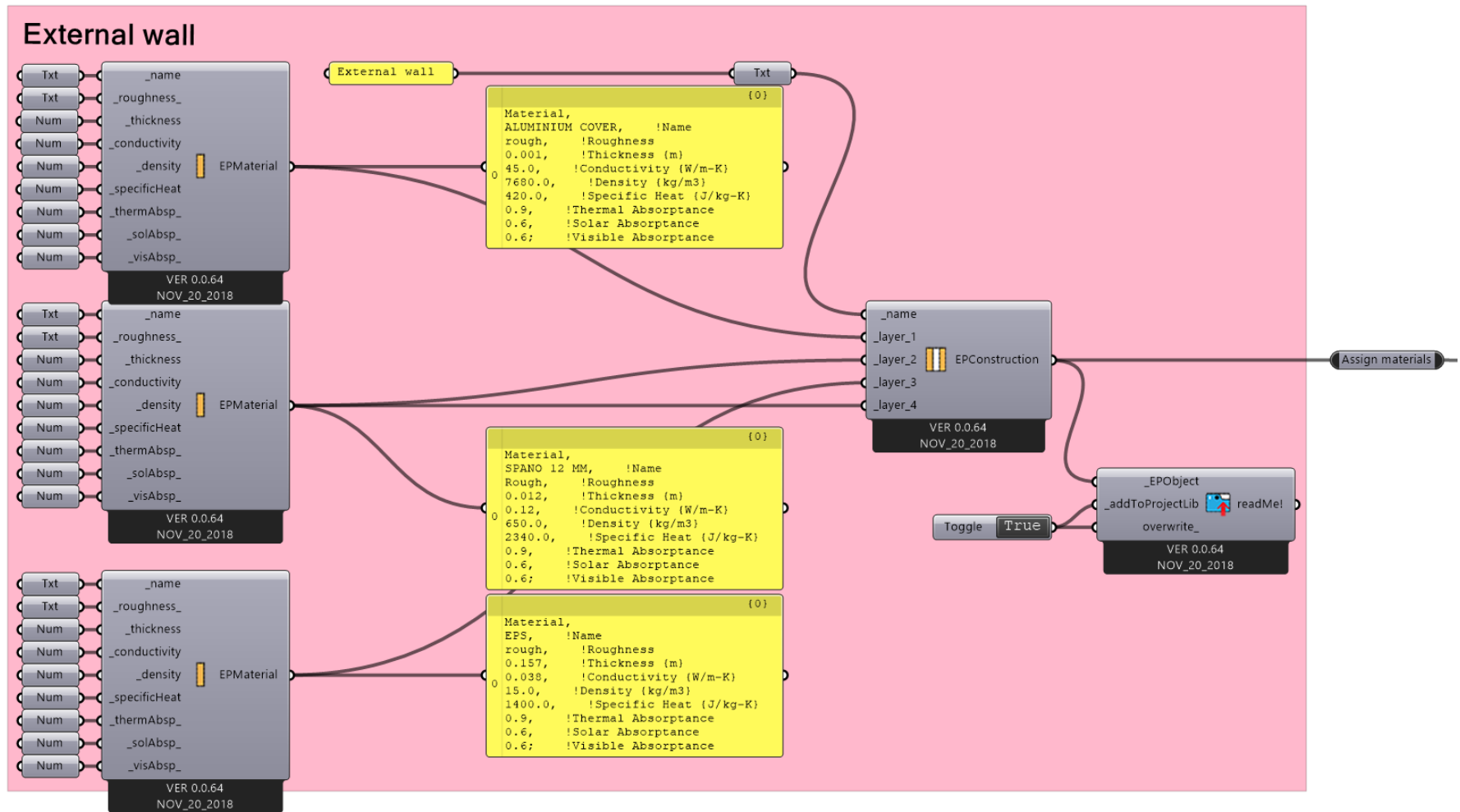


Figure A.2: Grasshopper model assign material properties external wall

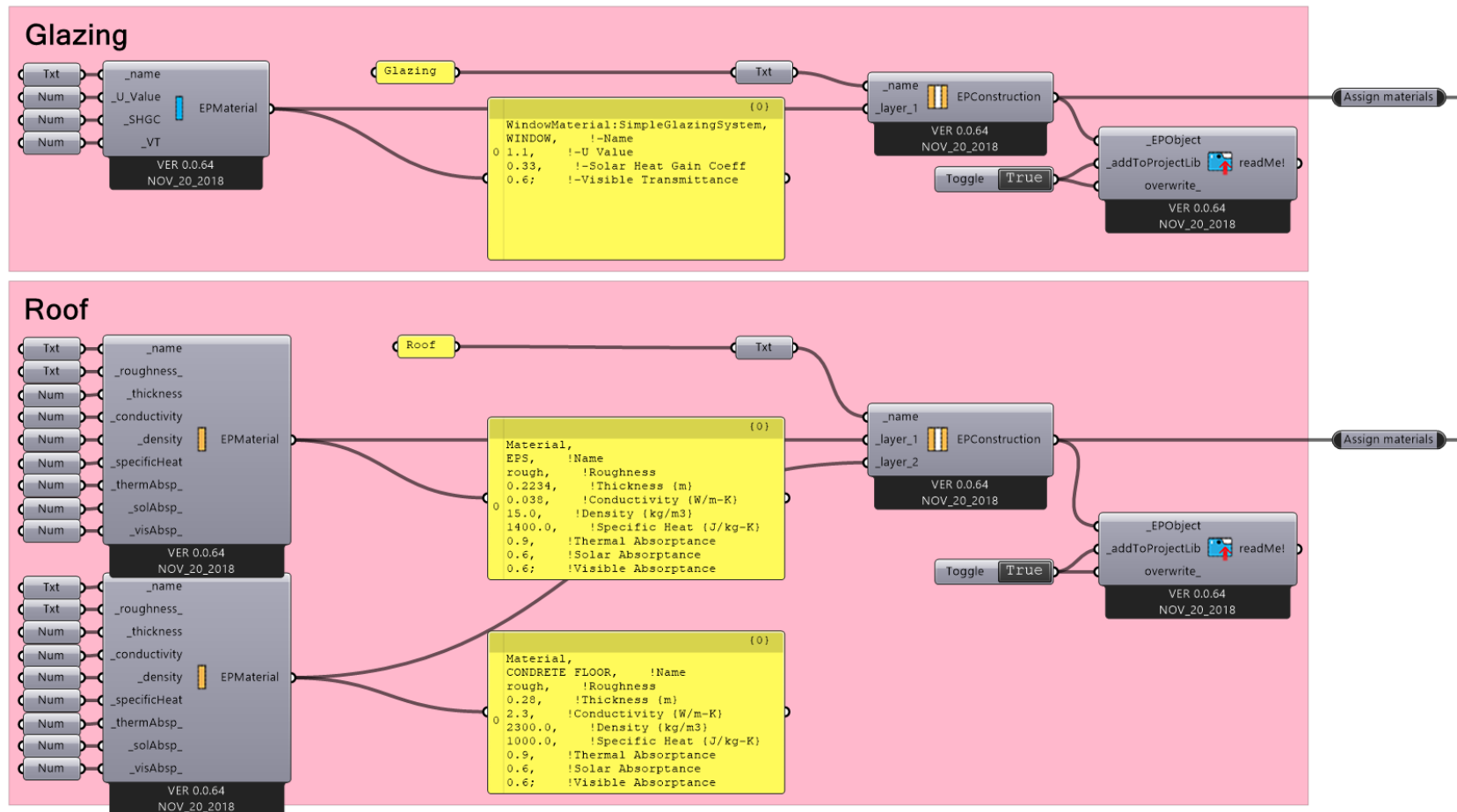


Figure A.3: Grasshopper model assign material properties glazing and roof

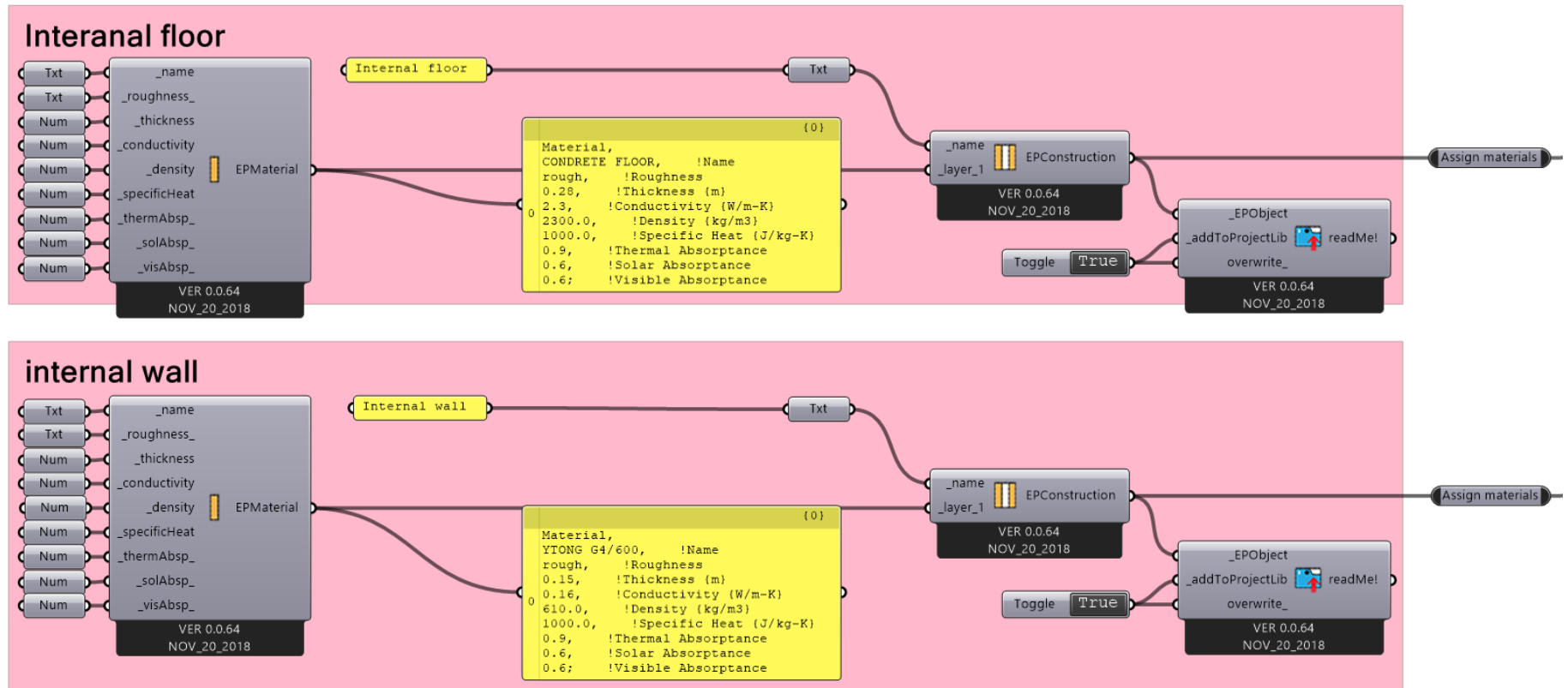


Figure A.4: Grasshopper model assign material properties internal floor and wall

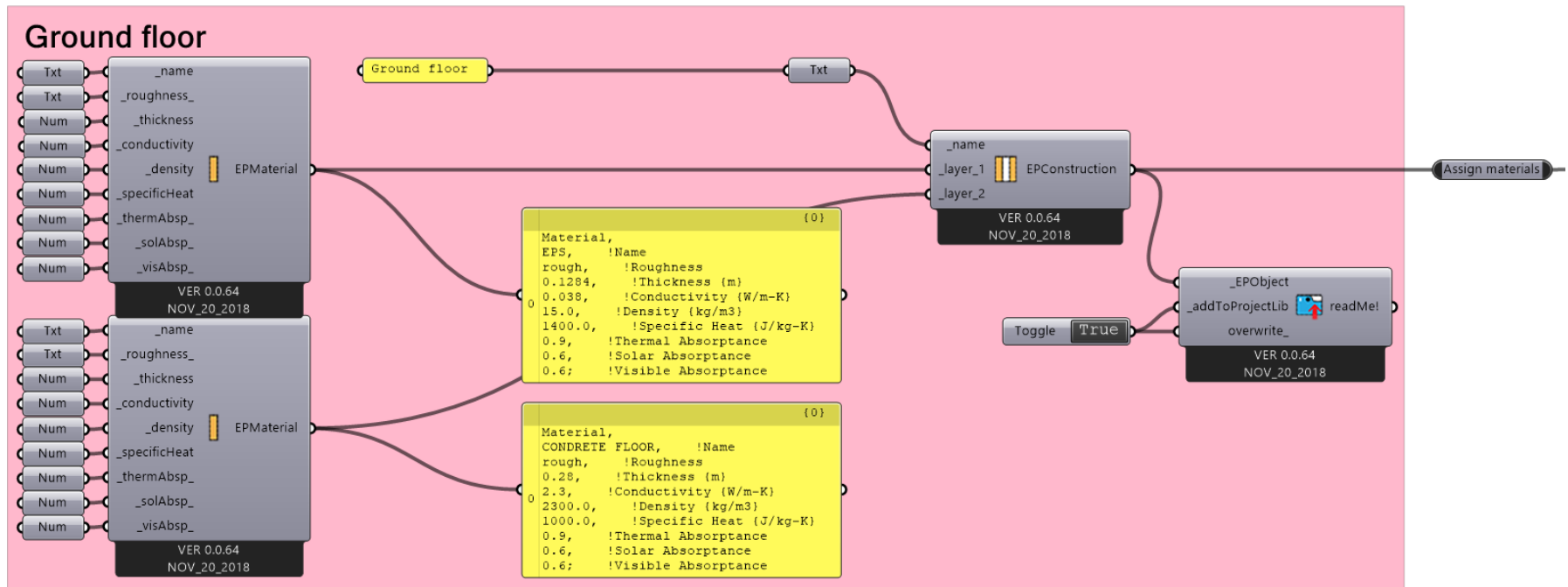


Figure A.5: Grasshopper model assign material properties ground floor

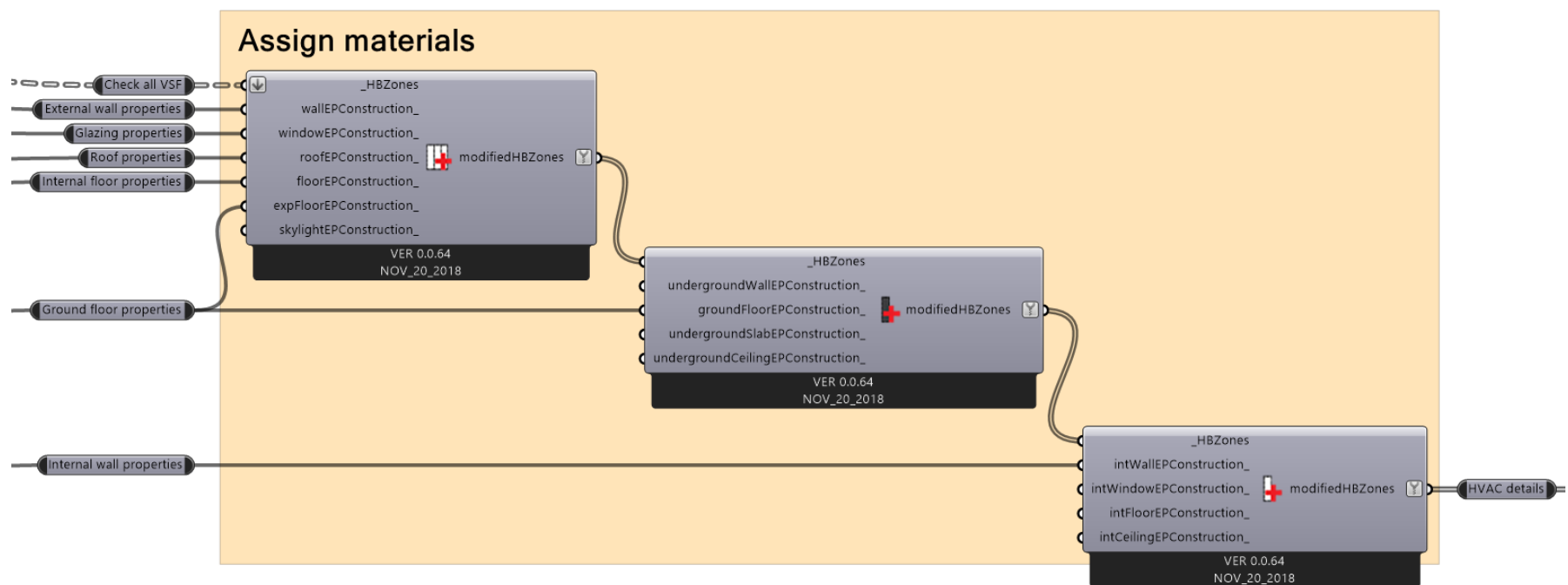


Figure A.6: Grasshopper model assign materials to building

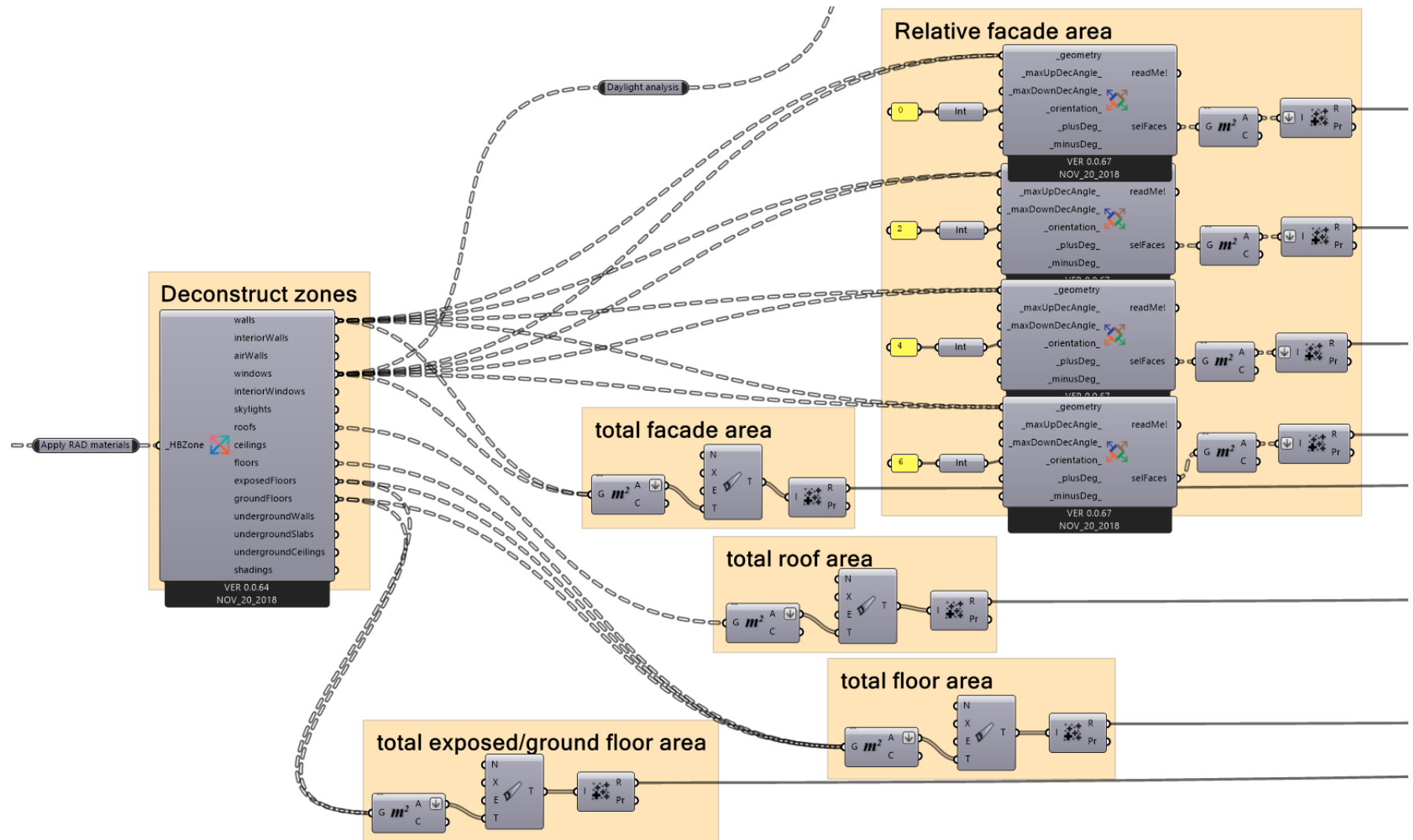


Figure A.7: Grasshopper model calculate building properties

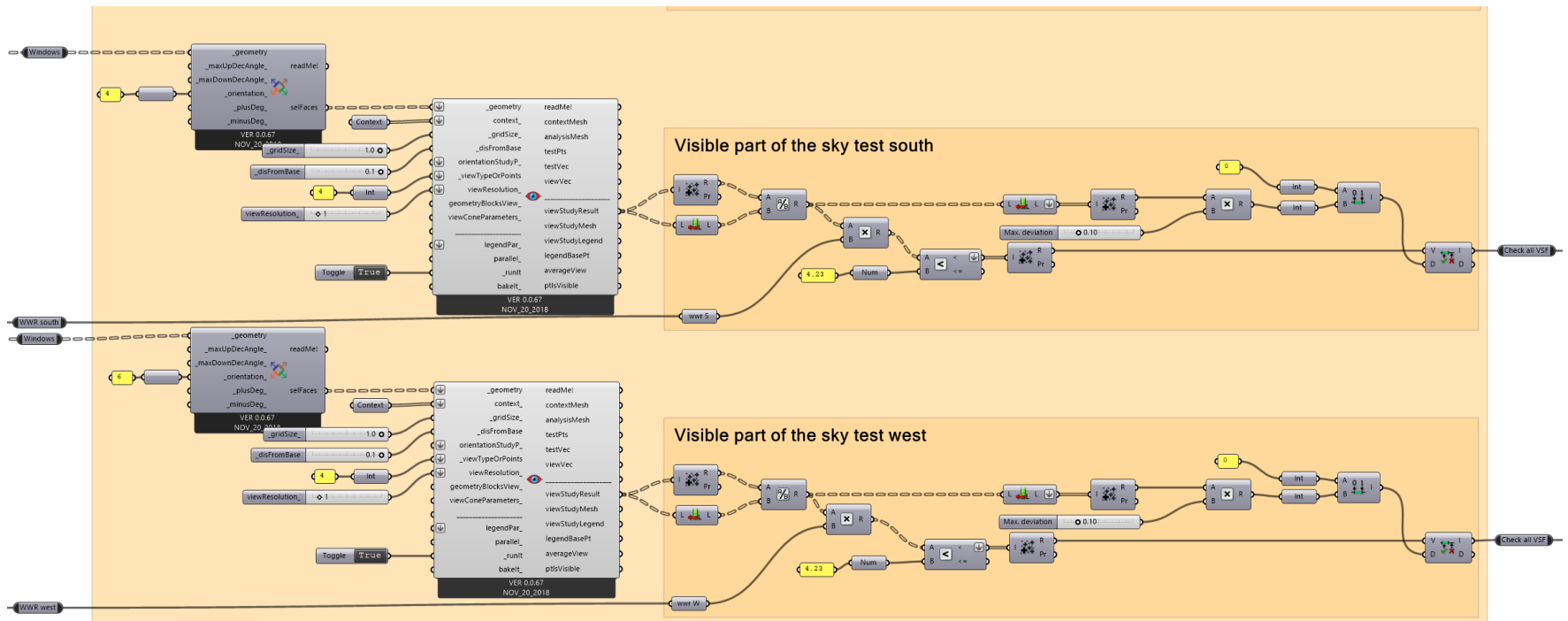
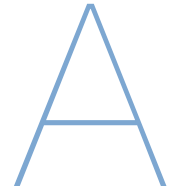


Figure A.8: Grasshopper model VSF calculation for the south and west facade

The screenshot displays the modeFRONTIER software interface, showing two simulation blocks for energy demand normalization. Each block contains a list of input variables (Zones, resultFileAddress, etc.) and a list of output variables (operativeTemperature, airTemperature, etc.). The outputs are connected to a central 'modeFRONTIER output' block, which lists various normalized energy demand metrics and building parameters.

Figure A.10: Grasshopper model normalise energy demand for winter and summer analysis and collect output values for mod-eFRONTIER





## Appendix E - Input variables DesignBuilder validation

Column1	Column2	Column3	Column4	Column5	Column6	Column7	Column8	Column9	Column10	Column11	Column12	Column13	Column14	Column15	Column16	Column17	Column18	Column19	Column20
DB report	01/07/2020 20:34:57	DB Version v5.4.0																	
Keyword	Key	U-Value (incl bridging) (W/m2K)	Km (KJ/K)	Cost per surface area (GBP/m2)															
CONSTRUCTION	Wall Erasmus	0.222	20.100	107.00															
CONSTRUCTION	Roof Erasmus	0.170	230.000	651.00															
CONSTRUCTION	Ground floor Erasmus	0.291	230.000	651.00															
Keyword	Name	Layers	UValue (W/m2K)	Trans Light (VT)	Trans Total (SHGC)	Trans Direct Solar	Cost per surface area (GBP/m2)												
GLAZING	Erasmus glazing	1	1.100	0.600	0.330	0.800	100.00												
Building Data																			
Building number of zones:	1																		
Building heated/cooled floor area (m2)	92.85																		
Building volume (m3)	278.56																		
Building external area (m2)	320.00																		
Building area-weighted average U-value (W/m2K)	0.337																		
Building external surface area/Volume (m-1)	1.149																		
Activity Area Summary																			
Activity	Area (m2)																		
Generic Office Area	92.85																		
Total	92.85																		
Zone	Activity	Floor area (m2)	Volume (m3)	Heated?	Heating SetPoint Temperature (C)	Cooled?	Cooling SetPoint Temperature (C)												
Block 1 - Zone 1	Generic Office Area	92.853	278.558	True	18.000	True	24.000												
	Element	Adjacent condition	Area-Nett (m2)	Flow path	U-Value (W/K-m2)	U-Value*Area (W/K)	Km (KJ/m2-K)	Km*Area (KJ/K)	SROut (m2-K/W)	SRIn (m2-K/W)	Orientation (deg E of N)	Slope (deg)	Heavyweight?	Embodied Carbon (kgCO2)	Embodied Carbon Flag	Equivalent CO2 (kgCO2)	Equivalent CO2 Flag	Cost of Surface Finish (GBP)	
	Infiltration	Outside	N/A	N/A	N/A	50.208	N/A	N/A	N/A	N/A	N/A	N/A	False	0.0					
	Ground floor	Ground	100.000	Ground floor Erasmus	0.291	29.0729	230.000	23000.0000	0.010	0.170	0.000	180.000	True	17186.880		17965.510		4,500.0	
	Roof	Outside	100.000	Roof Erasmus	0.170	17.0368	230.000	23000.0000	0.040	0.100	180.000	0.000	True	17543.130		18430.060		3,000.0	
	Wall	Outside	21.328	Wall Erasmus	0.222	4.7379	20.100	428.6928	0.040	0.130	90.000	90.000	True	1695.736		1847.032		853.1	
	Wall	Outside	21.328	Wall Erasmus	0.222	4.7379	20.100	428.6928	0.040	0.130	0.000	90.000	True	1695.736		1847.032		853.1	
	Wall	Outside	21.328	Wall Erasmus	0.222	4.7379	20.100	428.6928	0.040	0.130	270.000	90.000	True	1695.736		1847.032		853.1	
	Wall	Outside	21.328	Wall Erasmus	0.222	4.7379	20.100	428.6928	0.040	0.130	180.000	90.000	True	1695.736		1847.032		853.1	
	Glazing	Outside	8.672	Erasmus glazing	1.100	9.5392	0.000	0.0000	0.061	0.122	90.000	90.000	False	84.118	**	84.118	**	0.0	
	Glazing	Outside	8.672	Erasmus glazing	1.100	9.5392	0.000	0.0000	0.061	0.122	0.000	90.000	False	84.118	**	84.118	**	0.0	
	Glazing	Outside	8.672	Erasmus glazing	1.100	9.5392	0.000	0.0000	0.061	0.122	270.000	90.000	False	84.118	**	84.118	**	0.0	
	Glazing	Outside	8.672	Erasmus glazing	1.100	9.5392	0.000	0.0000	0.061	0.122	180.000	90.000	False	84.118	**	84.118	**	0.0	
														41849.4		44120.2		10912.5	
EMBODIED CARBON DATA																			
Table: 6, 5, 2																			
Materials Embodied Carbon and Inventory	Area (m2)	Embodied Carbon (kgCO2)	Equivalent CO2 (kgCO2)	Mass (kg)															
EPS Expanded Polystyrene (Erasmus)	285.3	1744.3	2274.5	697.7															
Wood derivatives - chipboard bonded with PF Dry	170.6	678.7	705.4	1330.9															
Metals - aluminium cladding	85.3	5601.9	6027.8	655.2															
Concrete Reinforced (with 1% steel)	200.0	33488.0	34776.0	128800.0															
Sub Total		41513.0	43783.7	131483.8															
Table: 5, 4, 2																			
Constructions Embodied Carbon and Inventory	Area (m2)	Embodied Carbon (kgCO2)	Equivalent CO2 (kgCO2)																
Wall Erasmus	85.3	6782.9	7388.1																
Roof Erasmus	100.0	17543.1	18430.1																
Ground floor Erasmus	100.0	17186.9	17965.5																
Sub Total	285.3	41512.94	43783.70																
Table: 5, 4, 2																			
Glazing Embodied Carbon and Inventory	Area (m2)	Embodied Carbon (kgCO2)	Equivalent CO2 (kgCO2)																
Erasmus glazing	34.7	336.5	336.5																
Local shading		0.0	0.0																
Window shading		0.0	0.0																
Sub Total	34.7	336.5	336.5																
Table: 1, 4, 2																			
Building Total	320.0	41849.4	44120.2																
COST DATA																			
Table: 2, 3, 1																			
Structure Costs	Floor Area (m2)	Cost (GBP)																	
Sub Total	92.9	19499.1																	
Table: 2, 3, 1																			
HVAC Costs	Floor Area (m2)	Cost (GBP)																	
Sub Total	92.9	0.0																	
Table: 2, 3, 1																			
Lighting Costs	Floor Area (m2)	Cost (GBP)																	
Sub Total	92.9	8356.8																	
Table: 2, 3, 1																			
Sub-Structure Costs	Floor Area (m2)	Cost (GBP)																	
Sub Total	100.0	11000.0																	
Table: 5, 3, 1																			
Super Structure Cost	Construction Area (m2)	Cost (GBP)																	
Wall Erasmus	85.3	9128.4																	
Roof Erasmus	100.0	65100.0																	
Ground floor Erasmus	100.0	65100.0																	
Sub Total	285.3	139328.4																	
Table: 5, 3, 1																			
Glazing Cost	Surface Area (m2)	Cost (GBP)																	
Erasmus glazing	34.7	3468.8																	
Local shading		0.00																	
Blinds and internal shades		0.00																	
Sub Total		3468.8																	
Table: 7, 3, 1																			
Renewables Cost	Area (m2)	Cost (GBP)																	
PV Panels	0.00	0.00																	
Solar Hot Water Panels	0.00	0.00																	
Wind Turbines	0.00	0.00																	
PV Electrical		0.00																	
Wind Turbine Electrical		0.00																	
Sub Total		0.0																	
Table: 5, 3, 1																			
Surface Finish Costs	Surface Area (m2)	Cost (GBP)																	
Walls	85.3	3412.5																	
Floors	100.0	4500.0																	
Ceiling	100.0	3000.0																	
Sub Total		10912																	
Table: 1, 3, 1																			
Building Total Cost (GBP)		192566																	